UNITED KINGDOM • CHINA • MALAYSIA

POST-TRANSLATIONAL MODIFICATION OF INTERFERON REGULATORY FACTOR 1 (IRF1)

AHMED HASSANEIN ABDELMAKSOUD KHALAF

THESIS SUBMITTED TO THE UNIVERSITY OF NOTTINGHAM FOR THE DEGREE OF MASTER OF RESEARCH

MOLECULAR AND CELLULAR SCIENCE

SEPTEMBER 2016

ABSTRACT

Interferon Regulatory Factor 1 (IRF1) was the first characterised member of the Interferon Regulatory Factor (IRF) family of transcription factors as an IFNβ activator during viral infection. IRF1 acts as a tumour suppressor protein through the induction of apoptosis and cell cycle arrest. IRF1 is exposed to several post-translational modifications that regulate its function. Ubiquitin modifies IRF1 post-translationally, where ubiquitin G76 ligates to IRF1 lysine amino acids, followed by the building of the polyubiquitin chain. The specific type of polyubiquitination depends on the coactivator that binds to the IRF1 transactivation domain (TAD). Subsequently, ubiquitin targets the IRF1 protein to a distinct molecular pathway mediated by the key molecular mechanism of each polyubiquitination. The ubiquitination requires an enzymatic cascade to form a chain on the surface of the protein substrate. IRF1 is also modified by the attachment of the Small ubiquitin-like modifier (SUMO). For instance, IRF1 SUMOylation suppresses the activity and stabilises IRF1 expression level, compared with IRF1 polyubiquitination, which mainly targets IRF1 for proteasome degradation. However, IRF1 domains and its lysines-modified by ubiquitin are still ambiguous. As such, to understand how the ubiquitin regulates IRF1 protein, this study aimed to identify precise lysine residues in IRF1 that are modified by different polyubiquitination types and determine the impact of this modification on IRF1 stability and transcriptional activity. We, therefore, focused on the IRF1 C-terminal lysine amino acids that carry the possibilities to be ubiquitin acceptors or modified by the SUMO1 variant. It was found that ubiquitin targeted the IRF1 C-terminal domain, mainly K240 was

found to be the main acceptor for the IRF1 K48-polyubiquitination. IRF1 transcriptional activity was reduced as a consequence of IRF1 C-terminal K-R substitution within its TAD. C-terminal substitutions K233R, K255R, K276R, or K300R, altered the stability of IRF1 in this pilot study. Finally, the E3 FBXW7α ligase enzyme was found to enhance K48-polyubiquitination and K63-polyubiquitination of IRF1.

CONTENTS

ACKNOWLEDGMENTS

I am ultimately grateful to ALLAH for giving me the great opportunity to learn what I did not ever know, who says in his Holy Quran versus;

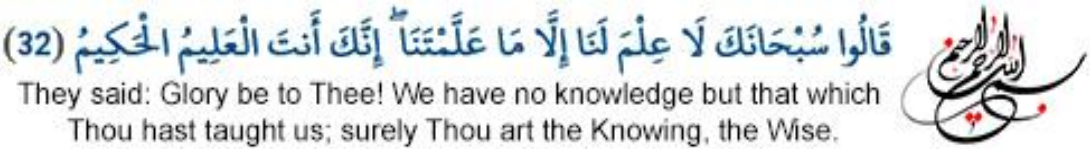

First, I am pleased to thank my supervisors, Dr. Nicole Clarke and Prof. David M. Heery, Center for Biomolecular Sciences, School of Pharmacy, University of Nottingham for their continuous support and inspiring words. She supported me in the laboratory work and let me to be self-dependent and Prof. David provided me his full support in managing the thesis writing.

Besides my supervisor, I would like to thank Dr. Hilary M. Collins, for her wonderful support, astute advices, encouragement and unending support for the successful presentation of my research work.

I am pleased to express my happiness towards The University of Nottingham, Citadel Capital Holding (NGO), and Beni-Suef University, for the financial support through Developing Master Solutions and QALAA Holding Scholarships, they believed in me and offered me the opportunity to acquire this knowledge which hopefully to transfer it back to our local students.

I would also like to express my gratitude for my parents, brothers and colleagues who motivated me a lot to move forward.

Finally yet importantly, I am gratefully full of positive thoughts owing to Cripps Centre, Crisis Team and Haven House for their urgent and tirelessly health support.

LIST OF FIGURES

LIST OF TABLES

ABBREVIATIONS

Abb	Definitions
°C	degree centigrade
µl	Microlitre
AB	Anti Body
Ad-IRF1	adenoviral vector
AEPSF	4-(2-aminoethyl) benzene sulfonyl fluoride hydrochloride
AML	Acute Myeloid Leukaemia
As-IRF1	antisense IRF1
BSA	Bovine Serum Albumin
Bak	Bcl-2 homologous antagonist killer
CAS9	CRISPR-associated Protein 9
CBP	CREB Binding Protein
CDK2	Cyclin-Dependent Kinase 2
CHX	Cycloheximide
cIAP2	the inhibitor of apoptosis
CKI	Cyclin-dependent Kinase Inhibitor
CML	Chronic Myeloid Leukaemia
CO_2	Carbon dioxide
Co-IP	Co-ImmunoPrecipitation
CRISPR	Clustered Regulatory Interspaced Palindromic Repeats
Cul1	cullin 1
DBD	DNA Binding Domain
ddH2O	Double distilled water
DMEM	Dulbecco's Modified Eagles Media
DMSO	Dimethyl sulfoxide
DNA	Deoxy Ribonucleic Acid
dsRNA	double-stranded RNA
DTT	1,4-Dithiothreitol
E.coli	Escherichia coli
EBV	Epstein-Barr virus
ECL	Enhanced ChemiLuminescence
ED	Enhancer Domain
FBXW7α	Fbox and WD 40 repeats domain-containing 7 α

GAS	IFNγ activated sequence
H_2O_2	Hydrogen Peroxide
HCV	Hepatitis C Virus
HECT	Homologous to E6AP Carboxy Terminus
HEK293	Human Embryonic Kidney 293
HLH	Helix Loop Helix
HRP	Horse Radish Peroxidase
HTH	helix-turn-helix
IAD	Interferon-associated Domain
ICSBP	Interferon Consensus Sequence Binding Protein
IFN	Interferon
IRF	Interferon Regulatory Factors
IRF1	Interferon Regulatory Factor 1
ISGF3G	IFN-stimulated gene factor 3
ISRE	Interferon Stimulatory response Element
kDa	kiloDalton
LOH	Loss of heterozygosity
Lox	Lysyl oxidase
LXRα	Liver X Receptors
MAPKs	Activated Protein Kinases
MDS	Myeloid Dysplastic Syndrome
MEF	Mouse Embryonic Fibroblast
MHC	Major Histocompatibility Complex
Min	Minute
Ml	Millilitre
MMP3	Metalloproteinases
MRC5	human foetal lung fibroblast cells
Mt	mutant type expressing plasmid
Na3VO3	Sodium Vanadate
NaCl	Sodium Chloride
NaF	Sodium Flouride
NEM	N-Ethyl-Maleimide
NF-KB	Nuclear Factor Kappa Beta
ng	Nanogram
NLS	Nuclear Localization Signal
NP40	nonyl phenoxypolyethoxylethanol (Nonidet P-40)

OA	Osteoarthritis
OD	Optical Density
PAMPs	Pathogen Associated Molecular Patterns
PBS	Phosphate buffered saline
PCAF	p300/CBP-associated factor
pDNA	plasmid DNA
PDSM	phosphorylation-dependent SUMOylation motif
PEI	Polyethylenimine
PK-R	RNA (dsRNA)-dependent protein kinase
PRRs	pattern recognition receptors
PUMA	p53 upregulated modulator of apoptosis
RBX1	RING-box 1
RING	Really Interesting New Gene
PIAS	Protein inhibitor of activated STAT
RIPA	Radio Immuno Precipitation Assay
qPCR	Quantitative polymerase chain reaction
RLU	Relative Luciferase Units
rpm	rotation per minute
S1P	Bioactive lipid
SCF	SKP1, CUL1 and Fbox Protein Complex
SDS-PAGE	Sodium Dodecyl Sulfate-Poly Acrylamide Gel Electrophoresis
sec	Second
SENP	Sentrin/SUMOspecific protease
Skp1	S-phase kinase-associated protein 1
ssDNA	single-stranded DNA
STAT1α	signal transducer and activator of transcription
SUMO	Small ubiquitin-like modifier
TAD	Trans-Activation Domain
TBST	Tris-Buffered Saline Tween
TEMED	TetraMethylEthyleneDiamine
TGS	Tris Glycine-Solution
TLR	Toll-like receptors
TNFα	Tumour Necrosis factor alpha
TRAF6	TNFα Receptor-Associated Factor 6
TRAIL	TNFα-Apoptosis Induced Ligand
Tris-EDTA	Tris-Ethylene Diamine Tetra Acetic Acid

Ubc9	Ubiquitin-like modifiers conjugating Enzyme 9
UIM	ubiquitin interactive motifs
WCE	Whole cell extract
αMEM	α Modified Eagles Medium
Δ	Truncation or Deletion

Chapter 1

Introduction

INTRODUCTION

1.1. Interferon Regulatory Factors (IRF)

Host defence mechanisms mediate important key roles through the stimulation of an immune response to exogenous pathogens and protection against tumours (Tamura et al., 2008). The IRFs are a group of transcriptional activators mediated by viral, bacterial and IFN-induced cellular signalling. They play a fundamental role in antiviral defence, immune response, cell growth regulation and apoptosis (Barnes et al., 2002). Known members of the IRF family are IRF1, IRF2, IRF3, IRF4/Pip/ICSAT, IRF5, IRF6, IRF7, ICSBP/IRF8 and ISGF3g/p48/IRF9. Also, virus-encoded analogues of cellular IRF have been discovered (Barnes et al., 2002). All IRF proteins share a highly conserved N-terminal 120 amino acids sequence called the DNA-binding domain (DBD) (Fig 1.1) characterised by highly conserved 5 tryptophan repeats. Three of the IRF-DBD tryptophan repeats bind a specific responsive motif within the promoters of target genes (GAAA and AANNNGAA) (Escalante et al., 1998). The specific role of certain IRF members is cell type-specific, and their transcriptional activity relies on their ability to dimerize with either, other IRF family members, or other transcription factors and co-activators (Taniguchi et al., 2001). The unique C-terminal domains of IRFs determines the transcriptional specificity (Takaoka et al., 2008).

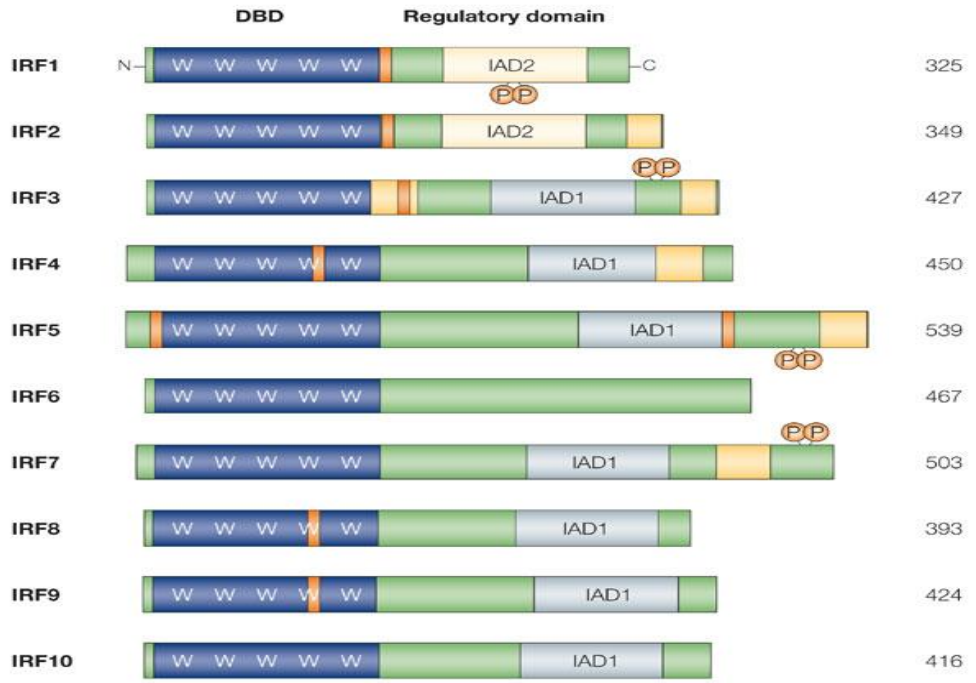

Fig 1.1. Schematic showing the structure of IRF family members.
Alignment study of the IRF family demonstrating the similarities within N-terminal region sharing a highly conserved DNA-binding Domain (DBD) where penta-repeats of Tryptophans are located. The family shows distinct differences in the position of NLS marked as orange lines and in the C-terminal domain for each member of the phosphorylated sites and their Interferon-Associated domain (IAD) or mentioned also as Trans Activation Domain (TAD). Consequently, they regulate the expression of different genes. Taken from (Lohoff and Mak, 2005).

1.1.1. IRF and Host immunity Defence

IRF1 was the first member of the IRF family to be discovered. It is constitutively expressed, activated by external stimuli and was first known as a transcriptional activator of IFN-β expression (Taniguchi et al., 2001). Its closest paralogue in the family is the IRF2 member. IRF2 is constitutively expressed and has been referred to as a repressor of IRF1 activity. It is also known to have tumourigenic activity as an oncoprotein (Harada et al., 1993b). Similarly, IRF3 is a constitutively expressed gene (Au et al., 1995). This family member varies in the fact that its Interferon-Associated Domain (IAD) is flanked by two inhibitory regulatory domains, which are unmasked during viral infection by

phosphorylation and induces the expression of IFN α and β. IRF4 is activated by T and B cells and expressed mainly in hematopoietic cell lineages. It possesses little DNA binding affinity when expressed alone (Eisenbeis et al., 1995). This IRF family member functions as a transcriptional repressor, especially in IRF1-dependent TRAIL activation (Yoshida et al., 2005). IRF5 expression is induced by IFNs, viral and DNA damage and may potentially have a role in tumour suppression (Takaoka et al., 2005). IRF6 has a critical role in controlling cell viability as IRF6-knockout mice are not viable and have severe craniofacial, dermal and limb growth retardation (Kondo et al., 2002). IRF7 is essential for type I IFN signalling, in co-operation with IRF3, although IRF3 is more predominant in the majority of cell types (Sato et al., 2000). IRF8 was first known as the Interferon Consensus Sequence Binding Protein (ICSBP), identified as a protein, which binds to the Interferon Stimulatory Response Element (ISRE), which activates expression of corresponding genes. This member of the IRF family may act as a tumour suppressor, as IRF8-null mice are vulnerable to developing CML (Chronic Myeloid Leukaemia) (Holtschke et al., 1996). Its DBD activity is weak. However, heterodimerization with IRF1 appears to overcome this issue (Taniguchi et al., 2001) as discussed below. IRF9 is a critical part of the IFNγ-Stimulated Gene Factor 3 (ISGF3) complex, in association with p48 and STAT1 homodimers which binds to ISRE and activates expression of correspondent genes (Majumder et al., 1998). IRF10 was identified in chickens and is absent in humans and mice (Nehyba et al., 2002). It binds to the ISRE of the MHC class I promoter. Both IRF1 and IRF10 have some of the same functional characteristics. However, IRF10 plays a role in the late stages immune

response by regulating the expression of some of the IFN target genes, in the absence of a cytotoxic effect (Nehyba et al., 2002). Elucidating the molecular mechanisms by which the IRF family controls these vital cellular activities has been proposed as an excellent pathway to developing immunotherapies (Nguyen et al., 1997).

1.1.2. Oncogenesis Regulation by IRF

Induced IRF1 expression activates target genes, leading to inhibition of cell proliferation and stimulation of cell apoptosis (Lohoff and Mak, 2005). For instance, the transcriptional induction of the gene encoding p21 (WAF1, CIP1), a cell cycle inhibitor, was found to be dependent on both IRF1 and p53, and the p21 promoter indeed contains functional IRF1 and p53-binding regions. This area is covered below in detail. IRF2 binds to the same DNA sequences as IRF1 but downregulates or blocks the activation of these IRF1 target genes. Accumulating evidence indicates that IRF1and IRF2 have anti-oncogenic and oncogenic potentials, respectively (Tanaka and Taniguchi, 2000). The correlation of IRF4 and oncogenesis has also been reported in Epstein-Barr virus (EBV)-transformed lymphocytes and HTLV-1-induced leukemogenesis (Mamane et al., 2002; Xu et al., 2008). Notably, IRF4 alone is not sufficient for oncogenesis in transgenic mice overexpressing IRF4 in lymphocytes, but it has been proposed that IRF4 may regulate cellular growth by targeting pro-apoptotic IRF5 during EBV transformation (Barnes et al., 2003). IRF6 may also act as a tumour suppressor via its interaction with maspin, a tumour suppressor gene (Bailey et al., 2005). Also, IRF8 has been revealed to exhibit antitumour activity through direct control of cell growth, differentiation, apoptosis and modulation of the immune system's anti-tumour activity (Deng and Daley, 2001). Together, these observations indicate that the IRF family is important in different Tumour types. So we are going to focus mainly on IRF1 as a tumour suppressor proteins and explore some aspects of its regulation.

1.2. *IRF1* gene

The human IRF1 gene is located in 5q31.1, detected using fluorescence *in situ* hybridization (Fig 1.2). The 5' regulatory area possesses GC-rich sequences and consensus binding elements for well-defined transcription factors, such as NF-ϰB. Interestingly, an IRF binding sequence was discovered within the IRF-2 promoter, and IRF1 expression reflects the level of expressed IRF-2. IRF1 has a single well-defined transcript, according to the NCBI database.

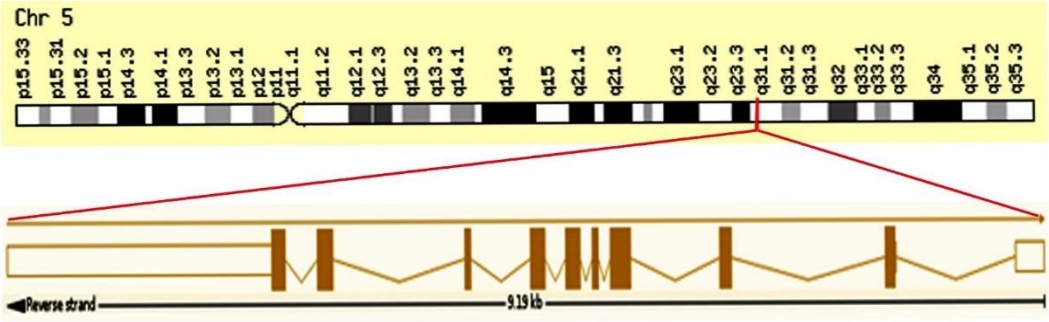

Fig 1.2. Schematic of chromosome 5 and the IRF1 gene Structure.
IRF1 gene is located in chromosome 5 q3.1.1. The Gene sequence locus consists of 10 exons, as gold boxes and 9 introns, shown as connecting lines. The translated region starts from the second exon. Data was taken from NCBEI and Ensemble (website mentioned at the end of References section).

1.2.1. *IRF1* gene Null Homozygous Mutant and Heterozygosity

An interstitial deletion inside chromosome 5q causes cytogenetic malformations, resulting in human leukaemia and myelodysplasia; The IRF1 tumour suppressor gene resides in 5q31.1 (Fig 1.2). When this gene is deleted in one or both alleles, it causes leukaemia and myelodysplastic syndrome (Deng and Daley, 2001). The inactivation of one or both IRF1 alleles and deletion of the other allele was discovered to occur in acute leukaemia patients. The loss of heterozygosity (LOH) increases tumour susceptibility as shown in Fig 1.3. Homozygous null mutants of IRF1 exhibit slow tumour

development in comparison with more tumourigenic induction with c-Ha-ras transgene or by knockout of p53, as evidence from mice, shows a higher mutation predisposition in the two latter cases (Nozawa et al., 1999). The activation of p53 activity for cell cycle arrest via its acetylation by p300 is indirectly activated by IRF1 (Dornan et al., 2004).

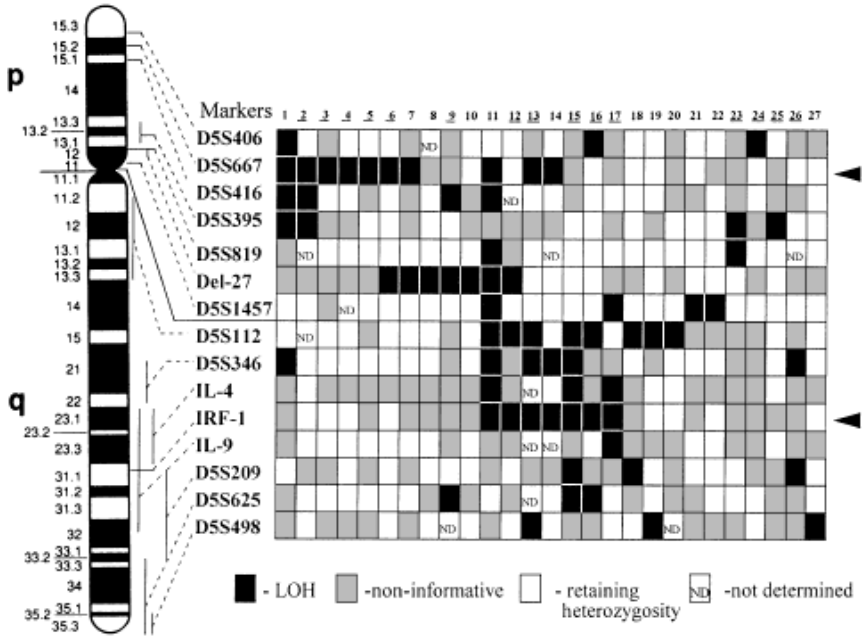

Fig 1.3. Loss of Heterozygosity in Chromosome 5.
The underlined numbers (1–27) represent Oesophageal carcinoma under LOH. Underlines represent squamous cell carcinoma. Arrowheads indicate the regions with frequent deletions in the panel of Examined Oesophageal carcinoma (Peralta et al., 1998).

1.3. Regulation of *IRF1* Expression

IRF1 is constitutively expressed within the cell; its expression level is a balance between its degradation and *de novo* synthesis with a short half-life (20~40 minutes). IRF1 needs activation or induction before it becomes functional in oncogenesis or an immune response. This gene is highly induced by IFN, viral double-stranded RNA (dsRNA), cytokines and particular hormones (Chen et al., 2013), (Pion et al., 2009).

1.3.1. Bacterial and Viral Infection

The transmembrane Toll-Like Receptors (TLR) and the IFN-inducible double-stranded RNA (dsRNA)-dependent protein kinase (PK-R) represent two types of pattern recognition receptors (PRRs) which has antimicrobial effect through the detection of viral Pathogen Associated Molecular Patterns (PAMPs), such as the lipopolysaccharides of bacteria and the nucleic acids of viruses. This results in the IRF1-dependent gene expression through indirect binding with ISRE (Pflugheber et al., 2002). TLRs stimulates NF-ϰB and Mitogen Activated Protein Kinases (MAPKs), which are essential for the cell's antiviral activity (Harikumar et al., 2014). Also, the accumulation of other viral components such as, Hepatitis C Virus (HCV) dsRNA, stimulates the IFN system which is activated by PK-R (Pflugheber et al., 2002).

1.3.2. Retinoic Acid.

Retinoic acid and IFNγ induces the IRF1 gene to regulate the expression of TNFα-Related Apoptosis Ligand TRAIL), and this induces apoptosis (Clarke et al., 2004). The experiments carried out to reveal this used a breast cancer cell line where the activation of chromatin acetylation and overexpression of TRAIL-dependent IRF1 occurs. Meanwhile, the overexpression of RA (Retinoic acid) and IFNγ in control cells does not induce TRAIL expression. This led to the conclusion that RA plays a synergistic role with the IFN machinery to converge coactivators on the IRF1 promoter, leading to TRAIL overexpression in cancer cells (Clarke et al., 2004).

1.3.3. STATs

IRF1 is induced and overexpressed in an indirect manner by IFNs, which activate STAT1, resulting in its binding to the IRF1 promoter at the IFNγ activated sequence (GAS). The expressed IRF1 may positively activate the STAT1 expression as a positive feedback. Subsequently, IRF1 activates a caspase 8 pathway that triggers apoptosis (Chen et al., 2013). Reported literature reveals that INFα/γ fail to induce the transcriptional expression of the IRF1 gene in the absence of STAT1 (Dou et al., 2014). Heterodimer formation between STAT1/2 has been found to activate IRF1, primarily through IFNα/γ activation of STAT1 and STAT2, which bind to the p48 protein to form a DNA-binding protein with IRF9 as a complex (ISGF3) (Li et al., 1996).

1.3.4. Tumour Necrosis Factor (TNFα)

TNFα or IFNγ are stimulated by the activation of the Interferon Receptor II (IFNRII) and Janus kinase and signal transducer and activator of transcription

(JAK/STAT1) signal cascade. This leads to the activation of GAS in the promoter of IRF1, leading to its overexpression and the induction of cellular processes, such as the activation of natural killers (NK cells) (Park et al., 2007; Taniguchi et al., 2001). TNFα with IFNγ increases the basal level of IRF1 expression and nuclear translocation in 15 different melanoma cell lines, as revealed by ImageStream IDEAS analysis software (Murtas et al., 2013). Also, it has been found that overexpression of TNFα and IL1 lead to increased levels of IFNβ and IRF1 mRNA expression (Fujita et al., 1989).TNFα and IFNγ invoke apoptosis in lipopolysaccharide-induced liver injury through IRF1 induction (Lee et al., 2007).

1.4. IRF1 Protein Structure

As shown in Fig 1.4, IRF1 contains:

1.4.1. DNA Binding Domain (DBD)

The N-terminal contains the initial 120 amino acids sequence called the DNA-binding domain (DBD) as shown in Fig 1.3 which is characterised by 5 conserved tryptophan repeats. Three of them bind specifically through the formation of a helix-turn-helix (HTH) as a structural motif, which mediates binding with target genes (GAAA and AANNNGAA) (Escalante et al., 1998). The research group of Kirchhoff et al., (2000), found that the first 60 amino acids of DBD is responsible for the inhibitory action on IRF1 activation as a regulatory sequence and truncation studies for these 60 amino acids resulted in same IRF1 transcriptional activity activity as the IRF1 TAD 185-256 amino acids activated motif does. They also have carried out further investigation into whether the DBD binding to its normal element is affected by this inhibitory

domain, and the conclusion is that these 60 amino acids have no effect on IRF1-DNA binding.

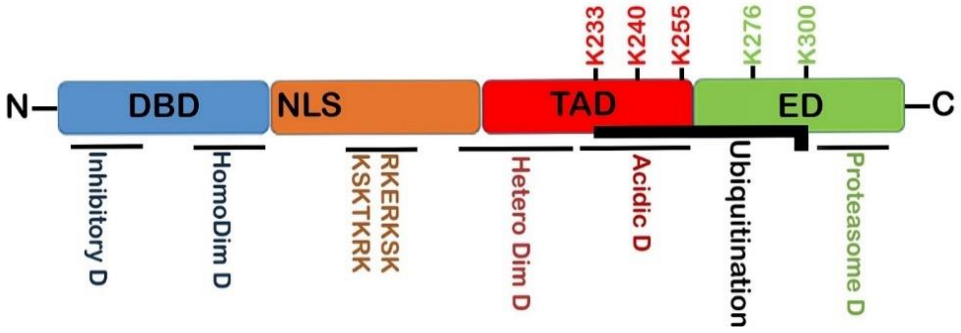

Fig 1.4. Schematic Shows IRF1 Protein and C-terminal Lysine Amino Acids.

DBD contains the inhibitory domain of IRF1 activity and homodimerization domain. NLS possesses two motifs that are responsible for nuclear localization of IRF1 within nuclear pores. The heterodimerization domain with ICSBP (IRF8) resides between NLS and TAD. TAD has three lysines that might be necessary for ubiquitination as acceptors. ED has a role in ubiquitination signalling and proteasome detection domain.

1.4.2. Nuclear Localization Signal (NLS)

NLS contains two potential sequences which direct the nuclear localization ; RKERKSK and KSKTK-RK and the role of them are to translocate the protein from the ribosomal cytoplasm to nuclear pores (Dou et al., 2014).

1.4.3. Trans-Activation Domain (TAD)

The Trans-Activation Domain (TAD) resides at the C-terminus of IRF1 (aa 185-256) and forms a Helix-loop-Helix (HLH) which is critical for activity, Kirchhoff et al., (2000) has shown IRF1 region between 185-256 comprises two central regions; (185-220) and an acidic motif (221-256) amino acids. TAD has an intrinsic activity equal to that of the full-length IRF1, but not other IRF1 domains.

1.4.4. Enhancer Domain (ED)

The IRF1 C-terminus possesses a 70 amino acid domain which increases the transcriptional activity of IRF1 10 fold. It stabilises the transcriptional activity of IRF1 . However, it possesses no intrinsic transcriptional capacity. This area is regulated by its sub-domains as follows, p300 binding domain which is required for enhanced transcription as a co-factor for p300 and PCAF transcriptional activity which in turn improves the acetylation of other transcriptional factors such as p53. The second sub-domain is a negative regulatory suppressor of the transcriptional activity. Additionally, the repressor sub-domain required for IRF1 mediated repression of Cyclin-Dependent Kinase 2 (CDK2) (LXXLL) which is necessary for IRF1 growth inhibition activity (Pion et al., 2009). Then ED has a role in regulating the protein stability and its c-terminal 25 amino acids are involved in the delivery of the IRF1 to proteasome degradation, the adjacent upstream region of the enhancer domain (255-300 amino acids) contains residues that are subjected to ubiquitin modification. The enhancer domain area includes the degradation motif and an ubiquitination signal (Pion et al., 2009). Another research group revealed that the truncation of the last 39 amino acids stabilised IRF1 protein in comparison to full IRF1 (Nakagawa and Yokosawa, 2000).

1.5. Post-Translational Modification by ubiquitin

Ubiquitin is a highly conserved polypeptide (76 amino acids) (Fig 1.5), which ligates to other functional target proteins to primarily bring them to the 26S multi-compartmentalised proteasomal degradation (Welchman et al., 2005).

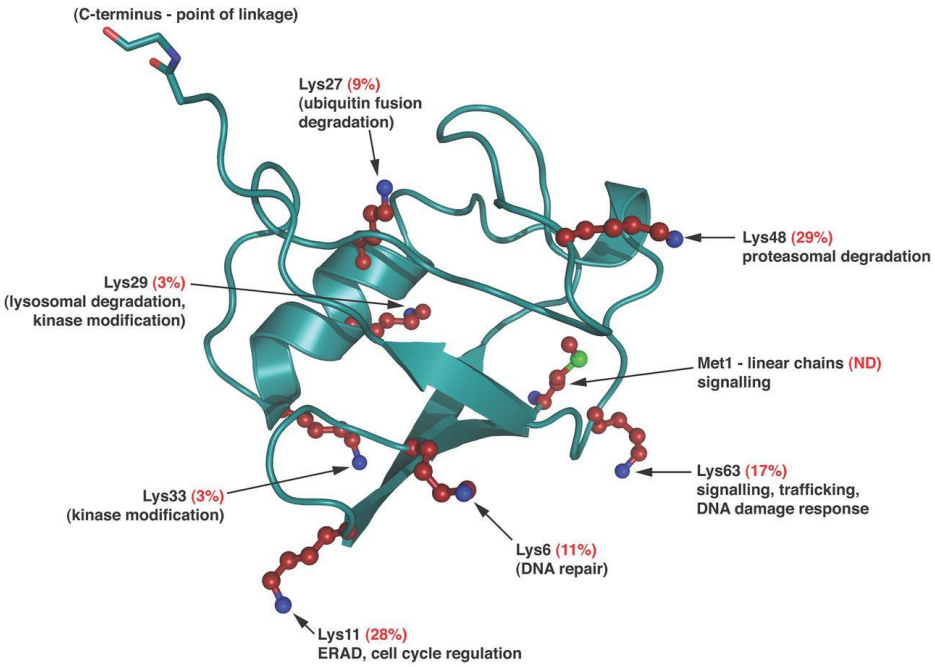

Fig 1.5. Ribbon structure of ubiquitin.

The Fig shows the ubiquitin highly conserved crystal structure with its C-terminus point of attachment (Gly76) and 7 lysine residues at which it can form different polyubiquitination (Komander, 2009).

The covalent ligation of ubiquitin to a substrate does not exclusively lead to a substrate degradation; it also covers a broad spectrum of different activities (Li and Ye, 2008). Ubiquitin binds to its target protein via formation of an isopeptide bond between ubiquitin C-terminal Gly76 and any Lysine (K) which resides on the target protein.

1.5.1. Ubiquitination requires Enzymatic Cascade.

The ubiquitination process involves an enzymatic cascade (Fig 1.6). Ubiquitin C-terminal Glycine forms a thioester bond with Cysteine residue on E1 activation enzyme, followed by its transfer to the conjugation enzyme E2, and finally, ubiquitin is ligated to an E3 Ligase multifunctional enzyme that ligates ubiquitin to the target protein. ubiquitin modifies its substrate through the formation of the isopeptide bond between ubiquitin C-terminal G76 and target protein lysine residue (Thrower et al., 2000). The diversity of polyubiquitination functionalities derives in part from the specificity of E3 ligases. E3 ligases are categorised into three main families; Homologous to E6AP Carboxy Terminus (HECT), Really Interesting New Gene (RING) domain which is larger in its size, and UFD2 homology (U-box) proteins. There is an important class of RING E3s, defined as SCF E3s (Pickart and Eddins, 2004) as discussed below. The mechanism of HECT E3 is unique and acts as a true enzyme through the formation of an intermediate thiol bond via its Cysteine residue with ubiquitin itself before transferring it to the substrate (Scheffner et al., 1995), as such ubiquitination occurs in two steps (Fig 1.6). RING E3s contains short, rich domains with cysteine and histidine residues with two zinc molecules which give a globular groove rigid conformation for the ligase. This hydrophobic groove carries the possibility to react with E2 enzyme without dealing with ubiquitin itself. In other words, it acts as a scaffolding machinery to transfer ubiquitin to the target substrate without forming any linkage with ubiquitin and yield a faster ubiquitination process than the intermediate formed by HECT (VanDemark and Hill, 2002).

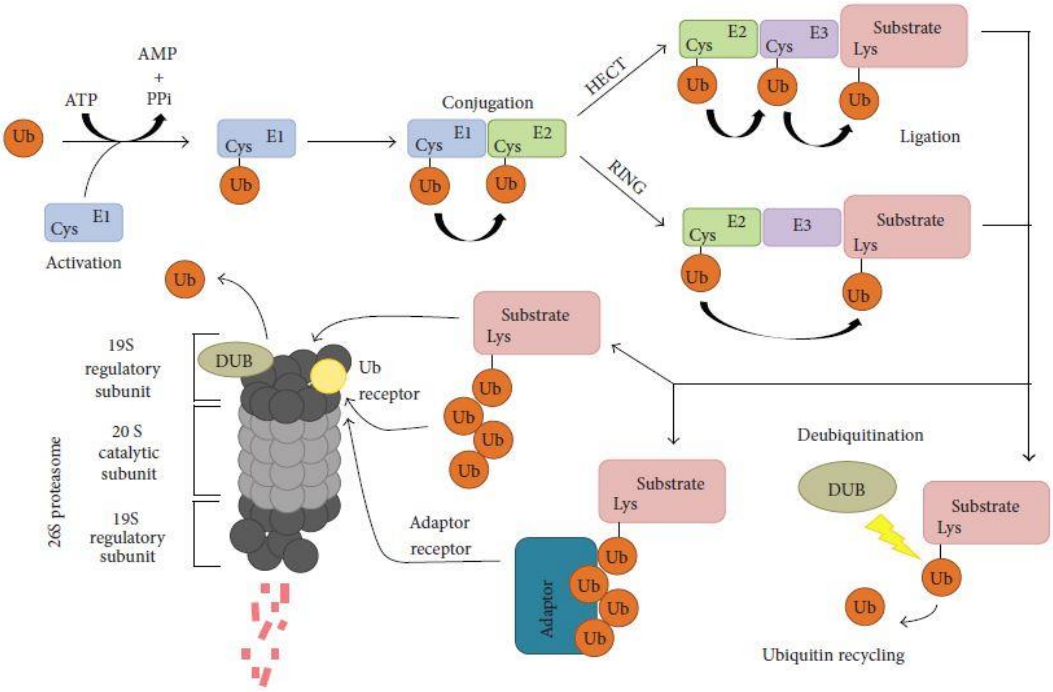

Fig 1.6. Schematic ubiquitination Process, Different E3 Ligases and Proteasome.

Ubiquitin is activated in an ATP-dependent manner with a sequential enzymatic cascade (E1, E2, and E3). **E3** may be HECT, which acts as a real enzyme, or RING which acts as a scaffolding protein. The fate of ubiquitinated substrate carries three possibilities. First is to be deubiquitinated by deubiquitination (DUB) enzymes. Second to bind with an adaptor to do more functions followed by substrate proteasome degradation, or to bring the substrate protein directly to the proteasomal degradation through the identification of ubiquitin by ubiquitin Interactive Motif (UIM) on 19S proteasome cap. Proteasome contains a catalytic 20S core particle structure and two 19S regulatory caps which together are termed the 26S proteasome (Lin and Man, 2013). **The proteasome** cylindrical stack of four 7-membered rings (20S) contains a narrow chamber that has no ability to digest large folded proteins. As such, before the internalisation of the protein, denaturation occurs at the first separated rings of unfolded polypeptides to that narrow chamber to hydrolyze small polypeptides and denaturate large proteins to release amino acids for cytoplasm for recycling of these amino acids (Thrower et al., 2000).

1.5.2. The E3 Ligase (SCF) SKP1, CUL1 and Fbox Protein Complex

One of the most complex RING E3 structure is SCF1 and SCF 2 (Skp1-Cul1-Fbox) and (Skp2-Cul1-Fbox) as illustrated in Fig 1.7. The SCF complex is composed of cullin 1 (Cul1) the long scaffolding part which interacts with Skp-1 on the C-terminus and RBX1 on the N-terminus. S-phase kinase-associated protein 1 (Skp1) binds to a specific part that carries the substrate. RING-box 1 (RBX1) possesses the motif for docking the E2~ubiquitin complex, and an Fbox domain for the attachment of Skp-1 protein and also carries the target substrate to be ubiquitinated (Orlicky et al., 2003).

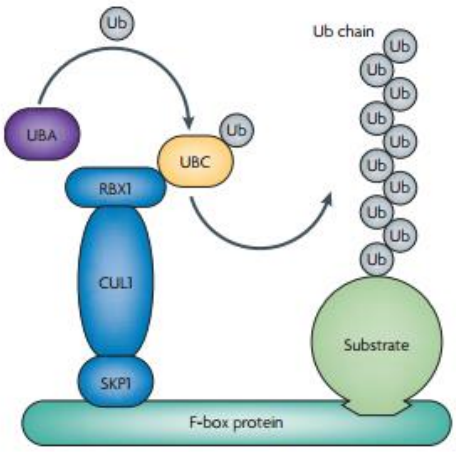

Fig 1.7. Schematic Diagram of SCF E3 enzymes.

SCF is a complex of SKP1, CUL1 and F-box proteins that act together to bring about substrate ubiquitination. CUL-1 (Cullin Protein) is the scaffolding part that binds with Skp1 and RBX1 from both sides. RBX1 (RING-box1) which possesses motif for docking the E2~ubiquitin complex, Skp1 (S-phase kinase 1) owns an Fbox domain. Fbox protein possesses different motif to recruit substrate protein for ubiquitination (Welcker and Clurman, 2008).

Either Fbox WD40 domains or leucine-rich repeats mediate substrate recognition by Fbox. As such, Fbox proteins are classified into Fbox (WD40)

or Fbls (Fbox Leucine-rich repeats), respectively (Welcker and Clurman, 2008).

1.5.3. Fbox and WD 40 repeats domain-containing 7 α (FBXW7α)

FBW7α is an Fbox protein that binds to central regulators of cell division and growth, including cyclin-E, MYC, JUN and Notch. Most FBW7 substrates are proto-oncogenes that are broadly implicated in the pathogenesis of human cancers (Welcker and Clurman, 2008). FBW7 binds to its substrates after they have been phosphorylated within conserved phospho-degron motifs (Fig 1.8). Substrate phosphorylation is highly regulated. Most substrates are phosphorylated by glycogen synthase kinase 3 (GSK3), or a mitogen-regulated kinase. FBW7α is a tumour suppressor, and loss of FBW7 function leads to chromosomal instability, probably owing to the hyperactivation of its many oncogenic substrates (Welcker and Clurman, 2008).

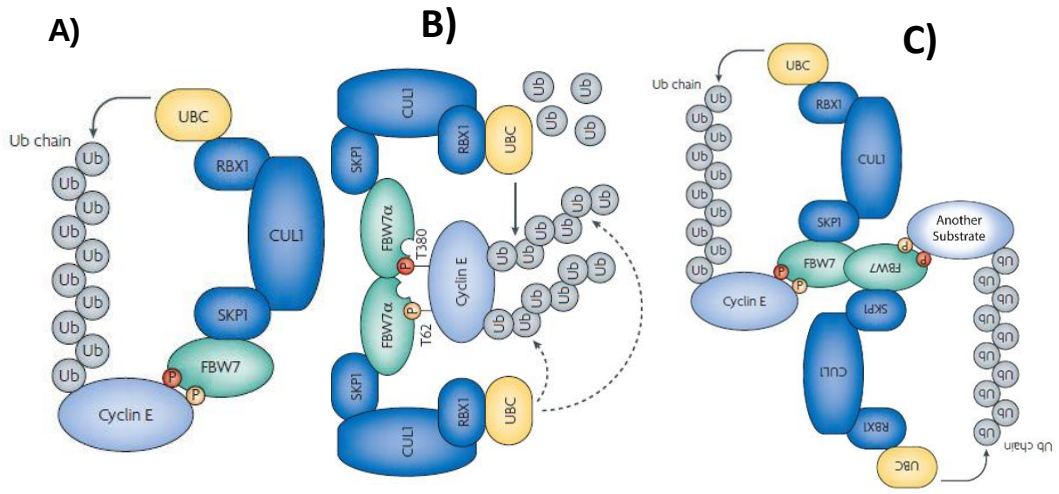

Fig 1.8. Schematic of E3 SCF binds to phosphorylated Cyclin E.

Models of different substrate cross ubiquitination by E3 complex and dimerization. Independently whether one or two substrates, bind to this dimer. It is possible that the lysine(s) in the area of the phospho-degron link to one SCF presented more optimally to the E2 active site of the adjacent SCF. As such, the improvement in the rate of ubiquitination and ubiquitin polyubiquitination may be enhanced by dimerization (Hao et al., 2007). **(A)** The diagram shows that FBXW7 binds to certain phosphorylated sites on the surface of its substrate. Such as Cyclin E, to bring about ubiquitination. **(B)** The diagram shows that FBXW7 carries the possibility to be dimerized on the same candidate substrate phosphor-degrons, which allow further ubiquitination of the substrate. **(C)** Dimerization of two complexes of FBXW7 to mediate ubiquitination of different substrates. Pictures were taken and optimised from (Welcker and Clurman, 2008).

1.5.4. Types of polyubiquitination Linkages

The current model suggests that target proteins are modified by a variety of ubiquitin post-translational modifications, and this depends on the functional flexibility of this post-translational modification that controls the formation of ubiquitin polymers, which encodes different signals (Li and Ye, 2008) (Fig 1.9). Mono-ubiquitination is the addition of one ubiquitin molecule to the target protein as a tag for endosomal detection and DNA-repair trafficking. Multi-ubiquitination indicates that several lysine residues on candidate substrate are mono-ubiquitinated (multi-mono-ubiquitination) which leads to multifunctional

signalling such as endocytosis and degradation (Haglund et al., 2003). Whereas polyubiquitination is the binding of several ubiquitin molecules to a single lysine residue on the target protein (Welchman et al., 2005). The reason behind the polyubiquitination at the same lysine residue that the ubiquitin itself has 7 lysine amino acids; K6, 11, 27, 29, 33, 48, and K63 (Fig 1.9.A). This allows the formation of isopeptide bonds between ubiquitin C-terminal G76 residue and another lysine residues of other ubiquitin molecules (Welchman et al., 2005). Polyubiquitination has been extensivelystudied and according to the type of polyubiquitination, the cellular mechanism of the ubiquitinated substrate is defined, as follows. A well-accepted theory that K48-polyubiquitination targets proteins for proteasomal degradation (Pickart, 1997). Whereas K63-polyubiquitination brings proteins to at least 4 non-proteolytic molecular mechanisms; cellular signalling, intracellular trafficking, biogenesis of ribosomes, and DNA-damage repair (Li and Ye, 2008; Chan and Hill, 2001; Kerscher et al., 2006). Beside those, K6-polyubiquitination which targets protein for the DNA-repair mechanism.

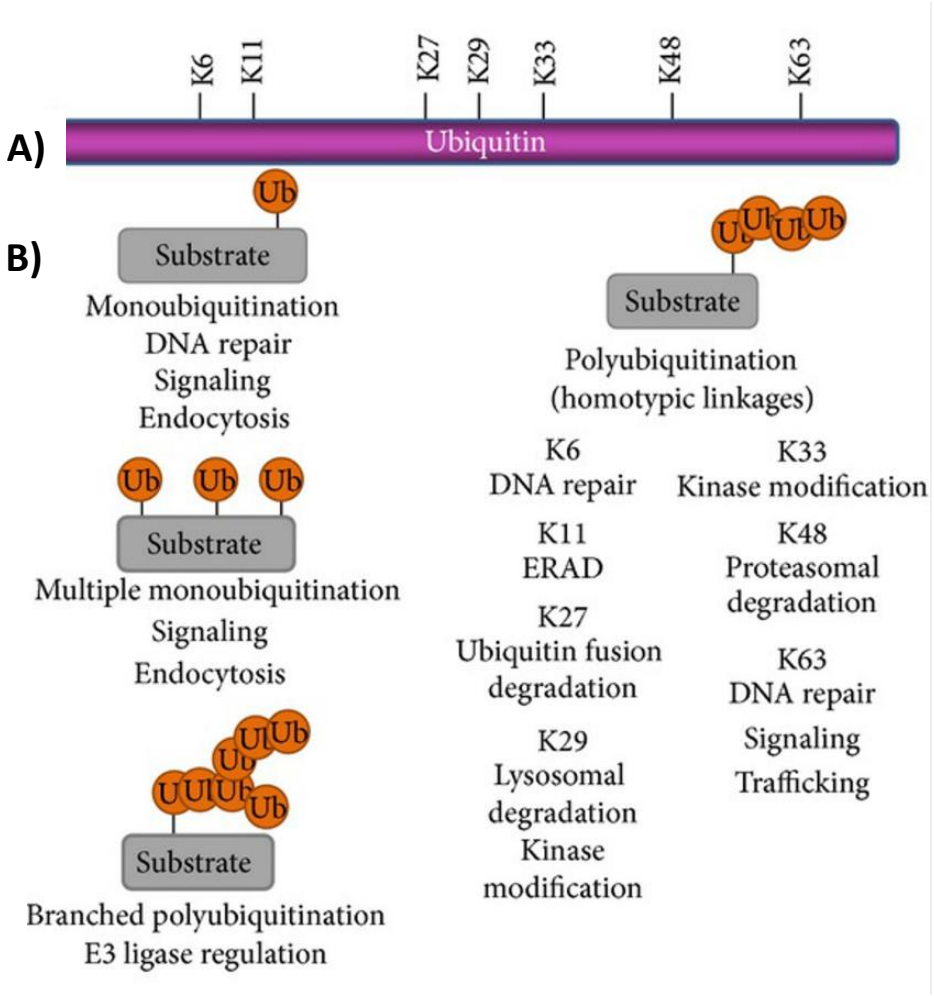

Fig 1.9. Schematic Diagram of ubiquitin and different types and functions of ubiquitination.

(A) Schematic Diagram shows Lysine residues reside within the ubiquitin structure that forms another isopeptide bond with ubiquitin, which leads to the formation of different polyubiquitination forms. **(B)** The various types of ubiquitin linkages (mono-ubiquitination, multi-mono-ubiquitination, or polyubiquitination either closed or branched chains) and their relative substrate cellular fate. The diagram was taken from (Lin and Man, 2013).

1.6. SUMOylation of Proteins

Small ubiquitin-like Modifier (SUMO) family of proteins that ligates with other proteins to affect various cellular mechanisms, such as apoptosis, protein stability, regulation of transcription, cell cycle progression and other functions (Hay, 2005). In humans, there are four SUMOylated protein paralogues: SUMO1, SUMO2/3, and SUMO4. There is a similarity between SUMO2, SUMO3, and SUMO4, however, SUMO4 shows a small difference in residue 90, where proline replaces glutamine, and this drives the intervention of SUMO4 in cellular processes of protein modification only when the cell is under starvation stress (Wei et al., 2008). SUMO family targets proteins within a hydrophobic consensus motif up to 80 % of SUMO modifications have been detected within this motif ψKxD/E (where ψ is a large hydrophobic residue), and K is a Lysine residue which allows the SUMO protein to form an isopeptide bond with its target substrate. However, non-consensus motifs can act as SUMO acceptors (Wilkinson and Henley, 2010). The ability of SUMO proteins to form chains depends on the presence of internal consensus sequences residing in the SUMO protein. SUMO2/3 have more than one consensus sequence. However, SUMO1 has no consensus sequence. Hence, SUMO1 has no ability to form a polySUMO1 chain. However, SUMO1 can take part in other SUMO2/3 chains resulting in *in vivo* chain termination (Geoffroy and Hay, 2009) and (Matic et al., 2008). Also, SUMO1 acts as a secondary signal to modify the substrate, followed by the chain ubiquitination and finally leads to proteasomal degradation and this is individually connected to the presence of SUMO-targeted ubiquitin ligases (Wilkinson and Henley, 2010).

1.6.1. Molecular consequences of SUMOylation

The molecular effects of SUMO modification are complex. SUMOylation promotes interactions with proteins that contain a SUMO Interactive Motif (SIM), which in turn may influence the transcriptional activity and subcellular localization. SUMO might interact with the substrate binding site as shown in Fig 1.10 and blocks other proteins from the modification of the same position. SUMOylation has the possibility to create a new interface to allow other proteins partners to be recruited to modify this substrate protein in the presence of SUMO protein. It may also introduce conformational changes at the moment of its substrate binding and form a new environment for another partner to modify the substrate in tandem with SUMOylation (Wilkinson and Henley, 2010).

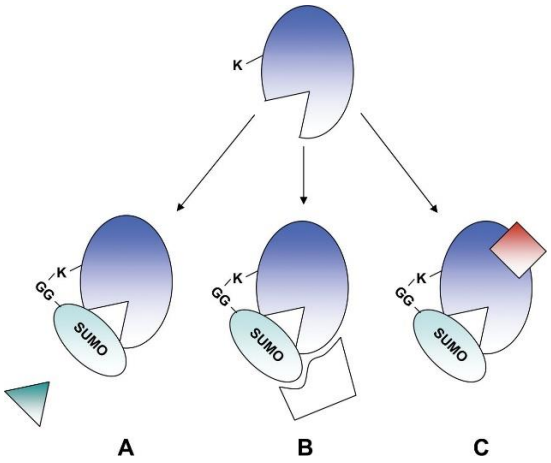

Fig 1.10. Molecular outcomes of direct substrate SUMOylation.

(A) SUMOylation might block the interactive site, **(B)** SUMOylation might form a new interface for other partner recruitment, **(C)** SUMOylation might change the dimensional structure of the substrate permitting another partner for attachment (Wilkinson and Henley, 2010).

1.6.2. SUMOylation may require Phosphorylation

Certain motifs located in the target substrate are known to enhance the phosphorylation-dependent SUMOylation motif (PDSM) defined as ψKxExxSP, whereas (ψ) is a hydrophobic residue, followed by Lysine to be SUMOylated and then directed SUMOylation in the presence of phosphorylatable serine amino acid. This motif is present in proteins such as the transcription factors HSF1 and MEF2A. In each candidate, the negative phosphate group charge conferred by phosphorylation of the serine residue enhances SUMOylation of substrate lysine (Wilkinson and Henley, 2010). IRF1 ψKxExx hydrophobic consensus sequence that might be SUMOylated (DFSC**K**EEPEID**SP**GDIGLS) carries the possibilities to follow this rule.

1.7. Similarities and Differences of SUMO and ubiquitin

SUMO1 has only 18% similarity with the ubiquitin structure and follows the enzymatic cascade with different E1, E2, and E3 enzymes (Nakagawa and Yokosawa, 2002). They have various functions within the cell (Gill, 2004). SUMO1 has an N-terminal domain that is absent from ubiquitin and requires activation before through the cleavage of C-terminus to expose di-Glycine amino acids for consensus lysine motif by Sentrin/SUMO-specific Protease enzymes (SENP). After cleavage, an enzymatic cascade proceeds to SAE1/2 (analogue of E1 activation enzyme), followed by the only well-known E2 Conjugating enzyme for SUMO1 (Ubc9) which directly binds to the substrate consensus sequence. E3 for SUMOylation called Protein inhibitor of activated STAT (PIAS) which functions similarly to the RING E3 ligase (Wilkinson and

Henley, 2010). RING and HECT were mentioned to be involved in ubiquitination, whereas only RING is involved in SUMOylation (Wilkinson and Henley, 2010).

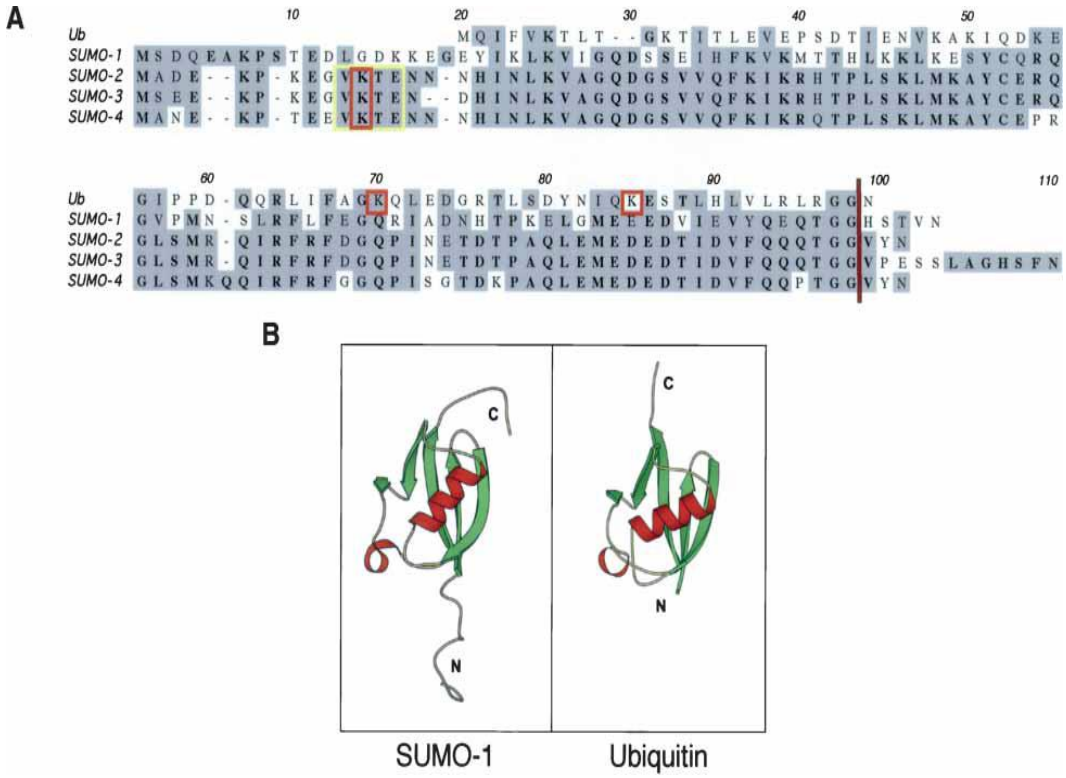

Fig 1.11. SUMO is Structurally Similar to ubiquitin.

(A) Amino acid maps alignment of ubiquitin and the 4 human SUMO variants. **(B)** Ribbon diagram of SUMO1 and ubiquitin where N-terminal at the sequence of all SUMO family not in ubiquitin, and C-terminal of SUMO1 needs cleavage and proline 90 at SUMO4 also is marked white (Gill, 2004).

1.7.1. Cross-Talk between ubiquitin and SUMO

The ubiquitination of any enzyme required in the cascade of SUMOylation machinery may lead to the inhibition of SUMOylation and as such degradation of the substrate protein. For example, ubiquitination of SUMO Activating E1 (SAE1) brings it to degradation and inhibits the anti-apoptotic GAM-1 substrate SUMOylation. Also, ubiquitination of SUMO E3 ligase leads to its degradation,

and this inhibits Parkin substrate protein SUMOylation which is important for Alzheimer's disease.(Wilkinson and Henley, 2010).

1.8. IRF1 Protein-Protein Interactions

IRF1 has interplay with other IRF member family; IRF2 is constitutively expressed and has been referred to as a repressor of IRF1 activity as it competes for the same binding target gene promoters as IRF1 (Harada et al., 1993a). Also, IRF4 competes with IRF1 dependent TRAIL activation (Yoshida et al., 2005). Moreover, IRF9 forms a complex with p-STAT1 to activate IRF1 as IFN-stimulated gene factor-3 (ISGF3) complex that binds to ISRE. In terms of dimerization between IRF1 itself or other IRFs as a heterodimer, it was found that IRF1 can form a homodimer with another IRF1 within the motif resides at the end of the DBD (90-115 amino acids). Also, IRF4 itself has a weak binding to DBD unless heterodimerization with IRF1 occurs to enhance the DBD binding of IRF4, in addition, IRF1 is well known to heterodimerize with IRF8 through binding of IRF8 within the Interferon Consensus Sequence Binding Protein (ICSBP) (Taniguchi et al., 2001). IRF1 can interact with other proteins apart from IRFs. It shows an ability to bind with the Hsp70/90 chaperone (Narayan et al., 2011). IRF1 also shares an important role in the acetylation of other proteins e.g. H4 lysine amino acids in Systemic Lupus Erythematosus (SLE) (Leung et al., 2015). IRF1 can also act as a coactivator for a broad range of proteins, such as p300, CBP and PCAF through p300 binding to the IRF1 C-terminal ED. IRF1 is also known to be phosphorylated as well on its C-terminal which is necessary for activity (Russell, 2013). Moreover, IRF1 is regulated post-translationally through its interaction with

Small ubiquitin-like Modifiers (SUMO), Protein inhibitor of activated STAT (PIAS) family and ubiquitin (Nakagawa and Yokosawa, 2002).

1.8.1. IRF1 Degradation

ED possesses a ubiquitination signal but does not include a ubiquitin acceptor. Because the mutated IRF1 (K276/K300) was substituted with Arginine to terminate their susceptibility for ubiquitination. The result did not change the ubiquitination profile compared with IRF1 WT. Also, the ED possesses an E3 ligase or related component motif which mediates the interaction of IRF1 with E3 ligase to recruit ubiquitination machinery outside the ED. The first motif of IRF1 ED 25 amino acids, especially 301-311 amino acids residues is required for the recognition of polyubiquitinated IRF1 by the proteasome (Pion et al., 2009).

1.8.2. IRF1 cellular Signalling

Studies conducted by Harikumar et al., (2014), found that IRF1 is essential for Interleukin1 (IL1) induced expression of chemokines *CCL5 and CXCL10* which recruit other cells to the site of sterile inflammation. The critical step that controls this signalling is the post-translational modification of IRF1, including K63-polyubiquitination and phosphorylation. The research group showed that, as a response to IL1 activation, newly synthesised IRF1 underwent K63-polyubiquitination by the interaction of other factors, such as Inhibitor of Apoptosis (cIAP2) which activates NF-kB, and Sphingosine kinasE1 (SphK1) which enhances E3 ligase activity of (TRAF6) and generates Bioactive lipid (S1P). They concluded that IRF1 N-terminal lysines (K75-K78-K95-K101) underwent K63-polyubiquitination, revealed by IRF1 K-R multi-mutations. The ability of those lysine residues to keep the level of IRF1 measured reporter activity as IRF1 WT was significantly noticed. Additionally, K48-polyubiquitination was conducted in this study, and they revealed that K48-

polyubiquitination is not involved in the cellular signalling of IL1 dependent IRF1 activation.

1.8.3. Direct SUMO1-IRF1 Modification

SUMOylation of IRF1 requires an enzymatic cascade, and this was revealed in the research conducted by Nakagawa and Yokosawa (2002). They mentioned that PIAS3 on IRF1 protein binding that mediates SUMO1-ylation through its action as SUMO1 ligase and the final protein-protein interaction resulted in the repression of transcriptional activity of IRF1. Studies have been carried out using different cell lines; that concluded that human K275 (mouse K276) is the primary SUMOylation site within IRF1 *in vivo*, and K275, K299 *in vitro* (Park et al., 2007). Overexpression of IRF1 WT with SUMO1 showed higher stability and a gradient decrease in luciferase reporter activity, which is an experimental method to quantify the relative transcriptional activity of any reported gene, with gradient increased SUMO1 overexpression. Whereas mutants of IRF1 (K275R, K299R) showed increased luciferase reporter activity compared with WT IRF1. Those mutations terminated the ability of the protein to be ubiquitinated correctly, concluding that SUMO1 and ubiquitin are competing on the same sites.

Overexpression of SUMO1 with IRF1 WT inhibits p21 (Park et al., 2007). IRF1 is exposed to SUMO1 modification through the interaction with its TAD, assuming that there is SUMOylation outside the hydrophobic (ψKxExx) consensus motif, and TAD of IRF1 is sufficient for SUMO1 binding with IRF1. SUMO1 does not target IRF2 for post-translational modification (Kim et al., 2008). The same group revealed, by GST pulldown assay, that Ubc9 is an interactive protein with IRF1 mainly through binding with its DBD and TAD.

This type of protein-protein interaction leads to co-localization of SUMO1-IRF1 in the nuclei of the cell. Intriguingly, Ubc9 is important for SUMOylation of IRF1 *in vivo* in tumourigenesis of ovarian cancer (Park et al., 2007).

SUMO1 appeared to be observed only under stress therefore the endogenous SUMO1 cannot be detected without *in vivo* overexpression, not only that but SUMO1ylated IRF1 cannot be detected without Ubc9 overexpression *in vitro* (Kim et al., 2008). It is indicated that the ubiquitination and SUMOylation residues in the IRF1 are the same. Consequently, SUMO1-IRF1 shows significant resistance to degradation, but also this sumoylated protein inactivates IRF1 tumour suppressor activity (Park et al., 2007). Moreover, it also gave an idea that there is a relationship between ubiquitination and transcriptional activity of IRF1. The same group found that Ubc9 and PIAS3 are overexpressed in ovarian cancer, and they showed that SUMOylated proteins enhance tumourigenic ity. This was evident from their experiments using non-cancerous MRC5 versus the cancer cell line MCF7. They detected SUMO1-IRF1 in MCF7, but not in MRC5 control cells.

They also found that SUMOylated IRF1 appeared as multiple bands, giving an indication that SUMO1 can modify various positions in cancerous cells (MultiSumoylation). Moreover, they could detect SUMO1-IRF1 using anti-proteasome MG132 to prevent any further IRF1 degradation, but this gives a future idea that SUMOylated IRF1 brings about degradation as well. The stability of IRF1 is under the control of post-translational modification by SUMO or ubiquitin and not at a transcriptional level. They compared the level of IRF1 in normal, and tumour cells and found that both were equally expressed. They then showed that SUMOylation of IRF1 governed protein stability and

abolished the ability of IRF1 to induce apoptosis upon treatment of cells with exogenous cytokines (Park et al., 2007). In addition, the IRF1 protein activates metalloproteinases gene expression in response to pro-inflammatory cytokines IL1β. Metalloproteinases (MMP3) and (MMP13) degrade the connective tissue matrix and type II collagen, respectively. When the α-Lipoic acid was used in this trial as a treatment for Osteoarthritis (OA), it did not decrease the level of IRF1 expression and reduces its transcriptional activity via SUMOyaltion of IRF1 as a post-translational modification step which was detected by the decreased expression level of metalloproteinases in synovial fluid treated with α-Lipoic acid (Sun et al., 2014).

1.8.4. SUMOylation Indirectly inhibits IRF1 Activity.

SUMOylation can regulate IRF1 transcriptional activity through other proteins that bind to IRF1 promoter and prevent IRF1 from activation. For instance, Liver X Receptors (LXRα, β) prevents p-STAT1 from binding to IRF1 as a response to IFNγ-induced lipopolysaccharide inflammation in brain astrocytes. This happens through the formation of a complex of SUMO1-LXRβ-PIAS on the surface of p-STAT1 and prevents its binding and activation of IRF1 expression. SUMO1ylation of LXRβ occurs mainly at its K30 hydrophobic consensus sequence (VKEEG). This led to the attachment of PIAS C-terminal region to p-STAT1 N-terminal domain and blocked its binding to the promoter of *IRF1* (Lee et al., 2009). The same group showed that the SUMOylation process happened without affecting the nuclear localization of any components through PPARγ receptors nor phosphorylation of STAT1.

1.9. IRF1 Protein Functions in Oncogenesis

Previous literature revealed that the hereditary deletion of *IRF1* gene from chromosomal 5q31.1 locus predisposes patients to Acute Myeloid Leukaemia (AML) and Myeloid Dysplastic Syndrome (MDS), and loss of one allele of IRF1 is also detected in oesophageal and gastric cancer. Moreover, a heterozygosity study correlates with low levels of mRNA IRF1 which leads to poor breast and hepatocellular cancer prognosis (Chen et al., 2013). Also, mRNA from *IRF1* lacking Exon2 and Exon3 via skipping mutation leads to the inability of expressed protein to bind DNA or act as a tumour suppressor, and this is a predisposition for MDS and leukaemia secondarily to MDS in peripheral mononuclear and bone marrow tissues (Harada et al., 1994). IRF1 has anti-oncogenic activity via induction of apoptosis and cell cycle arrest. Mouse Embryonic Fibroblast (MEF) cells that lack IRF1 have no ability to repress cell cycle progression in response to DNA damage. Subsequently, the absence of p21WAF/CIP dependent IRF1 activation acts as a Cyclin-dependent Kinase inhibitor (CKI) (Takaoka et al., 2008). The mechanism by which IRF1 plays its anti-oncogenic pathways may be due to activation of genes to induce apoptosis and cell cycles proliferation inhibition such as p21WAF/CIP , TRAIL, Lysyl oxidase (Lox), angiotensin type II receptor, and caspases pathways (1,7, and 8). Besides that, IRF1 inhibits survivin protein expression (Takaoka et al., 2008). Lox gene promoter contains an element for IRF1 binding; the experiment concluded that MEFs lacking IRF1 shows low expression level of Lox and activated *c-Ha-Ras.* MEFs lacking *IRF1* alleles showed transformation suppression only after cDNA overexpression of Lox (Tan et al., 1996). In response to serum starvation in cultured R3T3 cells,

Angiotensin receptor II is up-regulated and the level of apoptosis in these cells is increased, and this is related to ISRE found in angiotensin II gene promoter. This was revealed through the downregulation of this receptor in the presence of antisense IRF1 (AS-IRF1) (Horiuchi et al., 1997).

1.9.1. IRF1 Cell Cycle Arrest

IRF1 mediates γ-irradiation cell cycle arrest in collaboration with p53, but independently from p53 through the expression of genes such as p21WAF1/CIP1, which act as CKI. Also, p53 binds to p21WAF1/CIP1 promoter and induces G1/S cycle arrest (Nozawa et al., 1999). Moreover, IRF1 is the only IRF member that exerts this molecular mechanism of cell cycle arrest (Chen et al., 2013).

1.9.2. Role of IRF1 in Apoptosis

The mechanism by which IRF1 plays a role as a tumour suppressor protein is the induction of cell cycle arrest and induction of genes that leads finally to apoptosis (Chen et al., 2013). IRF1 can induce apoptosis in gastric cancer cell line, stable tetracycline-inducible clones at which phosphatidylserine, a chemical that causes gastric cancer, exposure activates IRF1 expression system. The IRF1 protein has a potential selective antitumour activity as it can induce apoptosis in two different breast cancer cell lines, C3-L5 and TS/A. It does not show any apoptotic effect upon pre-infection of the stable adenoviral vector (Ad-IRF1) towards non-cancerous breast cell lines; C127I and NMUMG as detected by Annexin V staining. The mechanism behind the breast cancer cell line apoptosis may be as a result of the upregulation of Bcl-2 homologous antagonist killer (bak), caspase8, and caspase7 (Kim et al., 2004). IRF1 shares an important role in apoptosis through the cellular intrinsic pathway

upregulation of p53 upregulated modulator of apoptosis (PUMA), independently from p53, where IRF1 is up-regulated by IFNγ (Gao et al., 2010). Retinoic acid and IFNγ induced IRF1 which shows antitumour activity through activation of TRAIL-dependent apoptosis in breast cancer cell line, whereas control cells are still unaffected. Enhanced *TRAIL* expression occurred following convergence of both, IRF1 and the coactivator on the *TRAIL* promoter. As a result, robust histone acetylation followed by concurrent induction of *TRAIL* IRF1-dependent expression, the TRAIL protein binds to Death Receptors (DRs) and activates caspases pathway (Clarke et al., 2004). In breast carcinoma cell lines (MDA-MB-468 and SK-BR-3), ectopic expression of IRF1 shows 14 fold down-regulation of anti-apoptotic protein (Survivin) independently from p53, and this was revealed by microarray and Western blotting (Pizzoferrato et al., 2004).

1.10. Regulation of immune response by IRF1

IRF1 is thought to be a linker between innate and adaptive immune response through its transcriptional activation of genes and their products that play a central role in the immunity systems (Chen et al., 2013). Dendritic cells which are considered as antigen-presenting cells shows a response in *IRF1* lacking mice as a decrease in mature CD8+ T cells. However, CD4+ T cells are not affected in thymus and peripheral lymphocytic cells. Due to the IRF1 dependent thymic genes regulation is responsible for specific T cell differentiation. This is shown from -/- IRF1 thymocytes that affect differentiation of CD8+ T cells from immature to mature cells and does not influence the development of CD8+ T cells itself because it does not reside in

the thymus (Penninger et al., 1997). As a response to T-lymphocyte mutations, IRF1 induces apoptosis, described as “altruistic suicidal action”, to inhibit its DNA damage modification and potential clone expansion. Overexpression of IRF1 activates IL1β converting enzyme gene10, a mammalian analogue of *Caenorhabditis Elegans* cell death gene *ced-3,* which enhances irradiation-induced apoptosis (Tamura et al., 1995). IRF1 is necessary for Th1 differentiation, and this may contribute to iNOS gene upregulation, which is Th1-dependent. IFNγ stimulates IRF1 which regulates genes encoding iNOS, eventually, catalysing NO (nitric oxide) release and activation of NK cells (Chen et al., 2013). IRF1 plays a role in the development and functionality of immune cells like NK cells. IRF1 knockout mice (Spleen and Liver) shows a significant decrease in count and functionality of NK cells. As such, IRF1 is thought to be necessary for IL15 gene expression in stromal cells of bone marrow which is important as a microenvironment for NK cells development. However, IRF1 does not affect NK cells progenitors because CD8+ T cells do not reside in the thymus (Ogasawara et al., 1998).

1.11. Aim of the Study

The study objective is to decipher the regulatory aspects of post-translational modification of IRF1 by ubiquitination and to map the acceptor site of ubiquitin on C-terminal Lysine amino acids. The study is based on an experimental design using IRF1 C-terminal K-R substitutions with evaluation of the impact on IRF1 stability and transcriptional activity. More specifically the experimental goals were to co-express IRF1 K-R mutants with epitope-tagged ubiquitin molecules mutated to allow linkages only at particular ubiquitin sites (K6, K48, or K63) and identify target residues in IRF1 that can be modified by these proteins. It was also planned to investigate how FBXWα affects these events and explore whether the K-R mutation affects the stability and transcriptional activity of IRF1. Moreover, the study focused on the possibility to detect whether IRF1 is SUMOylated by the SUMO1 variant.

Chapter 2

Materials and Methods

MATERIALS AND METHODS

2.1. Sources of Materials

2.1.1. General Suppliers

All general laboratory chemical reagents were of analytical grade from Fisher Chemicals or Sigma-Aldrich, and other companies reported accordingly. Sodium Chloride (NaCl) was from Alfa Aesar. Tris-Ethylene Diamine Tetra Acetic Acid (Tris-EDTA) preparation was from Gibco. PolyEthylineImine (PEI) reagent was diluted in the laboratory. 1X Phosphate buffered saline (1X PBS) solution was made in our lab. Double distilled water (ddH_2O) purified by Puriteselect/Neptune water purification system used for preparing solutions. The pH meter Janeway 3510 was used to adjust pH.

2.1.2. Molecular Biology reagents

Reagents Companies and their relevant biological purposes (Table 2.1).

Reagent	Purpose	Supplier
NucleoBond ; Maxi AX 500) kit	DNA Purification	Machery Nagel
EZ-RunTM Prestained Rec Protein Ladder	Western blot	Fischer's
Dulbecco's Modified Eagles Media (DMEM)	Cell Culture	Lonza
α Modified Eagles Media (αMEM)	Cell Culture	Lonza
Trypsin Enzyme	Cell Culture	Lonza
Penicillin-Streptomycin Antibiotic	Cell Culture	Sigma
protein G PLUS- Agarose beads	Co-IP	Santa Cruz
HisPur Ni-NTA superflow Agarose (nickel beads)	Chemical pulldown	Thermoscientific

(*)Magnetic Protein G Agarose beads gave better results regarding Western blot clarity.

2.1.3. Protein Assay Reagents and Western Blot Equipment.

Biorad Protein Assay Dye concentrate was purchased from Bio-Rad. Acrylamide/Bis-acrylamide, 30% solution, was purchased from Sigma-Aldrich. Other components for Sodium Dodecyl Sulphate-Poly Acrylamide Gel Electrophoresis (SDS-PAGE) preparation was purchased either from Sigma or Fisher's. Electrophoresis has been carried out using Biorad apparatus for both SDS-PAGE running and for Protein transfer onto Nitrocellulose paper. Nitrocellulose 0.2 µm was purchased from Bio-Rad.

2.1.4. Primary and Secondary Antibodies

Source of Primary Antibodies (Table 2.2).

Antibody	Type	Host	Dilution	Source
IRF-1 M20 Primary	Poly	Rabbit IgG	1:1000 (WB) 1µg/ml (IP)	Santa Cruz
FLAG M2 Primary	Mono	Mouse IgG	1:2000 (WB) 0.2µg/ml (IP)	Sigma-Aldrich
HA 12CA5 Primary	Mono	Mouse IgG	1:1000 (WB) 0.5ug/ml (IP)	Dr Nicole Clarke Group
β-actin Primary	Mono	Mouse	1:2000 (WB)	Sigma-Aldrich
c-Myc Primary	Mono	Mouse	1:2000 (WB)	Sigma-Aldrich
HRP Secondary (Mouse)	Mono	Mouse	1:5000	Santa Cruz
HRP Secondary (Rabbit)	Poly	Rabbit	1:5000	Santa Cruz

All Anti Bodies were diluted into 5% w/v milk in TBST as a vehicle. Also, 5% milk in TBST was used as blocking reagent for nitrocellulose membrane.

2.2. Cell Culture

2.2.1. HEK293T cell line

Human Embryonic Kidney 293 (HEK293) cells are considered a commonly used transformed cell line used for expression of exogenous proteins. The version used here, HEK293T, is a derivative transformed with the SV40 T antigen. This facilitates the propagation of plasmids containing the SV40 origin

of replication due to the ability of these cells to show anti-apoptotic response due to the down-regulation of its p53 but they are still non-tumourigenic cells. HEK293T is cultured in Dulbecco's Modified Eagles Media (DMEM) which was supplemented with other fresh components; 10% Heat inactivated FBS, 2mM L-Glutamine essential amino acid and 50 µl/ml Penicillin-Streptomycin. DMEM should be kept refrigerated at 4°C for up to a month for usage.

2.2.2. MRC5 cell line

MRC5 is a human foetal lung fibroblast cells. Similar culture conditions were used as for HEK293T cells, with the exception that, α Modified Eagles Medium (αMEM) was used instead of DMEM.

2.2.3. Passaging of Cell lines

Cell lines maintained in 10 cm plates were incubated at 5% CO_2, 37°C and optimised humidity, until 80% confluency. After that, the media was aspirated. Cells were washed with 1X PBS and detached out of the plate by the addition of 1 ml Trypsin-EDTA /10 cm plate incubation for 1 minute, followed by vigorously agitation to separate cells from plate and finally suspended in 5 ml of fresh media. The cell suspension was transferred to a 15 ml conical Falcon tube and seeded into new plates containing pre-warmed media. The seeded cells were incubated until the confluence ratio was up to 80% and re-passaged again. Certain limits of passaging intervals for the same cell line. We usually did not exceed 10 passages for each cell line.

2.2.4. Cell counting.

The cell counting was essential to perform accurate seeding into new plates. Harvested mammalian cells were diluted with an equal amount (30µl) of 0.4% Trypan blue dye or 1:1 ratio. The stained cells were loaded into a light

microscope (Nikon Eclipse) and counted according to manufacturer's instructions of Neubauer Marinefield Haemocytometer.

2.2.5. Cryopreservation and Resuscitation of cell lines.

Cells were detached from plates according to previous steps. The cryoprotectant Dimethyl sulfoxide (DMSO) was added to the harvested cell suspension at a ratio of (1:9) and mixed thoroughly to ensure equal distribution. The prepared mixture was aliquoted into cryotubes. Cryotubes were labelled and saved in -20°C for an hour and -80°C deep freezer overnight before keeping them for long-stand storage in liquid nitrogen canisters until passaging them later as required. When required, cryotubes preserved in liquid nitrogen were collected from liquid canisters through thawing the cryotube cell mixture for one minute at 37°C, spun down at 950 rpm (5 min). The supernatant containing DMSO was aspirated and finally cells were suspended, counted and seeded into pre-warmed appropriate media located into desired plates. The media was replaced the following day.

2.3. Biochemical Solutions

Urea Lysis Buffer: 8M urea, 0.1M pH 6.3 Sodium Phosphate, 0.001M pH 6.3 Tris-buffer, 10mM β-Mercaptoethanol, 5mM Imidazole, 0.2%w/v Triton X, and double distilled H_2O up to the desired volume. β-Mercaptoethanol was freshly added.

RIPA Lysis buffer: 50mM pH 7.5 Tris-buffer, 150mM NaCl, 1% NP40, (0, 0.1, or 1) % SDS, 0.5% Sodium Deoxycholate and 1mM EDTA. Enzyme inhibitors were freshly added.

Protease and enzyme Inhibitors: 1mM DTT, 10mM NaF, 1X complete protease inhibitor, 1X phosphatase inhibitor, 1mM AEPSF, 100mM NEM, 1mM Na_3VO_3 and 10mM β-GlyceroPhosphate.

WCE SDS-PAGE Protein Loading Buffer (5µl/20µg Protein): 5xLaemmli, prepared in the laboratory, 100mM DTT, ddH_2O

Nickel Beads Protein Elution and SDS-PAGE Loading Buffer (30µl/sample):

1x Laemeli buffer, 50mM DTT, 250mM Immidazole, ddH_2O up to needed volume**.** 250 mM Imidazole was used to elute any attached proteins from beads into the supernatant.

Protein G Agarose SDS-PAGE Loading Buffer (30µl/sample):5xLaemmli, 100mM DTT, ddH_2O

SDS-PAGE Electrophoresis Running (Migration) Buffer (1X TGS): 25mM Tris buffer, 200mM Glycine, 3.5mM SDS.

SDS-PAGE Components: (Table 2.3).

Reagents (in mls)	**Resolving gel (% acrylamide)**			**Stacking gel (% acrylamide)**
	6%	**8%**	**15%**	**5% acrylamide**
ddH2O	5.3	4.6	2.3	6.8
30% acrylamide gel	2	2.7	5	1.7
1.5 M Tris pH 8.8	2.5	2.5	2.5	--
1.0 M Tris pH 6.8	--	--	--	1.25
10% (W/V) SDS	0.1	0.1	0.1	0.1
10% (W/V) Ammonium PerSulfate	0.1	0.1	0.1	0.1
TetraMethylEthyleneDiamine(TEMED)	0.008	0.008	0.008	0.01

Electrophoresis Transfer Buffer: 39mM Glycine, 48mM Tris buffer, 0.037% SDS, 20% v/v pH 8.3 Methanol was used, and dd H_2O was added up to the desired volume.

Washing Buffer (1x TBST): 10mM pH 7.5 Tris-HCl, 150mM NaCl and 0.05% v/v Tween-20.

Enhanced ChemiLuminescence (ECL): (Table 2.4).

For each Nitrocellulose blot, a 5 ml ECL usually was used

Reagents	**5ml**	**10ml**	**15ml**
1M 8.5 Tris Buffer	5ml	10ml	15ml
Solution A (90 mM β Coumaric Acid in DMSO)	11µl	22µl	33µl
Solution B (250 mM Luminol in DMSO)	25µl	50µl	75µl
Hydrogen Peroxide (H_2O_2)	3µl	6µl	9µl

2.4. plasmids, Types and Preparation

2.4.1. Expression of plasmid used in Study (Table 2.4).

All Expressing plasmids were supplied by Dr Nicole Clarke's GRRB laboratory.

Plasmid Abbreviation	**Cloning Vector**
pCDNA3	pCDNA3.1
pCDNA3 IRF1	pCDNA3.1+Mouse IRF1
CMV FLAG	pCMV-FLAG
FLAG IRF1 WT	pCMV-FLAG-MouseIRF1
FLAG IRF1 K233R	pCMV-FLAG-MouseIRF1 K233R
FLAG IRF1 K240R	pCMV-FLAG-MouseIRF1 K240R
FLAG IRF1 K255R	pCMV-FLAG-MouseIRF1 K255R
FLAG IRF1 K276R	pCMV-FLAG-MouseIRF1 K276R
FLAG IRF1 K300R	pCMV-FLAG-MouseIRF1 K300R
HA FBXW7a	pCMV-HA Fbxw7α
6XHis-Myc ubiquitin WT	pCMV-6XHis-Myc-ubiquitin WT
6xHis-Myc ubiquitin K6 Only	pCMV-6xHis-Myc ubiquitin K6 Only
6xHis-Myc ubiquitin 48 Only	pCMV-6xHis-Myc ubiquitin 48 Only
6xHis-Myc ubiquitin K63 Only	pCMV-6xHis-Myc ubiquitin K63 Only
4X ISRE-Luc	p4XIRF1(ISRE)-Luc

2.4.2. Transformation using chemically competent Cells

E.coli (DH5α) competent bacteria prepared in the laboratory (Barbara Rampersad) were collected from -80°C and kept on ice 5 min to thaw out. Plasmid DNA was thawed on ice; tubes were gently tapped to ensure a uniform distribution of components and gently mixed a 100µl of a bacterial

suspension with 1µl of plasmid DNA. Cells were incubated on ice up to 30 min followed by transfer to 42°C water bath (45 seconds exactly). Cells were transferred to ice (2 min). One ml of LB media without antibiotic was added to polypropylene tubes and cells were placed in a shaker incubator (225-250 rpm) at 37°C for 45 min. One 10th of the transformed cell mix (100µl) was spread onto LB agar plates supplemented with the appropriate antibiotic using sterile spreader and incubated at 37°C overnight. Single colonies were inoculated into 3-10ml LB supplemented with selected antibiotic, (in most case 100µg/ml Ampicillin) and incubated in a shaker incubator at 37°C for 4 hours. This was used to inoculate 150 ml LB Ampicillin culture in Erlenmeyer flasks and grown in a shaking incubator at 37°C overnight for DNA purification step.

2.4.3. DNA Purification

High copy plasmid purification for large scale preparation was used according to manufacturer's instructions (Machery Nagel). Overnight transformed bacterial strain was pelleted via loading into 50 ml falcon tubes, spun down at 4000 rpm for 30 min at 4°C and the supernatant was removed. Pellets were subjected to alkaline lysis as follows:

Cell pellets were carefully resuspended in Buffer S1 + RNase (12ml). Lysis was analysed by adding Buffer S2 (12ml) and mixed gently by inverting the tube 6-8 times. The suspension was incubated for 5 min at room temperature (vortex is avoided to prevent the release of genomic DNA from cellular debris). Pre-cooled Buffer S3 (4°C) was added to the suspension followed by immediately mixing the lysate by inverting the falcon tubes 6-8 times until homogeneous suspension containing an off-white flocculate appeared and the suspension was kept for 5 min on ice. The selected column was equilibrated

with 6 ml Buffer N2 and was allowed to empty by gravity flow, and the flow-through was discarded. The lysate was filtered where the filter paper was folded in a small funnel for support and filter wetted with 5 ml sterile double distilled H_2O, followed by loading the bacterial lysate onto the wet filter where flow-through was collected. The collected flow-through lysate was loaded onto the column, and gravity flow was permitted to allow binding of the plasmid with column matrix. The column was washed with Buffer N3 (32 ml), and the flow-through was discarded. To elute DNA, Buffer N5 (15 ml) was added as soon as possible. Eluted plasmid DNA was precipitated via addition of iso-propanol (11 ml), carefully mixed and centrifuged at 4000 rpm for 30 min at 4°C. The supernatant was discarded, and the DNA pellet washed in Ethanol 70% (5 ml) at 4000rpm for 10 min at room temperature. Ethanol was carefully removed from the tube, and the wetted pellet was allowed to dry at room temperature. Plasmid DNA was dissolved in an appropriate volume of buffer TE (Tris-EDTA), kept on a shaker for 10 seconds and stored at -20°C.

2.4.4. DNA Quantification

Plasmid concentration and DNA quality were determined using Fisher NanoDrop® 1000 Spectrophotometer. Selected plasmid absorbance was read at 260nm. Plasmids were stored at -20°C.

2.4.5. Transient Transfections

Transfection was carried out by mixing each of required plasmids up to 8 µg pDNA for each 10 cm plate. plasmids were diluted with transfection media to 500 µL. The transfection media was without FBS. PolyEthylineImine (PEI) (Sigma) reagent considered as a chemical transfection reagent added with a ratio of 4 µl/ 1µg pDNA (32 µl/ 8 µg pDNA). The mixture Eppendorf tube

(plasmids, Media for transfection, and PEI) was quickly vortexed, spun down for a few seconds, and left for 30 min before its transfer into seeded cells. In the 30 min meantime, fresh cell culture medium was added to cell plates before plasmid transfection.

2.5. Whole Cell Extract Contents

Cultured cells at 80% confluency were harvested as follows:

The cell culture media was aspirated, and cells were washed once with 1X PBS. Following addition of 1 ml 1X PBS, cells were detached using a cell scraper, which was re-used after rinsing in 1X PBS. Cells were transferred to a 1.5 ml Eppendorf tubes followed by centrifugation at 1000 rpm for 5 min at 4°C. The supernatant was aspirated gently using a vacuum or by simple pipetting. Cells were ready for the addition of appropriate lysis buffer which was Urea lysis buffer in case of ubiquitin-IRF1 protein detection, and RIPA lysis buffer in both cases of SUMO1-IRF1 protein and Cycloheximide (CHX) chase reaction. Lysates formed were sonicated using Diagenode Biodisruptor was applied to ensure overcoming the sticky DNA present and extract total cellular proteins, where the highest frequency was used with time intervals 30 seconds off/20 seconds on for three times. Cellular debris and insoluble fractions were spun down at 3000 rpm for 4 min. The supernatant was collected as WCE which was ready for Western blot and immunoprecipitation.

2.5.1. Urea Lysis buffer.

Before application of cell scrapping and cell lysis, 10mM MG132 (proteasome inhibitor) was added to cells because of ubiquitinated proteins would be targeted to be lysed by the proteasome and this would hinder the purpose of

the experiment to detect the ubiquitinated proteins. Hence MG132 blocked the proteolytic activity of the 26S proteasome complex. Plates treated with MG132 incubated for 3 hours followed by preparation of whole cell extracts (WCE) for lysis. To facilitate the detection of ubiquitinated cellular proteins, cell lysates were prepared in Urea buffer because urea buffer solute acts as a chaotropic agent to disrupt the complex network of weak non-covalent intramolecular interactions as hydrogen bonds, van der Waals forces, and hydrophobic effects of the lipid bilayer to denature macromolecules like proteins and nucleic acids. Also, it reduces enzymatic activity and exerts stress on a cell to be lysed through decreasing the hydrophobic forces from amino acids of tertiary structure and finally denatures the proteins without affecting the high covalent isopeptide bonds which were very abundant in ubiquitin interactions with the substrate and with other ubiquitin molecules. Tertiary protein folding is dependent on hydrophobic forces from amino acids throughout the sequence of the protein. This solubilizes the hydrophobic interactions within the cell, thereby denaturing the protein. For each cellular pellet, a 500 µl Urea buffer was added and thoroughly mixed by pipetting to help in lysis of cells, until cellular matrix debris was formed. The cell lysate was left inside a fume hood for 5 min followed by sonication. The lysate was cleared at 3000 rpm for 4 min, and the supernatant was transferred to new tubes and stored at -80°C. The drawback of this method is the inability to quantify protein using Bradford assay method because some con10ts of lysis buffer might impede protein quantification. The supersaturated stock urea buffer was pre-warmed to increase its solubility and 10mM β-Mercaptoethanol solution was freshly added to the lysis buffer as mentioned before.

2.5.2. RIPA Lysis buffer.

Radio Immuno Precipitation Assay (RIPA) was the method used to extract proteins; it is very harsh lysis buffer because of the presence of SDS and sodium deoxycholate detergents. This carries the possibility to affect the interaction between SUMO and modified protein. However, presence of SDS is proper for sharing DNA sticky mass and this let us to avoid more sonication. Therefore, the procedure was carried out using RIPA with detergents and without detergents for each experiment. Each sample of prepared cellular pellets was treated with 300µl RIPA (0.1%SDS) buffer alongside freshly mixed enzyme inhibitors. Pipetting was applied, and the syringe is mixing (BD Microlance Syringe 100 23G) to ensure total lysis of cells, and warming up samples for 10 min at 95^{O}C. samples were let to cool down, and RIPA (without SDS) buffer was added for each to complete the lysate to be up to 1500µl. Sonication was applied as previously described to ensure overcoming the sticky DNA present and total cellular protein extraction. samples were centrifuged at 12,000 rpm for 10 min at 4 ^{O}C. The supernatant was then transferred to new 1.5ml tubes and kept at -80°C until detection by western blot.

2.5.3. Protein Assay.

The protein concentration was quantified using Bradford assay method (Bradford, 1976). Bio-Rad dye concentrate was used, where Protein assay buffer was diluted 5X (200µl and 800µl ddH_2O) which was aliqouted as 1ml for each cuvette and mixed. Bovine Serum Albumin (BSA) was taken as the standard with a serial concentration of BSA as (0, 2, 4, 6, 8,10,15,20 micrograms). Samples (1µl each), were added to 1ml of Protein Assay Buffer

and Optical Density (OD) was measured at 595 nm. The optical density (OD) of known BSA standard concentrations as measured on an Eppendorf spectrophotometer.

2.6. Nickel Beads Pulldown and Co-Immunoprecipitation.

2.6.1. Pulldown of His-tagged Proteins using Nickel Beads

FLAG-IRF1 different vectors and the 6XHis-Myc-ubiquitin expressing vector produced ubiquitin-protein contains a 6xHistidine N-terminal tag. Cellular lysates were tested for the presence of ubiquitin-IRF1 proteins via the interaction by affinity capture of His-tagged ubiquitin IRF1 on Nickel beads. For each cellular lysate, 10 µl pure nickel beads (30 µl nickel beads slurry) were prepared via washing the appropriate amount of slurry with PBS and spun them down. The supernatant was discarded, and the remaining beads were mixed with 30µl of urea lysis buffer to form 40 µl of 25% nickel beads suspension. Cellular lysate (230 µl) was mixed with 40µl nickel beads suspension and urea lysis buffer (250 µl) was added to bring the volume of each sample to 500 µl each. The cellular mixture was rotated overnight at 4°C to allow the chemical interaction between 6XHis tagged ubiquitin and nickel beads where the overnight incubation is to allow IRF1-ubiquitin interaction. Tubes were collected and spun down at 3000 rpm for 30 seconds. The supernatant was aspirated slowly to prevent any loss of beads. Beads were gently washed with 600µl freshly prepared urea lysis buffer and softly mixed 3-6 times followed by centrifugation at 3000 rpm for 30 seconds. The washing buffer was aspirated. The washing was repeated three times. The residual amount of lysis buffer was withdrawn from beads of interest with an insulin syringe. Beads were mixed with Nickel Beads Protein Elution and SDS-PAGE

Loading Buffer (30 µl/sample). Tubes containing beads were gently tapped with hands several times to suspend beads within the dye. Samples were warmed at 95^{o}C for 5 min and softly shaken in between. Tubes were collected and cooled at room temperature for 5 min, followed by centrifugation at 3000rpm for 1 minute. The supernatant containing eluted proteins was collected via withdrawal with syringes and spun down. Samples were kept at -20^{o}C or -80^{o}C until analysed by western blot.

2.6.2. Co-Immunoprecipitation using Protein G PLUS-Agarose Beads.

HEK293T cells were transfected with pCDNA3 IRF1 along with FLAG SUMO1, using PEI for transfection. After 48 hours, cells were harvested, washed with PBS, and lysed in RIPA buffer according to the protocol above. Half of the volume of each cellular lysate, nearly 500µg was diluted with same amount of RIPA lysis (without SDS) buffer with complete enzyme inhibitors. Diluted lysates were pre-cleared with 20µl of 50% Protein G PLUS-Agarose beads. Beads were pelleted at 12000 rpm, 20 seconds, at 4^{o}C and the supernatant was transferred to new tubes. 5 µl of Primary antibody was added to the precleared lysate, and the selected antibody was αFLAG (0.2 µg/ml), and samples were placed on a rotator at 4°C overnight. samples were collected, and 20µl of Protein-G beads (where no need for washing with PBS) were added and incubated at 4°C rotating for at least 2 hours. Beads were collected and washed in RIPA (0.1%w/v SDS) buffer (600µl each) for three times (including protease and other enzyme inhibitors), and excess buffer removed after the final wash to allow pellets to dry. Samples were prepared for SDS-PAGE by adding Protein G Agarose SDS-PAGE Loading Buffer (30

µl/sample). The samples were denatured for 5 min at 95°C followed by centrifugation at 12,000 rpm for 5 min to pellet any debris. Eluted samples could be saved at -20°C or -80°C deep freezer or used immediately.

2.7. Western Blot

2.7.1. SDS-PAGE gels Preparation

Resolving and stacking gels, containing different concentrations of Acrylamide and crosslinker TEMED were prepared as shown in (Table 2.3). An 8% Acrylamide gel was usually used because it was suitable for running of proteins from 25-200 kDa where our target IRF1 protein was located (50 kDa). Washing wells and overloading of samples were avoided to prevent poor distorted separation of protein bands.

2.7.2. Samples Preparation and Loading to SDS-PAGE gels

As mentioned before, Western Blot was carried out for 20µg of WCE by mixing the appropriate WCE volume with 5µl of (WCE SDS-PAGE Protein Loading Buffer). This was loaded to SDS-PAGE gel with Protein ladder (10 kDa-170 kDa). Protein amount of 20 µg was typically used to prevent any densitometry problems in case of using higher or lower values. Also, Co-IP and Pulldown samples were ready for SDS-PAGE loading as mentioned in (section 2.6).

2.7.3. Sample Running (Protein separation)

Running of loaded samples were applied using Bio-Rad mini-gel electrophoresis system (Bio-Rad Protean II) in the migration buffer 1X TGS, of constant voltage (120-135 V) for 90 min or usually when the migration front reached the bottom of the gel. Fisher BioReagents™ EZ-Run™ Prestained Rec Protein Ladder was used in this study (10-170 kDa).

2.7.4. Transfer to Nitrocellulose Membrane

The gel containing separated proteins was transferred to nitrocellulose paper, and other components of transfer Tetra System and Transfer Buffer were

used. The transfer was carried out at a voltage of 60V / 300mAmp at 4°C for 90 min, or overnight at 30V.

2.7.5. Blocking with 5% Milk and Immunoblot

Successfully transferred proteins on Nitrocellulose paper were exposed to incubation with 5% blocking milk in 1X TBST at room temperature for 1 hour under gentle shaking. The membrane was incubated with primary antibody in a 50 ml falcon tube containing (1:4000) primary antibody or as mentioned in (Table 2.2) for at least one hour at room temperature or preferably to be carried out at 4°C overnight for better binding efficiency. The blot was washed with 1X TBST (3 times/ 5 min each). The membrane was incubated in a 50 ml tube with 1:4000 secondary antibody which is usually HRP (conjugated Horse Radish Peroxidase) for 1 hour on rotating shaker at room temperature, followed by the same sequence of washing for three times. In the case of using 1X TBST as a washing vehicle, 1-minute washing with PBS was applied to the membrane before addition of ECL reagent (Table 2.4). Finally, the membrane was exposed to 5 ml (freshly prepared) ECL developing solution at room temperature for 1 minute. Hydrogen Peroxide was added directly before the incubation with the membrane. The ECL reagent was slowly removed from the blot within few seconds, directly followed by wrapping in a thin layer of saran wrap. The chemiluminescent signal was imaged and recorded using luminescent image analyser (Fujifilm LAS-4000). In the case of the requirement for another primary antibody incubation at the same blot, washing twice for 5 min was carried out with 1X TBST before incubation with the new primary antibody.

2.8. Densitometry Assay of Immuno-blot Bands

In some cases, normalisation was carried out through the measurement of the densitometry of the input lysate protein band and the pull-down proteins also. The relative ratio of the protein-protein interaction was outlined by dividing the quantified pulldown results protein by Input lysate results for the densitometry as a tool for normalisation of ubiquitinated IRF1 where the loading control was WCE IRF1 band which used as a means to normalise the final data (Fig 2.1).

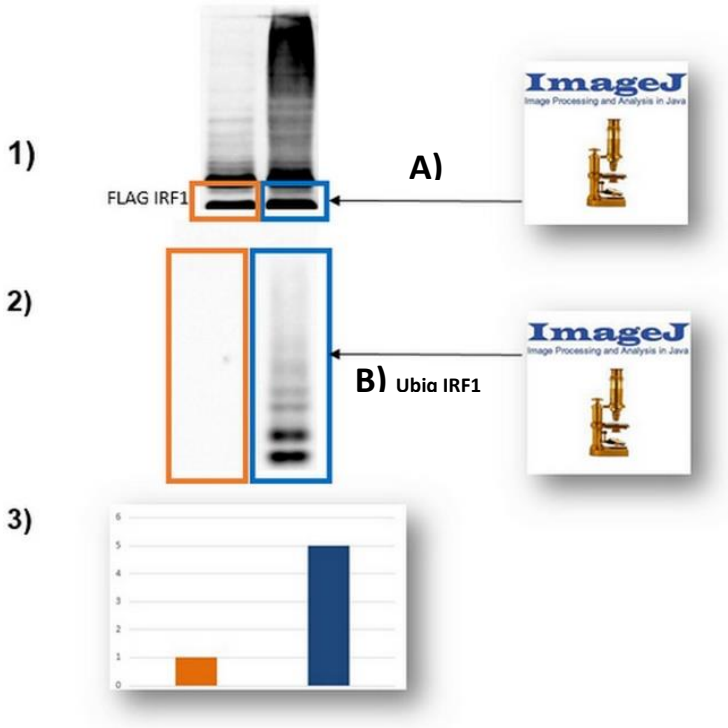

Fig 2.1: Schematic Shows Densitometry Measurements Using ImageJ Software. **(1)** Western Blot shows rectangular frames drawn around WCE FLAG IRF1 by ImageJ software which measures the intensity of each band, denoted as **(A). (2)** Western Blot shows rectangular frames cover the whole ubiquitinated IRF1 bands at each lane and measured bands intensity indicated as **(B). (3)** The *average* ubiquitination level of IRF1 measure by dividing **(B) by (A)** which can be represented as a graph.

2.9. Dual gene reporter Luciferase activity assay

Using Glomax luminometer (Promega) reporter assays were carried out in MRC5 cells. Cells were seeded in 24-well plates at a $0.01x10^{6}$ cells/well in αMEM media for 24 hours. After 24 hours, transfection of the following amount of plasmids to each plate. For each well, cells were transfected with 50ng of IRF1 expression plasmid, 75ng of 4X ISRE (interferon stimulatory response element) and 3ng of conserved control β-Galactosidase plasmid, single-stranded DNA (ssDNA) added to each to complete the amount of plasmid to be up to 250ng. plasmids were diluted with an appropriate media for transfection which is free from FBS (Foetal Bovine Serum) followed by addition of PEI as recommended with a dose of 1 µg/250 ng DNA, vortexed for 10 seconds each and left for 30 min before its transfer to seeded cells. Cells were exposed to lysis protocol (optimised Applied Biosystems®) after 48 hours or 36 at least after transfection as following; Cells were washed with PBS twice (each well 1ml PBS) and transferred to ice. Reporter Lysis buffer was added as 50 µl/well. Cells are exposed to the shaker for 15 min on ice. Cells were scraped from wells by pipette tips and transferred to new tubes. Tubes were centrifuged at (6,000 rpm /5 min) to remove any cellular debris, and the supernatant was collected and might be kept at 80°C until measuring luciferase according to the following steps. All assays were performed in triplicate at room temperature and manufacturer's GLOMAX® 96 microplate luminometer. Buffer A and B were equilibrated to room temperature. Galacton-Plus® substrate was freshly diluted in a 1:100 in Buffer B (50 µL/ well). Solution A and cellular lysate were mixed in a fixed time interval manually for all 96 well plate, Solution A (12.5 µL/ well) was mixed with lysate

(5 µL/ well). Within 10 min, Buffer B mixture was injected with Buffer a mix automatically at the same time interval. After a 1-2 sec delay, read the luciferase signal for 0.1-1 sec/well. The microplate was incubated for 30-60 min at room temperature before addition of an accelerator-II solution (50 µl/well) to measure internal control of β-Galactosidase. After a 1-2 sec delay, read the β-galactosidase signal for 0.1-1 sec/well. Data was normalised via dividing of luciferase reading with internal galactosidase control. Results are equalised as a fold induction of empty vector for each treatment, and the obtained results were expressed as Relative Luciferase Units (RLU). Data is from 3 independent biological experiments, and each was carried out in triplicate transfection procedure.

2.10. Cycloheximide Chase Reaction

MRC5 cell line was co-transfected with FLAG IRF1 (WT, Mt) expressing plasmids with a limit of 8µg/ 10 cm plate. The transfection was carried out according to (Section 2.5). After two days of incubation, plates were treated with Cycloheximide (25µg/ml) for each type of expressed plasmids and allowed to be incubated for (0, 30, 60, 120 min) time intervals. Cycloheximide stops any further translation and expression of cellular proteins, and this gave a chance to track the stability of already expressed proteins during the time intervals. Cells were harvested according to (Section 2.5.1.1). Lysates were collected, and Western blot detected proteins (Section 2.7).

Chapter 3

Results

RESULTS

In this study, we aimed to investigate the precise residues that are modified by ubiquitin and SUMO is, therefore, important to understand IRF1 function.

IRF1 C-terminal Lysine Amino Acids

NCBI Gene database describes a single mature transcript mRNA for IRF1 in humans. As mentioned in the introduction, the IRF1 protein contains multiple domains (Fig 3.1). This study focuses on the IRF1 C-terminus. The first domain is the transactivation domain (TAD) (185-256), this is critical for gene regulation by IRF1 (Schaper et al., 1998). The enhancer domain increases IRF1 transcriptional activity 10-fold although it appears to have no intrinsic activity (Kirchhoff et al., 2000).

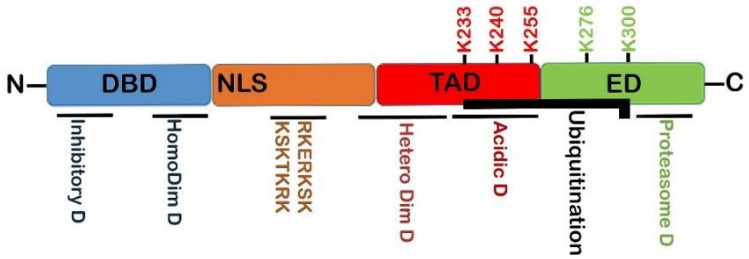

Fig 3.1. Schematic shows IRF1 Main Domains and C-terminal Lysine Amino Acids. The IRF1 C-terminal region contains 5 Lysine residues (K233, K240, K255, K276, and K300) approximately shown in the Fig that is located within the potential motifs for ubiquitin attachment. Three locations reside within TAD (K233, K240 and K255), whereas K276 and K300 are within the enhancer domain.

An outline of the experimental approach is described in Fig 3.2, and the representative Western blots are shown in similar results below in Figs 3.A,B. Whereas the average ubiquitinated-IRF1 of at least 3 independent biological replicates was shown in Figs 3.C.

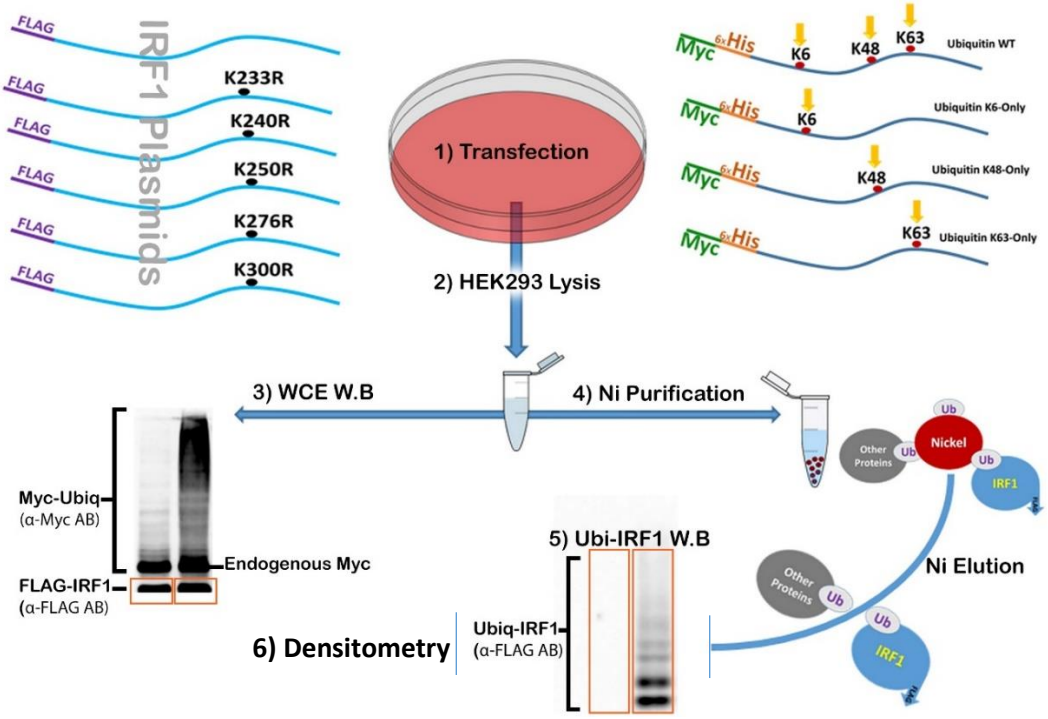

Fig 3.2. Diagram of Experimental Procedure for ubiquitinated-IRF1 identification.

1) HEK293T cells were transfected with one type of IRF1 plasmids, with or without one type of ubiquitin plasmids. **2)** Cells were harvested after two days of incubation Cells were lysed by urea. **3)** W.B of WCE (20 µL proteins) was tested for the expression of FLAG-IRF1 using α-FLAG antibody and quantified using ImageJ Densitometry tools. Myc-ubiquitin was detected on the same immunoblot using α-Myc antibody, and this step was just to confirm that WCE was being ubiquitinated (smeary band) and did not be quantified by ImageJ. **4)** Nickel beads were used to purify ubiquitin-proteins through overnight incubation of WCE with Nickel beads followed by beads spinning down and washing. ubiquitin-proteins was eluted from Nickel beads, and W.B was carried out for supernatant. **5)** Immunoblot of Pulled down ubiquitin-proteins with α-FLAG to detect FLAG-IRF1-ubiquitin. The blot band appeared as multiband which represent polyubiquitination levels of IRF1. ImageJ software quantified the whole immunoblot bands. **6)** Numerical data of the Average ubiquitnated-IRF1was done by dividing ubiquitin-IRF1 band intensity by WCE IRF1 band intensity, and data was graphed after doing at least statistical independent replicates.

3.1. K240 is Required for IRF1 ubiquitination

To identify which C-terminal K acts as an acceptor for ubiquitin, series of IRF1 mutants which were already present in our laboratory were used. These C-terminal candidate Lysine amino acids were substituted with arginine to abolish their ability to be ubiquitinated but maintain the structural integrity, due to the similarity of the side chains between Lysine and arginine. The experimental procedure for detection of ubiquitinated IRF1 was carried out as shown schematically (Fig 3.2.). Representative Western blots are shown in Figs 3.3.A,B and the average ubiquitinated-IRF1 of at least 3 independent biological replicates was shown in Figs 3.3.C. The western blot of the whole cellular extract (WCE) indicates that all expressed unmodified-IRF1 proteins WT, K240, K255, K276, or K300R ran at 50 kDa (Fig 3.3.A. Unmodified-IRF1). However, the level of their expression appeared unequal. For instance, unmodified-IRF1 lanes 2, 4, 6, or 8 was higher compared with adjacent ubiquitin overexpression in lanes 3, 5, 7, or 9. This indicates that ubiquitin has amended the IRF1 protein to a higher level. Except K300R which showed the contrary where the level of expressed unmodified-IRF1 protein at lane 11 showed increased than lane 10, and the level of modified-IRF1 of the same upper lane 11 increased compared with lane 10. As such, it was concluded that IRF1 K300R stabilised the ubiquitinated IRF1, whereas other residues underwent ubiquitination but did not affect the stability of the IRF1 protein. Unmodified-IRF1 bands were quantified by densitometric tools using ImageJ software. Also as shown in Fig 3.3.A, Myc-ubiquitin expression was checked with α-Myc antibody and approximately equal levels of ubiquitin WT interacted with other proteins which were seen as smeared bands running from nearly

70 kDa-250 kDa. Moreover, as shown in Fig 3.3.B, nickel-beads pulldown purification was carried out to capture any His tagged-ubiquitin or associated His tagged-ubiquitin interacting proteins. Polyubiquitnated-IRF1 bands were detected by immunoblotting with α-FLAG. Whereas nothing was observed in the event of the absence of ubiquitin co-transfection at lanes 2, 4, 6, 8, and 10 (Fig 3.3.A, B). After densitometric assay of ubiquitin-IRF1 multi bands, it was concluded that IRF1 K240R lowered the ubiquitination compared with IRF1 W. This indicated that K240 is critical for ubiquitination process or even acts as ubiquitin acceptor. As shown in Fig 3.3.C**,** K240R significantly decreased the level of IRF1 ubiquitination as compared with WT IRF1. In contrast, IRF1 K300R significantly increased the relative level of IRF1 ubiquitination. As such, the mutation within the ED far 25 amino acids subdomain did not inhibit ubiquitination but increased the stability of IRF1. Other IRF1 mutants showed no significant difference when compared to WT ubiquitin. In summary, it was concluded that IRF1 was successfully ubiquitinated. Besides that, the major acceptor site was IRF1 K240, and other Lysine sites may act as secondary acceptor sites because ubiquitination of IRF1 K240R was reduced but still detected.

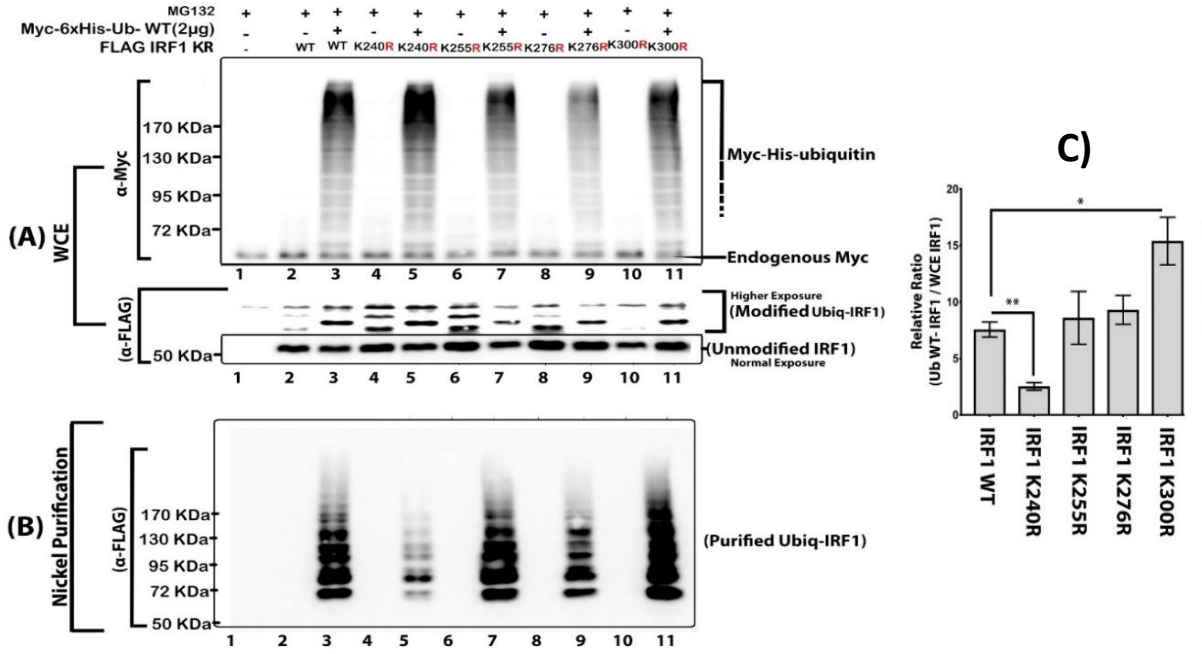

Fig 3.3. K240R significantly decreased the relative level of IRF1 ubiquitination.

(A) HEK293T cells were transfected with Wild-type or mutant IRF1 expressing vectors along with Myc-6XHis-ubiquitin expressing plasmid. Cells were incubated for two days, followed by 3 hours of treatment with anti-proteasome reagent MG132 to block any proteasome degradation of ubiquitinated IRF1. Cells were harvested, lysed with urea buffer and Western blot was carried out. FLAG-IRF1 was detected with α-FLAG antibody. IRF1 band ran at 50 kDa which was quantified using ImageJ software Densitometry. The same blot was washed, and Myc-6XHis-ubiquitin interacting proteins were detected with α-Myc as primary antibodies. Ubiquitinated proteins appeared as smeary bands running from nearly 70 kDa-250 kDa. **(B)** The WCE was overnight incubated with Nickel beads to allow 6XHis-ubiquitin to interact with Nickel beads followed by elution of Nickel beads, and the supernatant was immunoblotted with α-FLAG to detect WT Ub-IRF1. Densitometry was applied using ImageJ densitometry tools. Note: modified-IRF1 shown at a section was under higher exposure, meanwhile the lower Unmodified was normally detected by normal exposure. **(C)** Graph represents the average ubiquitinated-IRF1 from at least 3 independent replicates. Error bars represent the Standard error of Mean (SEM), student t-test was used as to compare between WT IRF1 and a candidate IRF1 mutant type in terms average ubiquitination level of IRF1. Values were from three independent experiments.

3.2. polyubiquitination on IRF1 C-terminal Domain

The next experiment was to identify the type of polyubiquitination on IRF1 the C-terminal and the main acceptor for this polyubiquitination. As discussed in the introduction, the C-terminal Glycine of ubiquitin-protein can ligate to another ubiquitin molecule at Lysine (K6, K48, or K63) and this leads to the formation of branched polyubiquitinations after first isopeptide bond with its target protein. Previous studies suggest that polyubiquitination of different acceptors perform various functions. For instance, K6-polyubiquitination targets the candidate protein for DNA repair through activation of Breast Cancer Susceptibility Gene (BRCA1-BARD) repair mechanism mediated by E3 ligases (Thakar et al., 2010). In addition, K48-ubiquitination recruits its substrate proteins for proteasome degradation. K63-polyubiquitination mainly involves the modified protein in cellular signalling. As reported in the literature IRF1 C-terminal domain is responsible for IRF1 proteasomal degradation (Nakagawa and Yokosawa, 2000). The aim of the current study was to ascertain the type of polyubiquitination formed on IRF1 C-terminal domain and the IRF1 Lysine acceptor for this polyubiquitination. To achieve this objective, FLAG-IRF1 WT, K240R, K255R, K276R, and K300R expression plasmids were co-transfected into HEK293 cells alongside one type of-Myc-6XHis-ubiquitin according to the same experimental procedure (Fig 3.2).

3.2.1. K63-polyubiquitination does not modify IRF1 C-terminus.

The aim of the subsequent experiment was to ascertain whether IRF1 is modified by K63-polyubiquitination and the probability to form this type of ubiquitin isopeptide bond with IRF1 C-terminal Lysine amino acids. The same experimental procedure was used, where FLAG-IRF1 plasmids were

transfected with Myc-6XHis-ubiquitin K63-Only in HEK293 cells. Results indicated the equality in FLAG-IRF1 protein expression as outlined in western blot assay using α-FLAG antibody (Fig 3.4.A). FLAG-IRF1 bands were at 50 kDa at similar levels**.** The indication is that IRF1 K-R mutations have no major impact on the expression level of IRF1. Overexpressed Myc-6XHis-ubiquitin ubiquitously modified cellular proteins, and this was revealed using the α-Myc antibody as shown in the upper section of Fig 3.4.A. The Fig 3.4.B showed ubiquitin-IRF1 proteins purified with Nickel beads affinity capture and directly incubated with α-FLAG to detect FLAG-IRF1-K63-polyubiquitination. The results of Western Blot revealed that K63-polyubiquitination does not modify IRF1 C-terminus. Although, IRF1 K240R-K63-polyubiquitination appeared at a higher level of expression (lane B.3) compared with IRF1 WT-K63-polyubiquitination (lane B.1), the triplicate repetition of the experiment showed the no significant difference in the relative levels of ubiquitination of IRF1 between mutants and WT. This was revealed graphically in Fig 3.5.C, resulted in no strong significant difference between the relative K63-polyubiquitination level of FLAG-IRF1 K-R and FLAG-IRF1 WT. Finally, IRF1 is possible that K63 polyubiquitination occurs at a site outside the c-terminal domain of IRF1.

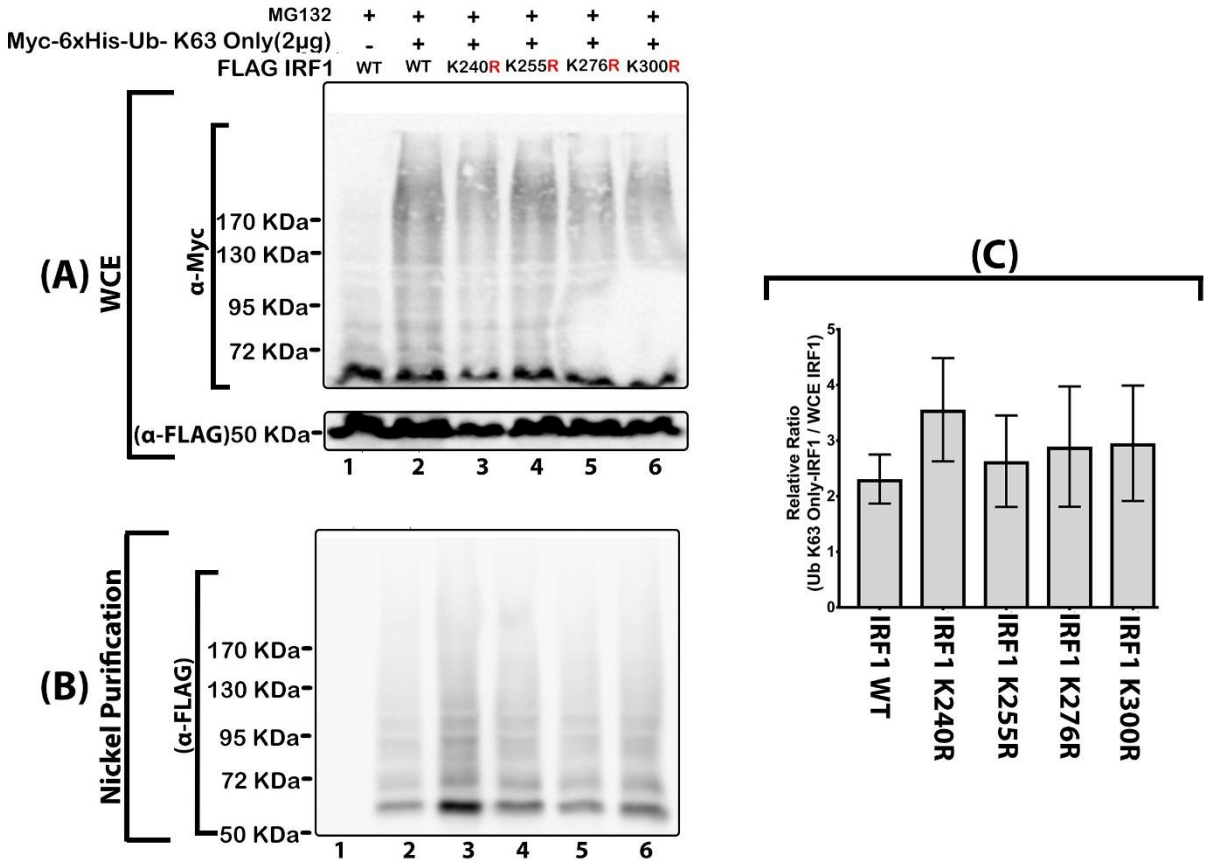

Fig 3.4. IRF1 C-terminal domain is not a target for K63-polyubiquitination.

(A) Western Blot of WCE of FLAG-IRF1 and-Myc-6XHis-ubiquitin K63-Onlyoverexpression in HEK293 for 2 days followed by treatment with MG132(10µg/ml) for 3 hours and cells were collected and lysed with 8% urea lysis buffer. WCE proteins (FLAG-IRF1,-Myc-6xHis-ubiquitin) detection where carried out using α FLAG and α-Myc, respectively at the same blot. **(B)** Western Blot data from overnight incubation of the large remained WCE with Nickel beads to allow 6XHis-ubiquitin K63-Only with or without associated proteins to interact with beads followed by beads elution and the supernatant was immunoblotted with α FLAG to detect Ub K63-Only-IRF1. **(C)** Graph represents Average ubiquitination level of IRF1 (Ub K63-Only-IRF1/WCE IRF1). Error bars represent the Standard error of Mean (SEM), student t-test was used as to compare between WT IRF1 and a candidate IRF1 mutant type in terms of relative K63-polyubiquitination level. Values were from three independent experiments.

Note: The relative level of IRF1 ubiquitination was measured as a relationship between the level of WCE IRF1 and the level of Ubiquitinated-IRF1 using ImageJ densitometry. As such the defect in upper part of Fig 3.4.A, with α-Myc did not affect the densitometry measurement because it was not included in densitometry analysis.

3.2.2. K48-polyubiquitination modifies IRF1 C-terminal K240

In addition to previously used IRF1 K-R mutants (K240R, K255R, K276R, K300) in WT-polyubiquitination, an additional IRF1 K233R was available for subsequent experiments. The co-transfection of different plasmid vectors of FLAG-IRF1 with Myc-6XHis-ubiquitin K48-Only (where ubiquitin K48 was the only lysine able to form a chain). The result was successful FLAG-IRF1 Expression. IRF1 ran at similar 50 kDa levels as shown in Fig 3.5.A, indicating that the C-terminal Lysine amino acids substitution has no impact on the process of IRF1 expression. In addition to the detection of IRF1 bands, HEK293 equally overexpressed Myc-6XHis-ubiquitin K48-Only detected with α-Myc antibody as smeary bands running approximately around 70 kDa and reached the modification of higher molecular weight cellular proteins. To quantify the level of IRF1-K48 polyubiquitination, nickel beads experimental purification procedure was performed to ascertain that K48-polyubiquitination modified-IRF1 C-terminal. The results of Fig 3.5.B revealed that IRF1 proteins were changed by Myc-6XHis-ubiquitin K48-Only as multi bands at each lane. However, densitometry analysis verified that only IRF1 K240R decreased the K48-polyubiquitination level of IRF1 compared with WT FLAG-IRF1 (Fig 3.5.C) after conducting the three independent biological experiments. Although IRF1 K240R showed a significant drop in the level of K48-polyubiquitination, it did not entirely abolish the ubiquitination, suggesting that other minor sites could be K48-polyubiquitinated. In conclusion, IRF1 mainly is modified by K48-polyubiquitination and IRF1 K240 is critical for K48-polyubiquitination which targets the protein primarily for proteasome degradation.

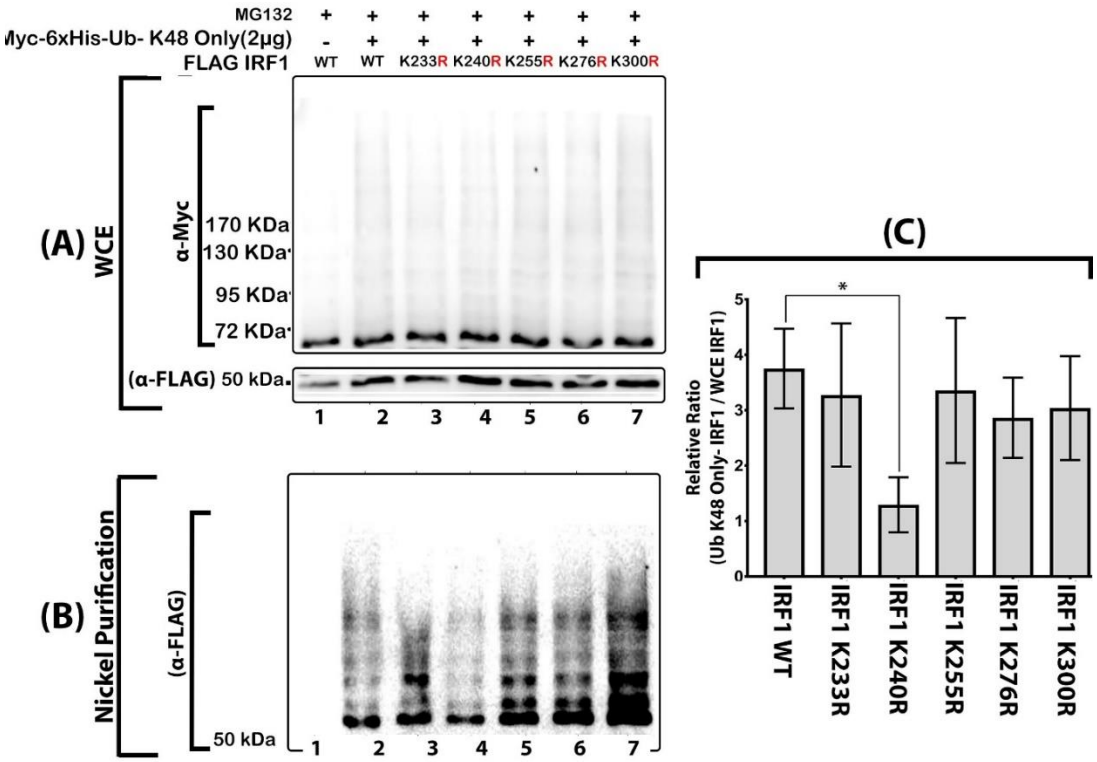

Fig 3.5 K240 is required for K48-polyubiquitination of IRF1 C-terminus.

(A) WCE Western Blot at which the FLAG-IRF1 and Myc-6XHis-ubiquitin K48-Only proteins were detected. HEK293 cells were co-transfected with FLAG-IRF1 vectors as indicated along with Myc-6XHis-ubiquitin K48-Only. Cells lysed after 2 days of transfection and 3 hours of cell culture plates treatment with anti-proteasome reagent MG132 (10µg/ml) to prevent proteasome degradation of ubiquitinated IRF1. FLAG-IRF1 was detected with α-FLAG which appeared as 50 kDa and densitometric analysis was carried out using ImageJ software. At the same blot α-Myc was used to detect WCE ubiquitinated proteins as primary. **(B)** Western Blot data from overnight incubation of WCE with Nickel beads to allow 6XHis-ubiquitin K48-Only with or without associated proteins to interact with beads followed by beads elution and the supernatant was immunoblotted with α-FLAG to detect IRF1 interacted with K48-Only-ubiquitin which quantified using densitometry. **(C)** Graph represents Average ubiquitination level of IRF1 (Ub K48-Only-IRF1/WCE IRF1). Error bars represents Standard error of Mean (SEM) and (*) is referred to the significance difference (<0.05), student t-test was used as statistical representation for comparison between WT IRF1 and a candidate mutant type. Values were from three independent experiments.

Note: This was the first experiment IRF1 K233R included.

3.2.3. K6-polyubiquitination does not target IRF1 C-terminus

As reported in the literature, K6-polyubiquitination inhibits protein degradation and induces DNA damage repair, via the BRCA1 pathway. However, this type of polyubiquitination is poorly studied and still needs more clarification about the mechanism of interaction with IRF1 and the fate of IRF1 modified by this K6 ubiquitin linkage. We aimed specifically to ascertain whether K6-polyubiquitination modified the C-terminal IRF1 lysines. The different FLAG-IRF1 expressing plasmids indicated before were overexpressed alongside Myc-6XHis-ubiquitin K6-Only in HEK293 and the experimental procedure described in Fig 3.2 was used. As shown in Fig (3.6.A) IRF1 was successfully expressed regardless of K6-polyubiquitination overexpression, nor IRF1 K-R mutations. Nickel beads purification revealed a level of IRF1 K-R ubiquitination in Fig (3.6.B) which did not show any significant difference to the level of K6-polyubiquitination compared with IRF1 WT. The conclusion was to exclude both K6 and K63-polyubiquitinationation on IRF1 C-terminal Lysine amino acids, and this suggests other IRF1 domains may be the target for these types of ubiquitin linkages such as the nuclear localization signal domain (NLS) or even the DBD, and these motifs reside in the N-terminal domain of the protein.

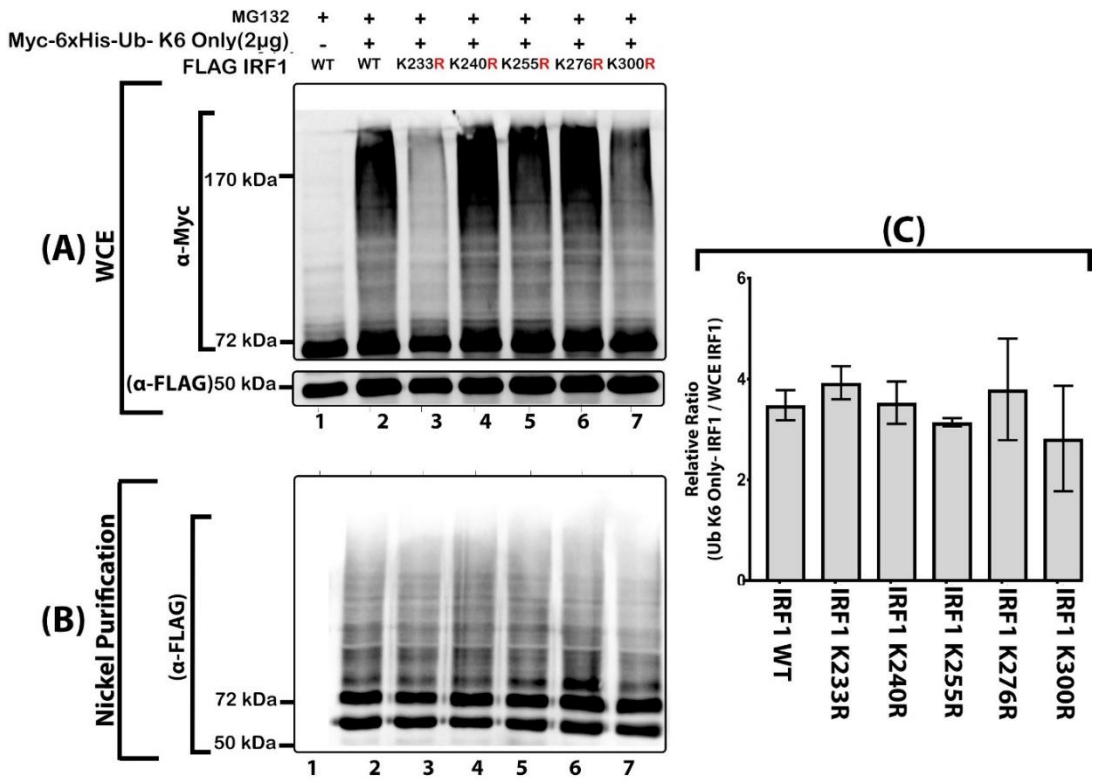

Fig 3.6. IRF1 C-terminal domain is not a target for K6-polyubiquitination.

(A) Western Blot of WCE of FLAG-IRF1 and-Myc-6XHis-ubiquitin K6-Only overexpression in HEK293 for 2 days followed by treatment with MG132(10µg/ml) for 3 hours and cells were collected and lysed with 8% urea lysis buffer. WCE proteins (FLAG-IRF1,-Myc-6xHis-ubiquitin) detection where carried out using α FLAG and α-Myc, respectively at the same blot. **(B)** Western Blot data from overnight incubation of the large remained WCE with Nickel beads to allow 6XHis-ubiquitin K6-Only with or without associated proteins to interact with beads followed by beads elution and the supernatant was immunoblotted with α FLAG to detect Ub K6-Only-IRF1. **(C)** Graph represents Average ubiquitination level of IRF1 (Ub K6-Only-IRF1/WCE IRF1). Error bars represent the Standard error of Mean (SEM), student t-test was used as to compare between WT IRF1 and a candidate IRF1 mutant type in terms of relative K6-polyubiquitination level. Values were from three independent experiments. Densitometric analysis were carried out using ImageJ software.

3.2.4. **K233 is not a major IRF1 C-terminal ubiquitin acceptor**

The IRF1 C-terminus was evaluated to harbour of ubiquitin acceptor sites for K6, K48, or K63-polyubiquitination. IRF1 K233R mutant was received later, and we aimed for determination of the role of IRF1 C-terminal K233 on WT-polyubiquitination and K63-polyubiquitination. In this experiment, we carried out the same sequential technical steps to ascertain whether IRF1 K233 was an ubiquitin acceptor and whether it was critical for WT-polyubiquitination or K63-polyubiquitination. Here, HEK293 cells were co-transfected with FLAG-IRF1 K233R alongside one expression either-Myc-6XHis-Ubitiquitin WT or Myc-6XHis-ubiquitin K63-Only and Western Blot results were compared with the relative polyubiquitination (WT or K63) levels of IRF1-WT (Fig 3.7). IRF1 (WT or K233R) resulted in successful expression at 50 kDa. However, the levels of IRF1 expressions were not equal. In the case of Co-transfection of ubiquitin-WT with IRF1 (WT or K233R), the level of basal IRF1 expression was decreased compared with co-transfection of IRF1 with ubiquitin K63-Only as shown in Fig 3.7.A. When ubiquitin K63-Only was co-expressed, K48-polyubiquitination and K11-polyubiquitination were blocked and this prevented IRF1 proteasome degradation, leading to the accumulation of expressed IRF1 (lane A 4 and 5). This also was noticed at the level of K63-polyubiquitination of IRF1 (WT or K233R) as shown in Fig 3.7.B. Where nickel beads, purification of His-tagged proteins were immunoblotted with α-FLAG. Also, that difference may be due to the accumulation of K63-polyubiquitinated-IRF1. The main focus that K233 has no significant difference effect on the relative level of IRF1 ubiquitination, neither with WT ubiquitin nor K63 ubiquitin as compared with WT IRF1, as shown in Fig 3.7.C.

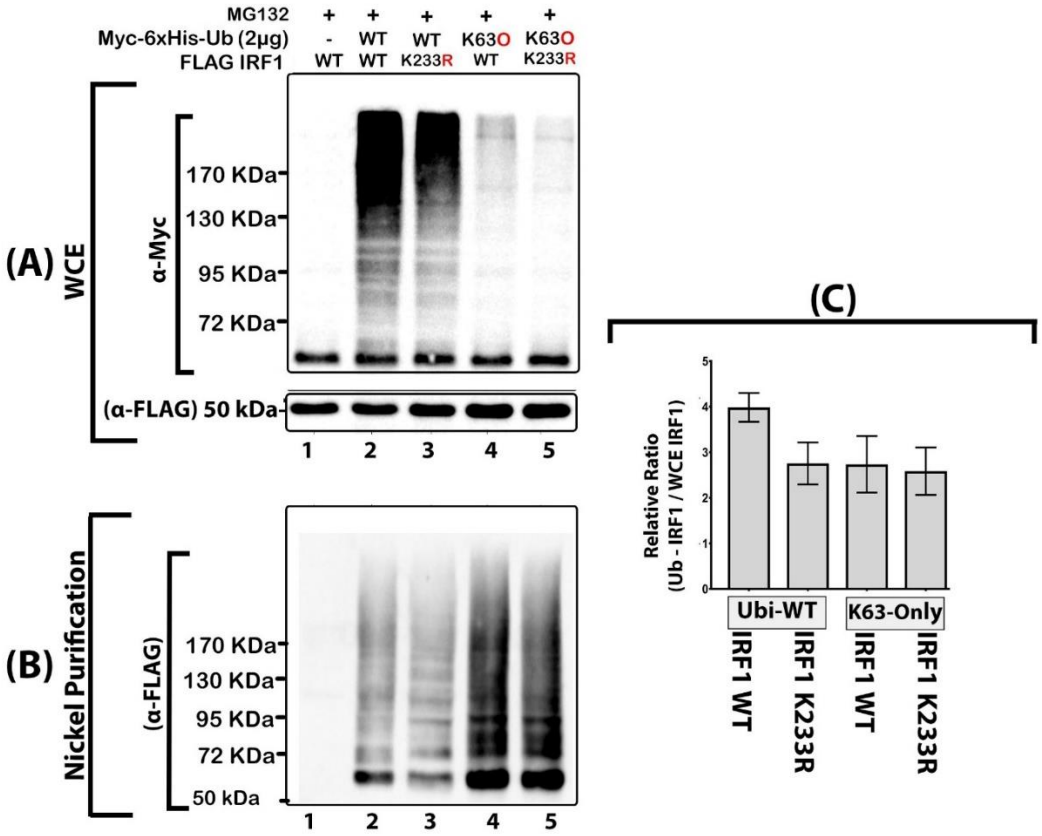

Fig 3.7. IRF1 K233 has a weak impact on formation of WT polyubiquitination and K63-polyubiquitination.

(A) Western Blot of WCE of FLAG-IRF1 (WT or K233R) alongside-Myc-6XHis-ubiquitin (WT or K63-Only) matching overexpression in HEK293 for 2 days followed by treatment with MG132(10µg/ml) for 3 hours and cells were collected and lysed with 8% urea lysis buffer. WCE proteins (FLAG-IRF1,-Myc-6xHis-ubiquitin) detection where carried out using α FLAG and α-Myc, respectively at the same blot. **(B)** Western Blot data from overnight incubation of the large remained WCE with Nickel beads to allow 6XHis-ubiquitinated proteins to interact with nickel followed by elution and the supernatant was immunoblotted with α FLAG to detect Ub-IRF1 accordingly. **(C)** Graph represents Average ubiquitination level of IRF1 (WT or K233R) with either WT ubiquitin or ubiquitin K63-Only. Error bars reveal the Standard error of Mean (SEM), student t-test was used. Values were from three independent experiments. Densitometry numerical data using ImageJ software and the Average ubiquitination level of IRF1 was a subsequent outcome of subdivision the in10sity of B bans by FLAG-IRF1 (A) bands.

3.3. FBXW7α stimulates K48 and K63-polyubiquitination.

As reported in the introduction, ubiquitination requires an enzymatic cascade, summarised as the activation by E1, followed by conjugation by E2 and finally the ligation of an ubiquitin molecule to a substrate by an E3 ligase enzyme. E3 ligases are categorised mainly into two families: RING and HECT. Those ligase enzymes are formed by converging of different small proteins together to function properly. Such as SKP1-Cullin-1 Fbox proteins (SCF) E3 complex. The component is known as Fbox WD40-repeats α isoform (FBXW7α) functions in substrate binding and triggering other SCF E3 ligase components to ubiquitinate this substrate in RING sequential manner. FBXW7α brings protein substrates to the SCF as the largest member of E3 ligases (Sun and Li, 2013). FBXW7α mainly binds to phosphorylated residues on its substrate protein to be ubiquitinated, referred as phospho-degrons motifs. FBXW7α can dimerize with another FBXW7α polypeptide to function together on one candidate substrate on different phospho-degrons or even different substrates. We, therefore, investigated whether FBXW7α overexpression improved IRF1 ubiquitination and ascertained types of this polyubiquitination. First of all, we optimised the required amount of Myc-6XHis-ubiquitin WT plasmid (either 0.5 µg or 1.0 µg) overexpressed with FLAG-IRF1 WT to enable the detection of the concurrent overexpression of HA-FBXW7α expressing plasmid on the level of IRF1 WT-ubiquitination. As shown in Fig 3.8, the co-expression of 1 µg of 6XHis-Myc-ubiquitin WT resulted in a robust increase of Ubiq-IRF1 pulled down by affinity purification and detected with the α-FLAG antibody when co-expressed with HA-FBXW7α. As such, FBXW7α recruits

ubiquitination of IRF1 and, therefore, 1 µg of 6XHis-Myc-ubiquitin in subsequent experiments was used.

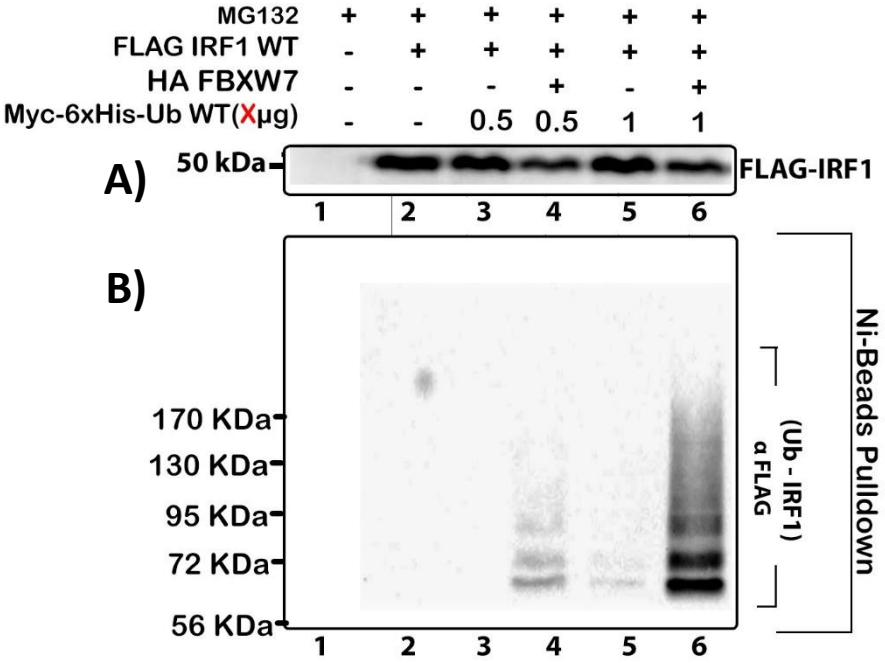

Fig 3.8. Optimization the required Amount of Myc-6XHis-ubiquitin to enable the observation the Effect of FBXW7α.

(A) Western Blot of WCE of FLAG-IRF1 and 2 different amounts of-Myc-6XHis-ubiquitin WT overexpression in HEK293 with or without HA FBXW7a for 2 days followed by treatment with MG132(10µg/ml) for 3 hours and cells were collected and lysed with 8% urea lysis buffer. WCE proteins (FLAG-IRF1,-Myc-6xHis-ubiquitin) detection where carried out using α FLAG and α-Myc, respectively at the same blot. **(B)** Western Blot data from overnight incubation of the large remained WCE with Nickel beads to allow 6XHis-ubiquitin WT associated proteins to interact with beads followed by elution and the supernatant was immunoblotted with α FLAG to detect the effect of HA FBXW7a on the level of Ub-IRF1.

We next examined whether IRF1 modification is enhanced with a specific type of polyubiquitination (K6, K48, and K63 chain) by FBXW7α. To achieve that HEK293 cells were co-transfected with 1 µg of 6XHis-Myc-ubiquitin different expressing plasmids used in the current study (WT, K6-Only, K48-Only, and K63-Only), with or without HA-FBXW7α. FLAG-IRF1 WT was co-expressed in all conditions. Cells were collected and lysed followed by western blot. As shown in Fig 3.9.A, the immunoblot with the α-Myc antibody on WCE ubiquitinated proteins were not equal between different wells. This revealed that E3 ligase enzyme affected all cellular proteins in specific types of polyubiquitination modification. This was revealed that the ubiquitination smeary bands in the case of co-transfection of FBXW7α showed higher intensity level of ubiquitinated proteins than the other non-co-transfected FBXW7α. To ensure that HA-FBXW7α was successfully overexpressed, other WCE proteins were examined by Western blot using α-HA antibody which resulted in the detection of FBXW7 α in lysate between 56-72 kDa, above IRF1 bands and at the same range of monoubiquitinated IRF1 marker level. It might be the other components of E3 ligase enzyme interacted with FBXW7α. Next Fig 3.9.B, we tried to detect whether HA-FBXW7α enhanced a particular type of IRF1-polyubiquitination. The same nickel beads purification technique used on to capture ubiquitinated proteins, followed by immunoblot with α-FLAG to detect IRF1-Ub-(WT, K6-Only, K48-Only, or K63-Only)**.** In Fig, 3.9.C where average IRF1-ubiquitin was estimated from at least 3 replicates resulted in a significant increase in the level of WT, K48, or K63-polyubiquitination of IRF1 was detected in response to FBXW7α. However, FBXW7α caused a no

significant increase in the IRF1 average K6-polyubiquitination level when compared with ubiquitin K6-Only without FBXW7α transfection. Intriguingly, the IRF1 average level of WT polyubiquitination in the presence of FBXW7α (bar graph 2) was collectively equal to the consensus sum of average IRF1 K6-Only, K48-Only, and K63-Only polyubiquitination levels of bar graphs 4, 6, and 8. This was logic that the enzymatic cascade could recruit multi-substrates or multiple phosphors- degron residues of the same substrate for a specific type of polyubiquitination,

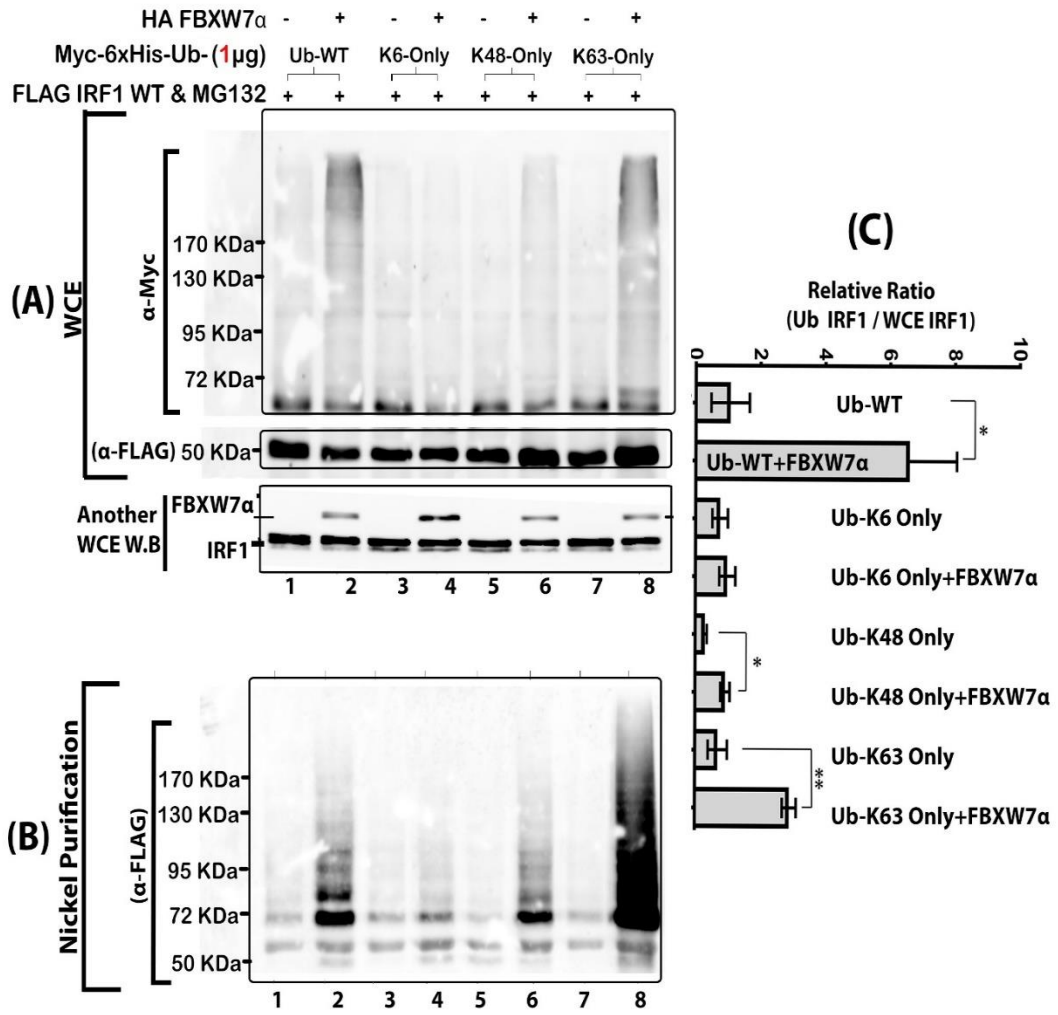

Fig 3.9. FBXW7α stimulates IRF1 for K63 and K48-polyubiquitination of IRF1.

(A) Western Blot of WCE of FLAG-IRF1 and-Myc-6XHis-ubiquitin (WT, K6-Only, K48-Only, or K63-Only), and with or without HA FBXW7α for each single type of ubiquitin plasmid. Overexpression occurred in HEK293 cells for 2 days followed by treatment with MG132 (10µg/ml) for 3 hours and cells were collected and lysed with 8% urea lysis buffer. WCE proteins (FLAG-IRF1,-Myc-6xHis-ubiquitin) detection where carried out using α FLAG and α-Myc, respectively at the same blot. In another WCE western blot HA FBXW7α was investigated using α HA. **(B)** Western Blot data from overnight incubation of the large remained WCE with Nickel beads to allow 6XHis-ubiquitin to interact with beads, followed by elution and the supernatant was immunoblotted with α FLAG to detect Ub-IRF1. **(C)** Graph represents Average ubiquitination level of IRF1. Error bars represent the Standard error of Mean (SEM), student t-test was used. Values were from three independent experiments.

Conclusions of IRF1 polyubiquitination

In summary, the experiments in this study have successfully detected the ubiquitination of IRF1 in HEK293 cells where the mutation of IRF1 C-terminal Lysines indicates that K240 is the major site for K48-polyubiquitination. However, other minor sites may be able to be modified by this type of polyubiquitination event. FBXW7α was found to enhance polyubiquitination of IRF1 via K48 and K63 type of linkages, but not K6-polyubiquitination. This may be expected as experiments were not performed under conditions of DNA damage which stimulates K6-polyubiquitination. The data is schematically shown in Fig 3.10.

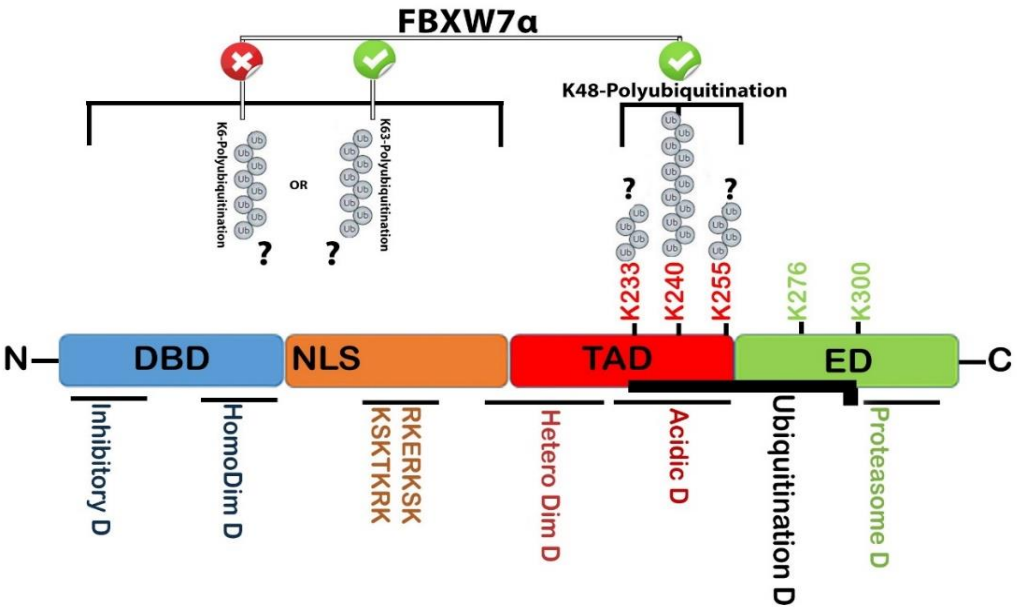

Fig 3.10. Schematic Diagram of IRF1 selected polyubiquitination Domains.

Ligase E3 complex component FBXW7α increased the level of IRF1 modification through the formation of K48-polyubiquitination and K63-polyubiquitination, but not K6-polyubiquitination. IRF1 K48-polyubiquitination modified IRF1 through the formation of an isopeptide linkage with IRF1 K240 as a major acceptor residue for this type of modification. Whereas, other adjacent residues might be altered as minor residues. Modification of IRF1 by K6- and K63-polyubiquitination were formed outside TAD and ED, not known where exactly the main acceptors for those types of modification.

3.4. IRF1 TAD Lysine Amino Acids are essential for Activity

Having determined that IRF1 C-terminal lysines are critical for its modification by ubiquitin, we next assessed the effects of K-R mutation on IRF1 transcriptional activity in reporter assays. The transactivation domain (TAD) of IRF1 binds to co-activators or co-repressors. We focused on certain residues within TAD (K233, K240 and K255). We conducted gene reporter luciferase assays in the MRC5 cell line co-transfected with the IRF1 K-R mutants and the Interferon Stimulatory Response Element promoter-luciferase (4X-ISRE-luc) as shown in Fig 3.11.A. IRF1 K233R, IRF1 K240R, or IRF1 K255R significantly decreased the IRF1 reporter luciferase transcriptional activity compared with IRF1 WT. Whereas IRF1 K276 or K300R, did not cause a significant difference in reporter activation. Although, K300R and K276R showed more average experimental variability as indicated. The variability of data had the possibility that the K-R substitution within Enhancer Domain changed the conformational structure of IRF1 or affected the stability of the protein. Western Blot detection showed IRF1 proteins were equally expressed (Fig 3.11.B). This indicated the expression level of IRF1 is not altered by the C-terminal mutation. Except for K300R which increased the stability of IRF1 rather than IRF1 expression because K300 resides at the start of IRF1 C-terminal proteasomal degradation recognition motifs and its mutation to Arginine affected the recognition of ubiquitinated-IRF1 by the proteasome. In conclusion, IRF1 (K233, K240, and K255) located within the TAD are essential for IRF1 transcriptional activity. These data to some extent was consistent with the data of the ubiquitination acceptor site where IRF1 K240 has been concluded to be the major key site for ubiquitination. The indication was that

attachment of co-activators, such as E3 ligases, to enhance IRF1 ubiquitination required the total TAD integrity to function correctly. Also, IRF1 K240 was suggested to interact with ubiquitin directly.

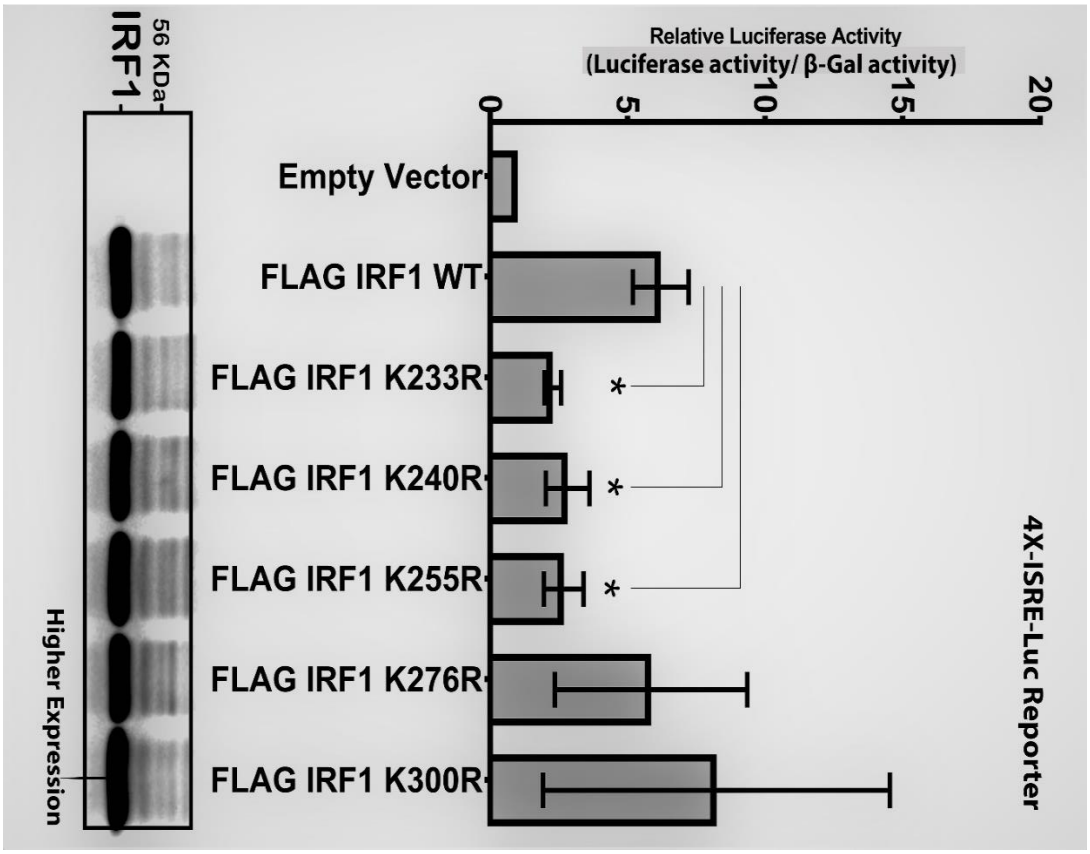

Fig 3.11. C-terminal TAD Lysine amino acids are required for IRF1 transcriptional activity.

The graph shows RLA of IRF1. MRC5 cells transfected with 2ng βGAL, 50ng IRF1 and 75ng 4X-ISRE-Luc for 48 hours. Cells were collected, and Luciferase assay was done. Results were normalised with βGalactosidase activity and presented as a fold induction of empty vector, where empty vector luciferase activity was equalised as 1 (RLU). Data were from 4 independent experiments carried out in triplicate. Error bars denoted the Standard Error of Mean (SEM) and (*) represented the significant difference as determined by Students t-test ($p<0.05$). Western Blot from our lab works where IRF1 K-R mutants were transfected in HEK293. Two days left then treated with MG132 (10µg/ml) for 3 hours and harvested and western blot was carried out. The primary antibody α-FLAG was used to quantify IRF1.

3.5. C-terminal K-R mutations alter IRF1 Turnover

Cycloheximide reagent inhibits the protein biosynthesis due to its prevention of translational elongation and cells treated at zero point cycloheximide are prevented from *de novo* protein synthesis. This enables protein half-life to be determined at different time intervals. Based on this, we identified the importance of C-terminal Lysine amino acids residues on IRF1 stability. FLAG-IRF1 has a short half-life (20-40 min). It is well known that K48-polyubiquitination of IRF1 brings about protein degradation. To achieve this aim, Cycloheximide (CHX) time chase was carried out in the MRC5 cell line co-transfected with IRF1 WT and mutant expression plasmids. As shown in Fig 3.12.A, FLAG-IRF1 WT half-life was nearly 30 minutes, and this was consistent with previous reports. Total degradation of FLAG-IRF1 was observed after 1 hour. All other FLAG-IRF1 (K-R) showed slower degradation rate as compared with FLAG-IRF1 WT. Especially IRF1 K300R. Although IRF1 K240 showed rapid degradation nearly equal to IRF1 WT. This requires more elucidation because the level of β-Actin of IRF1 K240R was not equally expressed. However, after the quantification of each IRF1 bands and normalising them with their β-Actin, the below Fig 3.12.B indicates K240R stabilised IRF1 longer than two hours followed by K233R which has higher half-life compared with IRF1 WT but frequently IRF1 steadily degraded at 60 minutes. Moreover, this experiment was carried out once, and further investigation in the future for statistical analysis was required. Unfortunately, there was not enough time to repeat the experiment.

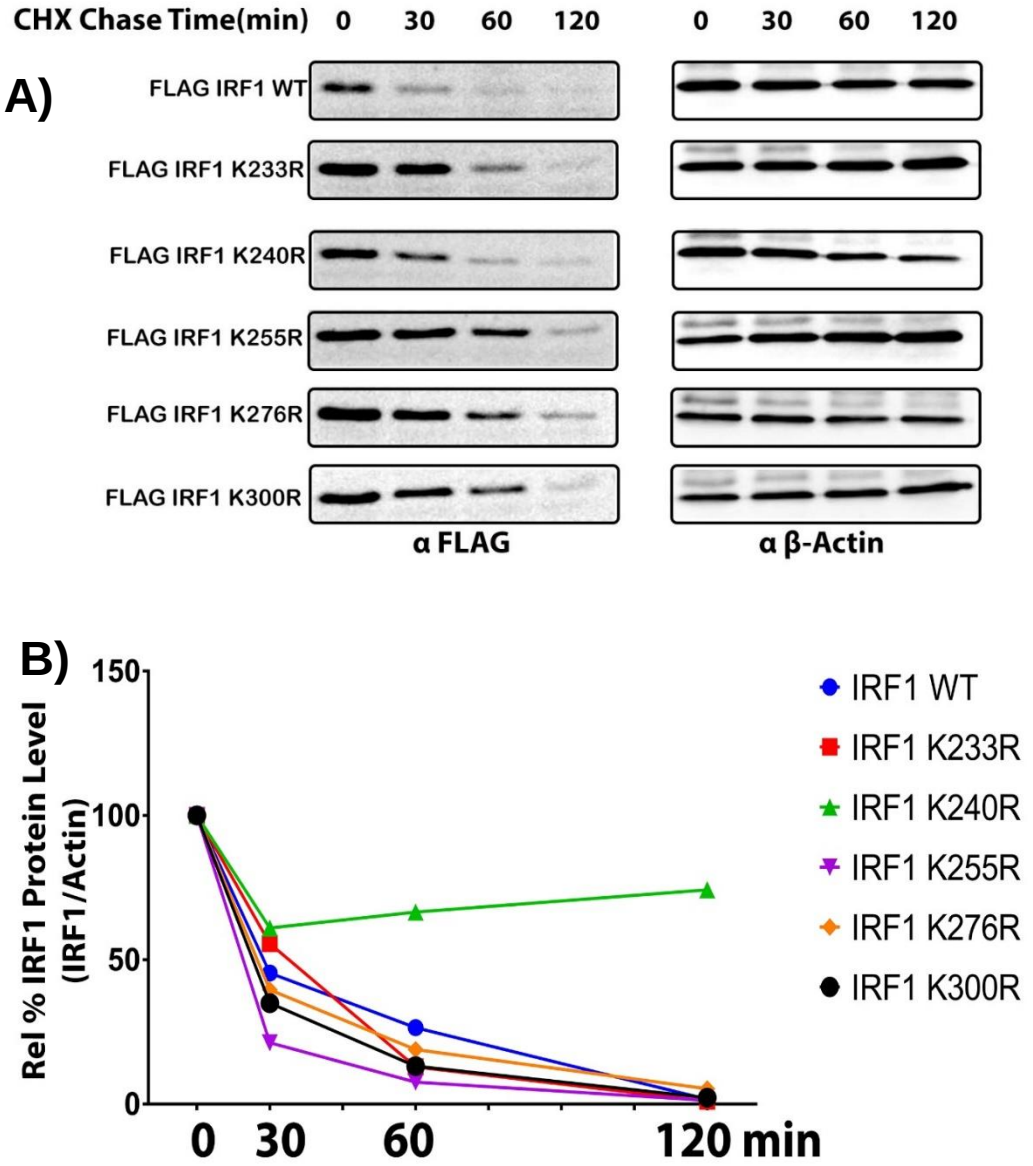

Fig **3.12. IRF1 C-terminal Lysine amino acids appear to regulate IRF1 stability.**

(A) MRC5 cell line was cotransfected with different FLAG-IRF1 expression plasmids. Cells were incubated up to two days. Cycloheximide reagent was added to each plate (25 µg/ml) at time intervals of (zero, 30 minutes, 1 hour, and 2 hours), to block any further transcription of IRF1 and this gave an opportunity to measure expressed IRF1 proteins. After CHX treatment cells were harvested using 50 µl RIPA buffer (0.1 % SDS) and Western blot was carried out into WCE. The antibody (α FLAG) used to detect different FLAG-IRF1, and the same blots were incubated with (α Actin) later. **(B) Curve** line represents the relative percent of IRF1 stability over 30, 60 and 120 minutes. The experiments have been carried out once so this data just for normalisation of Pilot study and for statistical analysis it is required to be repeated at least 3 times.

Conclusions on IRF1 K-R mutation on Stability and Activity of IRF1

In summary, the IRF1 C-terminal TAD lysines are required for IRF1 transactivation. K233, K240, and K255 are essential for activity, and the relation between K240 as a primary C-terminal ubiquitin acceptor and IRF1 transcriptional activity requires more clarification. Moreover, IRF1 C-terminal lysine amino acids are necessary to keep IRF1 stability within its reasonable limits. Hence, any mutation within these residues may stabilise the protein due to defective protein-protein interactions or even introduces hitherto IRF1 structure unable to be detected by the proteasome. In addition, FBXW7α may play a role in the connection between stability and activity as shown in Fig 3.13.

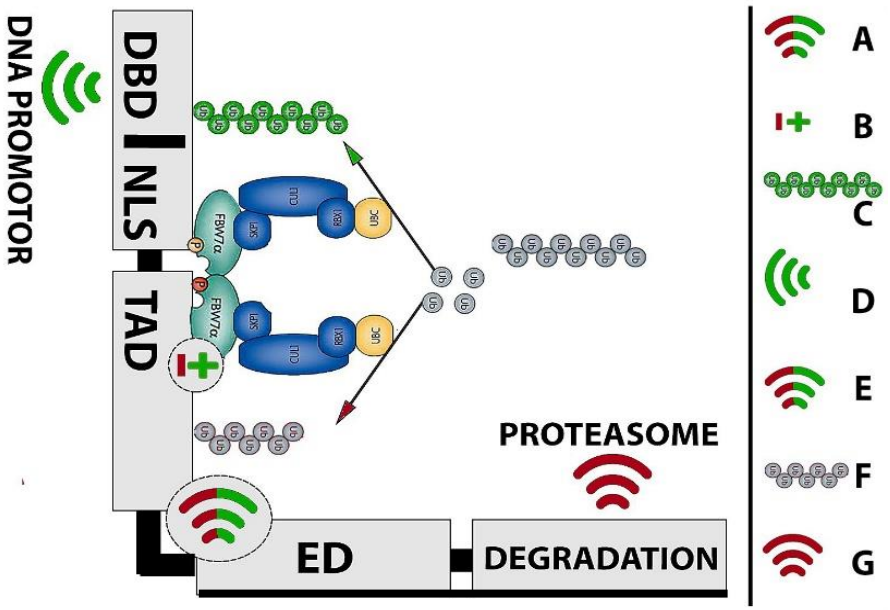

Fig 3.13. FBXW7α possible Sequential IRF1 mediated IRF1 activation and Degradation.

A) ED first 25 amino acids possess the cofactor-binding motif that mediates coactivators/ corepressors interaction with TAD. **B)** TAD interacts with coactivators/ corepressors which recruits other regulatory proteins to modulate IRF1 modification. For instance, certain coactivator mediates FBXW7α binding to phosphor degrons within ED which triggers IRF1 polyubiquitination within TAD or N-terminus. **C)** FBXW7α mediates N-terminal K63-polyubiquitination. **D)** IRF1 DBD acquires new conformational interface and interacts with DNA element to activate certain cellular signalling. **E)** After IRF1 activation of Gene promoter or certain enhancer downstream sequence, ED permits other coactivators/corepressors to recruit another FBXW7α (dimerization) to induce K48-polyubiquitination of IRF1 C-terminal K240. **F)** K48-polyubiquitination of IRF1 K240 as a primary acceptor residue mediates the activation of the farthest part of ED (Degradation). **G)** Degradation domain calls for IRF1 the proteasomal degradation which interacts with IRF1 K48-polyubiquitin through UIM

3.6. SUMOylation of IRF1?

This study tested whether SUMOylation of IRF1 could be detected using HEK293, and what is the molecular mechanism that regulate the interplay between SUMO1 and ubiquitin? To achieve this aim, we firstly had to show that IRF1 was SUMOylated. To perform this experiment, HEK293 cells were co-transfected with FLAG-SUMO1 with pCDNA3 IRF1 and cells were lysed with RIPA buffer and Western blot was carried out to check WCE (Fig 3.14). Co-IP was conducted to identify SUMOylated-IRF1. Sequentially, the WCE was incubated overnight with the α-FLAG antibody followed by the incubation with magnetic agarose beads to capture FLAG-SUMO-IRF1. Finally, immunoprecipitated proteins were analyzed using Western blot and primary antibody was α-FLAG followed by another primary α-IRF1 (Fig 3.14). The results in Fig 3.13 revealed IRF1 was successfully expressed. Interestingly, higher IRF1 expression levels at lanes 3, 4 and 5 were noticed, where the co-transfection of SUMO1 was done, compared with the IRF1 alone at lane 2. This indicates that SUMO1 enhanced the stability of IRF1. As shown in Fig 3.13 many proteins, detected by Western blot with α-FLAG, were SUMO1-ylated in normal non-cancerous HEK293, and there was a specific band at lane 4 within the range of 95 kDa, which might be SUMO1-IRF1. Unfortunately, the immunoblotting with α-IRF1 did not reveal any particular band on the expected range of SUMO1-IRF1 of 61 kDa-95 kDa. We were unable to detect SUMO1-IRF1 complexes. This may be due to the masking of IRF1 protein on the blot by IgG Heavy and Light chains. In addition to that, Sumoylation of proteins constitutes lower than 1% of the protein proportion. Thirdly, we overexpressed SUMO1 in non-cancerous cells which affected the

SUMOylation machinery required pathway. Finally, proteases enzymes could break down the interaction and this is thr reason behind the inability to detect SUMOylated proteins.

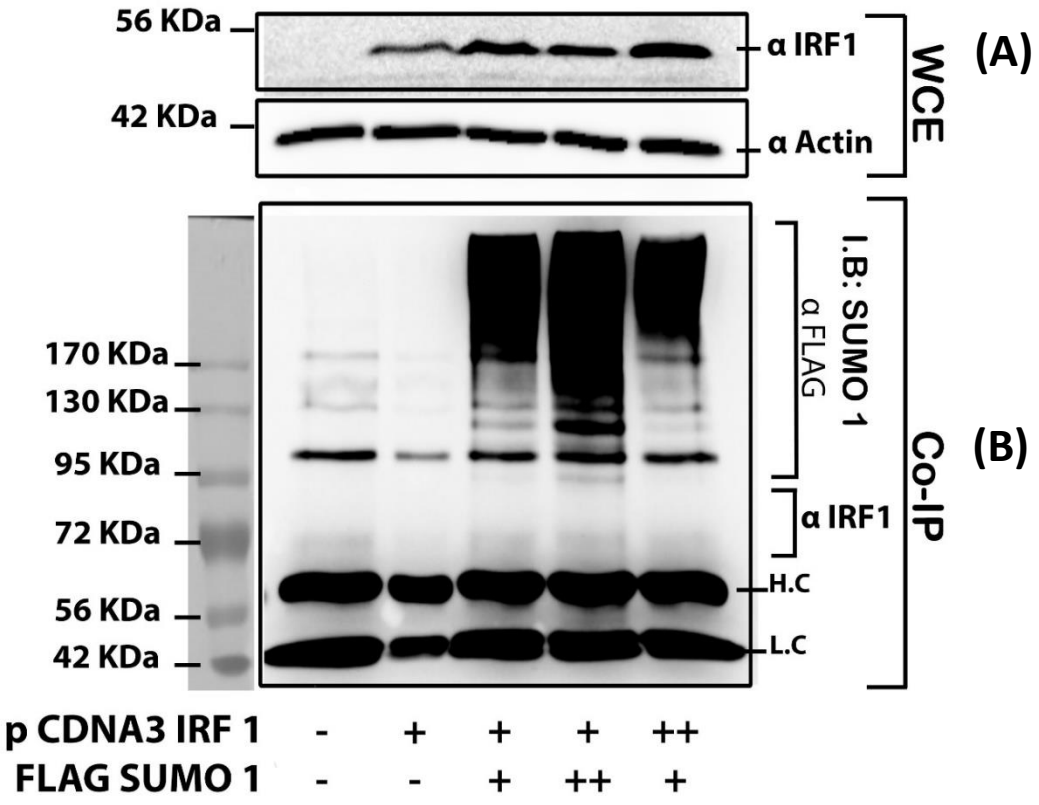

Fig 3.14. IRF1 and SUMO1 Western Blot Detection.

(A) HEK293 cells were co-transfected with FLAG SUMO1 alongside pCDNA3 IRF1 or their double amounts (4µg plasmid for up (++) legend). Cells were harvested after two days, and RIPA buffer lysed the cells (1% SDS). Followed by SDS-PAGE running of WCE. Western Blot was carried out incubating the cellulose paper with first α M20 (α IRF1). **(B)** Co-IP was performed for WCE. Incubated for 2 hours with α FLAG followed by addition of magnetic Protein G-agarose beads which gave better blot clarity than standard non-magnetic beads. Finally, α M20 used as a primary antibody to detect SUMO1-IRF1 by western blot. Followed by addition of α FLAG to identify any other SUMOylated proteins. NEM was added to all samples to prevent deSUMOylation by SENP enzymes.

Chapter 4

Discussion and Conclusions

DISCUSSION AND CONCLUSIONS

4.1. polyubiquitination linkages to IRF1 are Domain Selective.

The data generated reveals that IRF1 can be polyubiquitylated within the C-terminal domain (Fig 3.3), and IRF1 C-terminal K240 is the major ubiquitin acceptor, especially for K48-polyubiquitination (Fig 3.5). Also, IRF1 modification by K6-polyubiquitination and K63-polyubiquitination are successfully identified, suggesting the presence of other IRF1 domains of ubiquitin acceptors of K63 and K6-polyubiquitination as shown respectively in Figs 3.6.B and 3.7.B. However, the IRF1 C-terminal K-R mutations did not alter the average K6-polyubiquitination, nor K63-polyubiquitination in Fig 3.7.C and 3.6.C, which indicates that those types of linkages do not target IRF1 C-terminal modification. The inability of C-terminal K63-polyubiquitination detection is consistent with other research reporting that K63-polyubiquitination, but not K48-polyubiquitination, modifies the IRF1 N-terminal domain (Harikumar et al., 2014). Our results are also consistent with reports that K6-mediated polyubiquitination of IRF1 is observed only under conditions of DNA damage (Shang et al., 2005), (Lin and Man, 2013). In conclusion, IRF1 N-terminal DBD may possess a ubiquitin Lysine acceptor site for K63-polyubiquitinaion and IRF1 C-terminal harbours K240 which is the major K48-polyubiquitination, whereas K6-polyubiquitination, known to abolish IRF1 proteasome detection through alteration of IRF1 conformational structure, might require other conditions to be precisely detected, such as DNA damage (Lin and Man, 2013).

4.2. TAD is essential as acceptor for K48-polyubiquitination.

As a complementary study for (Pion et al. 2009) that ED K276 and K300 are not ubiquitin acceptors but other lysines are considered for this modification, we found that K240 is the primary ubiquitin acceptor site for the major K48-polyubiquitination. Also, the K48-polyubiquitination is not restricted to K240 only, but also there are other K48-polyubiquitination adjacent lysines considered as minor acceptors. These lysines do not reside within the N-terminus based on the report mentioned before that N-terminal is the primary acceptor domain for K63-polyubiquitination, and K48-polyubiquitination modifies the C-terminal domain. Subsequently, those sites are K233 and K255 which reside within the C-terminal TAD. Our results also showed that K240 amino acid located downstream on IRF1 C-terminus has a significant impact on the majority of IRF1 polyubiquitination, and the same amino acid controls the level of K48-polyubiquitination in particular. This confirms the research of (Pion et al. 2009), in tandem with reported literature (Thrower et al., 2000) that K48-polyubiquitination is the primary ubiquitin modification of IRF1. Concluding that, the enhancer domain is necessary for other components of ubiquitination signalling, such as E3-ligase reaction towards IRF1 and it does not appear that the lysine amino acids within this domain are acceptors for ubiquitination of IRF1. Hence, the ubiquitin acceptor lysine/s reside on the C-terminal domain within the TAD (K233, K240, and K255) located directly beside the enhancer domain.

4.3. Coactivator or repressors Recruitment to TAD.

4.3.1. Uncoupling polyubiquitination and Proteasome Recognition.

Pion et al (2009) mentioned that the ED contains 2 major subdomains; the first 25 amino acids permits or inhibits the recruitment of coactivators or corepressor to bind with TAD. Subsequently, the transcriptional activity and protein-protein interactions are regulated by first 25 amino acids of the ED. The remainder of the ED receives a signal of K48-polyubiquitin chain linked to IRF1 for the proteasomal degradation. Their conclusions are based on the truncation studies of IRF1 301-325 which abolished proteasome degradation, meanwhile the polyubiquitinated-IRF1 accumulates. Truncation studies of the entire ED (256-325 amino acids) entirely abolished the polyubiquitination of IRF1.

4.2.2. TAD is not sufficient alone to activate polyubiquitination.

As mentioned above, the IRF1 K240 resides within the TAD is the ubiquitin acceptor as shown in this study. This polyubiquitination requires an enzymatic cascade machinery and as reported before that the ED contains a motif for E3 signalling pathway (265-300 residues), but not an E3 acceptor (Pion et al., 2009). Subsequently, the ED truncation studies abolished entire IRF1 polyubiquitination, where the truncation of the ED (300-325 residues) prevented the proteasome-dependent degradation and the polyubiquitination was still detected (Pion et al., 2009). This suggested a role of ED to ensure the balance of IRF1 steady state level and the required level of IRF1 activation via signalling mediated by the first motif of ED (265-300) and the proteasomal degradation mediated by the other ED degradation motif. Our results

confirmed the IRF1 point mutation within the ED K300R, located at the end of first ED. This increased the stability and accumulation of polyubiquitinated IRF1 (Fig 3.13) and (Fig 3.3) respectively. The point mutation of K300R leads to polyubiquitin-IRF1 accumulation because the ED first subdomain area is thought to be activated as toK48-polyubiquitination of ED.

4.4. TAD Lysines and Transcriptional activity of IRF1.

IRF1 TAD is essential for transactivational activity of IRF1 (Dou et al., 2014). The relationship between TAD ubiquitination and the transcriptional activity of TAD is still ambigous. The reporter luciferase activity assay revealed that K-R mutations within the TAD lessened the IRF1 transcriptional activity (Fig 3.11), and this is consistent with the view that the TAD is important target for coactivator/corepressors binding. The loss of transcriptional activity of IRF1 TAD K-R mutations may arise from diminished cofactor interactions with a specific lysine. K300R and K276R did not affect the transcriptional activity of IRF1, it might slightly change the conformational IRF1 structure, especially because their location within ED. It is possible that different types of ubiquitin linkage mediate different regulatory cofactors or various types of polyubiquitination on IRF1 lysines to modulate the conformational structure of IRF1. This, in turn, mediates its recognition by other regulatory proteins harbouring ubiquitin interactive motifs (UIM) in a ligand-receptor manner or expose the IRF1 DBD for binding to gene promoters or enhancer sequences which in turn alters the transcriptional activity of IRF1 protein. For instance, it has been shown that IL1 overexpression induces *IRF1* expression through recruitment of the inhibitor of apoptosis (cIAP2) to activate IRF1 protein through the cIAP2 converging on certain IRF1 domain with other regulatory

factors, most probably on TAD, to mediate the conjugation of the preformed K63-polyubiquitin chain conjugated with E3 TNFα Receptor-Associated Factor 6 (TRAF6) to ligate it with the IRF1 N-terminal K75, K78, K95, and/or K101 amino acids (Upreti and Rath, 2005). Subsequently, IRF1 acquires a new conformational structure modification by K63-polyubiquitination which can be detected by IRF1 promoter of chemokines *(CCL5 and CXCL10)* to be expressed and directed to the sterile inflammation sites (Harikumar et al., 2014). TRAF6 mediates IRF1 polyubiquitination as an E3 RING ligase enzyme, whereas cIAP2 is the coactivator. Meanwhile, cIAP2 does not recognise other E3 ligases that carry K48-polyubiquitination. As such, IRF1 does not acquire the conformational structure required for proteasome recognition, and IRF1 degradation pathway is avoided. Instead, IRF1 is targeted for cellular signalling pathways mediated by K63-polyubiquitination on the N-terminus. Also, these experiments revealed that TRAF6 does not ligate its K63-polyubiquitin to IRF1 C-terminus (Harikumar et al., 2014).

4.5. FBXW7α Dimerization might amplify Multipolyubiquitin.

The E3 ligase FBXW7α orchestrates the transfer of either K63-polyubiqutination or K48-polyubiquitination to a variety of protein substrates because the E3 complex can dimerize as previously illustrated in Fig 1.7 and 3.13. The selectivity of FBXW7α does not only modulate IRF1 for degradation via K48-polyubiquitination. It also mediates K63-polyubiquitination and subsequently induces IRF1 cellular signalling in tandem. This leads IRF1 to the proteasome-dependent degradation afterwards to ensure steady state level of IRF1 between its activation and degradation. This partially confirms other literature which commented on the role of the SCF E3 complex to bring

about the protein degradation (Welcker and Clurman, 2008). Our results introduce a novel approach that FBXW7α can ubiquitinate IRF1 on different acceptors on IRF1 domains (Fig 3.11, Fig 3.13). This indicates that IRF1 has the possibility to be multi-ubiquitinated which is consistent with previous studies (Komander and Rape, 2012). The E3 enzyme specifically mediates the transfer of individual polyubiquitin chains to link with a particular IRF1 domain to confirm that IRF1 is suitable for UIM groove on regulatory acceptor molecule to modify IRF1 stability or to be exposed to DNA gene element, and finally, the transcriptional activation is analysed. Hence, coactivators trigger IRF1 specific polyubiquitination that refers IRF1 in a suitable particular conformation for transactivation. So lysine is required for IRF1 activity before proteasome-dependent degradation, or even ubiquitination facilitates ubiquitin interaction to UIM at the19S proteasome cap. Finally, the proper sequence of modification is binding of IRF1 to coactivators FBXW7α to enhance IRF1 activity by K63-polyubiquitination which triggers K48-polyubiquitination that simultaneously activates IRF1 activity and promotes its degradation.

4.6. Why was SUMO1ylation of IRF1 interaction not detected?

Reports in the literature suggest that SUMO protein modifies IRF1 but we were unable to replicate these findings in HEK293T cells. There are a variety of possible explanations for this. Typically, only a small fraction (<1%) of a given protein is SUMOylated and being reversible and SUMO1 is easily to be removed by specific SUMO proteases, such as SENP. In budding yeast, the SUMO protease (Ulp1) is bound at the nuclear pore, whereas SUMO protease (Ulp2) is a nucleoplasmic enzyme. The distinct subnuclear localisation of SUMO protease enzymes is conserved in higher eukaryotes (Mukhopadhyay

and Dasso, 2007). SUMO1 has only one ψKxD/E consensus sequence, as a consequence, it has no ability to form detectable polySUMOylation itself unless the binding to another chain of SUMO2/3 and terminate its elongation. However, SUMO2/3 is activated only under cellular stress so to enable SUMO1 detection we should expose the cells to stress to activate other factors, SUMO-2/3 modifications seem to be involved specifically in the stress response (Saitoh and Hinchey, 2000) (Geoffroy and Hay, 2009) (Matic et al., 2008). SUMOylation *in vitro* requires the overexpression of Ubc9 E2 overexpression and media supplemented with cellular cytosol as a source of essential E1 enzyme to activate SUMO1 activation and ligation to substrate protein (Hilgarth and Sarge, 2005), as shown in Fig 4.1. Intriguingly, Ubc9 is important for SUMOylation of IRF1 *in vivo* in tumourigenesis of ovarian cancer (Park et al., 2007). Because SUMO1 appeared to be observed only under stress so endogenous SUMO1 cannot be detected without *in vivo* overexpression, not only that but also SUMO1ylated IRF1 cannot be detected without Ubc9 overexpression *in vitro* (Kim et al., 2008). The same group found that Ubc9 and PIAS3 are overexpressed in ovarian cancer, and they showed that SUMOylated proteins are present in cancer to enhance tumourigenic ity. This was evident from their experiments using non-cancerous MRC5 versus MCF7 (Breast Cancer cells). They detected SUMO1-IRF1 in MCF7 cells, not in MRC5 control cells, not only that but also they found that SUMOylated IRF1 appeared as multiple bands, and this gave an indication that SUMO1 can form polySUMOylation with SUMO2/3 in cancerous cells (Park et al., 2007).UBC9 interaction to DBD and SUMO interaction with Enhancer domain may make protein conformational changes and prevent any protein-protein interaction or

recognition by any other cellular proteins such as proteasome components, ubiquitin components or others. For that reason, SUMO1 and ubiquitin may not compete on the same site.

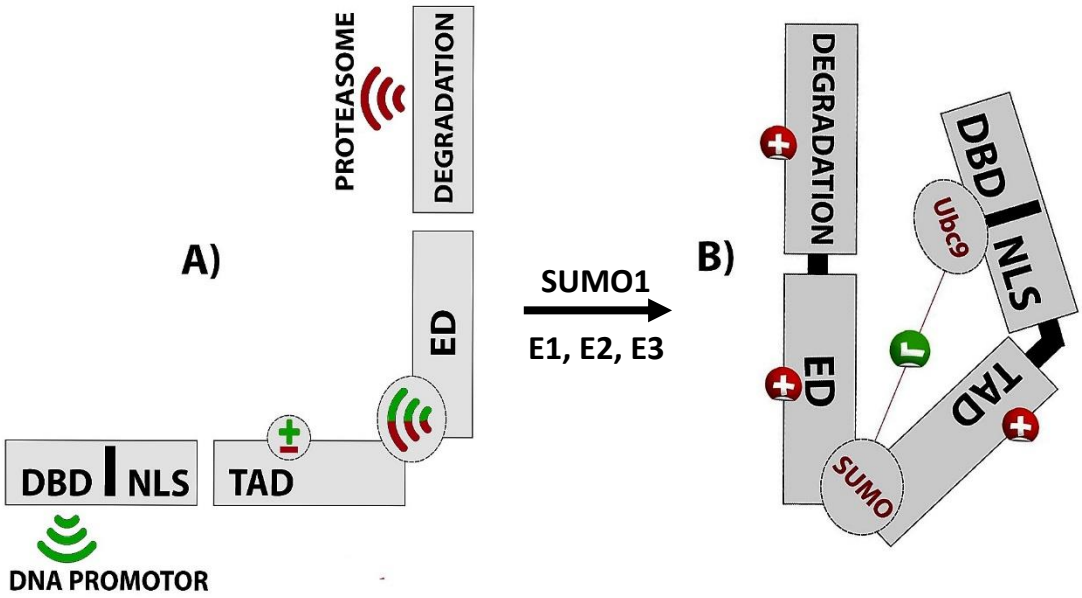

Fig 4.1. Schematic summarises IRF1 Mediated Structural modulation by SUMOylation.

(A) Conformational structure that enbles IRF1 to be activated or even degraded by the proteasome system, through the orchestration between IRF1 different domains. **(B)** SUMOylation of IRF1 successfully occurs as a result of SUMO-IRF1 binding either on K276 hydrophobic consensus or TAD lysines. This is mediated by Ubc9, which was revealed to be overexpressed in Tumour MCF-7 cells to interact with IRF1 DBD or TAD, and this SUMOylation leads to conformational changes which disable the interplay between ED and TAD. Green mark illustrates the strong isopeptide bond formed between Ubc9 and SUMO1 which finally makes conformational IRF1 structure changes and flanks its critical domains from the interplay between each other, which marked as wrong red marks.

Chapter 5

Future Work

FUTURE WORK

IRF1 is a well-characterized member of tumour suppressor proteins and its regulation may enable researchers to treat patients with Breast cancer, AML, CML, and MDS genetically, or therapeutically through targeting certain genes or pathway that regulates IRF1 activity and stability.

5.1. ED May regulate Recruitment of Coactivators and IRF1 stability

The ED are is thought to regulate the binding of cofactors that are important for TAD functionality and stability. Subsequently, an experimental approach to ED truncation studies might use the Clustered Regulatory Interspaced Palindromic Repeats-CRISPR associated Protein9 (CRISPR-CAS9) to produce IRF1-ΔED and K276R/ K330R mutants which may elucidate the ED function and its impact on the recruitment of cofactors for the TAD.

5.2. polyubiquitination and Transactivation of IRF1 through TAD

It would be beneficial to shed light on the role of the TAD on IRF1 and determine genes that are affected by the K-R mutations. As mentioned, CRISPR-CAS9 will be used to generate stable IRF1 K-R mutants. The generation of such mutants would allow us to ascertain the genes that are affected by mutated IRF1. We might use the microarray experimental approach to track genes are possible to activate IRF1 protein and whether K233R, K240R and/or K255R are affected by SiRNA mediated knockdown of the corresponding genes. The quantitative real-time polymerase chain reaction (qPCR) would be useful analysis tool for illustration of mRNA gene

levels that might mediate the pathway intervene between ED and TAD interplay.

5.3. FBXW7α

The FBXW7α requires acidic phosphate groups to link with IRF1 motifs and the prediction of phosphorylation sites that are potential to be the acceptor of FBXW7α using new approaches are required (Zhao et al., 2012). In addition, as reported this has a significant impact on IRF1 K48-polyubiquitination and K63-polyubiquitination. Those types of linkages are important for IRF1 cellular signalling and proteasome IRF1-dependent degradation. Subsequently, an experimental approach can be performed to knockdown *FBXW7α* gene through co-transfection of FBXW7α-siRNA, followed by illustrating whether the relative IRF1-polyubiquitination, stability, and transcriptional activity of IRF1 are altered. We can measure the activity through Reporter assays, ubiquitination by Western blot, and stability with CHX chase time reaction. Hence, another approach may be useful, if we silence the endogenous mRNA FBXW7α by siRNA mediated knockdown and measure the subsequent differences of IRF1 transcriptional activity, polyubiquitination and stability will be helpful and more precise for FBXW7α.

5.4. SUMOylation of IRF1

IRF1 is reported to be modified by SUMO1 on TAD (Kim et al., 2008). The group revealed by GST pulldown assay that Ubc9 is an interactive protein with IRF1 mainly through binding with its DBD and TAD, this type of the protein-protein interaction leads to co-localization of SUMO1-IRF1 in the nuclei of the cell through SIM binding. As such, an enzymatic cascade of SUMO1 reported

revealed the ability of Ubc9 binds to DBD and TAD of IRF1. However, in their study they did not map the acceptor residues for SUMOylation, and they did not truncate ED when they showed that SUMO1 binding site was TAD. However, they confirmed that Ubc9 binds to DBD and suggested that SUMO1 targets either TAD lysine or the hydrophobic consensus that SUMO1 modifies K276 as K276R decreases SUMOylation of IRF1. The hypothesis behind the inhibition of IRF1 activity via SUMOylation arises from two points of views that SUMO1 targets ψKxD/E hydrophobic consensus sequences of either, the expressed IRF1. This leads to conformational disruption of IRF1 or, the hydrophobic consensus of other regulatory proteins that leads to IRF1 expression, such as p-STAT1 where its SUMOylation prevents p-STAT from binding with *IRF* ISRE and this prevents IRF1 expression or activation. It is not known if the ubiquitination and SUMOylation are co-incident. Consequently, SUMO1-IRF1 shows significant resistance to degradation, but also this sumoylated protein inactivates IRF1 tumour suppressor activity (Park et al., 2007). However, according to our results that K276 is not an acceptor for polyubiquitination. We can track the effect of SUMO1 which is enhanced in tumourigenesis through overexpression of Ubc9 and measure the level of SUMOylation of targeted proteins using Western Blot to know whether this modification required Ubc9 which is activated in cancerous cells. Or an *in vitro* approach may be utilized, and cellular cytosolic extract as a source of E1 enzyme for SUMO1 activation may be required, and Ubc9 to conjugate SUMO1 to E3 enzymes which in turn ligate the SUMO1 to IRF1 and finally measure the level of IRF1 SUMOylation (Hilgarth and Sarge, 2005).

5.5. IRF1 K6-polyubiquitination

The K6-ubiquitin linkage inhibits protein degradation (Shang et al., 2005), and IRF1 degradation is supposed to be regulated by C-terminal modification by K6 ubiquitin. However, our results revealed that K6-polyubiquitination has no role in IRF1 C-terminal polyubiquitination under normal conditions. Hence, the conformational structure change of IRF1 that may prevent other molecules like FBXW7a from mediating IRF1 modification. Or FBXW7α does not target K6 under normal circumstances using control HEK293T cells and only may occur during the DNA-damage repair mechanisms. Another method that K6-polyubiquitination antagonises the role of FBXW7α regarding IRF1 proteasome recognition and degradation as mentioned (Shang et al., 2005).

The future studies might induce the DNA-damage of cancerous cells used to illustrate the change in the level of K6-polyubiquitination on C-terminal of IRF1.

Chapter 6

References

REFERENCES

AU, W.-C., MOORE, P. A., LOWTHER, W., JUANG, Y.-T. & PITHA, P. M. 1995. Identification of a member of the interferon regulatory factor family that binds to the interferon-stimulated response element and activates expression of interferon-induced genes. *Proceedings of the National Academy of Sciences,* 92**,** 11657-11661.

BAILEY, C. M., KHALKHALI-ELLIS, Z., KONDO, S., MARGARYAN, N. V., SEFTOR, R. E., WHEATON, W. W., AMIR, S., PINS, M. R., SCHUTTE, B. C. & HENDRIX, M. J. 2005. Mammary Serine Protease Inhibitor (Maspin) Binds Directly to Interferon Regulatory Factor 6 IDENTIFICATION OF A NOVEL SERPIN PARTNERSHIP. *Journal of Biological Chemistry,* 280**,** 34210-34217.

BARNES, B., LUBYOVA, B. & PITHA, P. M. 2002. Review: on the role of IRF in host defense. *Journal of interferon & cytokine research,* 22**,** 59-71.

CHAN, N.-L. & HILL, C. P. 2001. Defining polyubiquitin chain topology. *Nature structural biology,* 8**,** 650-652.

CHEN, F. F., JIANG, G., XU, K. & ZHENG, J. N. 2013. Function and mechanism by which interferon regulatory factor-1 inhibits oncogenesis (Review). *Oncology letters,* 5**,** 417-423.

CLARKE, N., JIMENEZ-LARA, A. M., VOLTZ, E. & GRONEMEYER, H. 2004. Tumor suppressor IRF-1 mediates retinoid and interferon anticancer signaling to death ligand TRAIL. *The EMBO journal,* 23**,** 3051-3060.

DENG, M. & DALEY, G. Q. 2001. Expression of interferon consensus sequence binding protein induces potent immunity against BCR/ABL-induced leukemia. *Blood,* 97**,** 3491-3497.

DOU, L., LIANG, H.-F., GELLER, D. A., CHEN, Y.-F. & CHEN, X.-P. 2014. The regulation role of interferon regulatory factor-1 gene and clinical relevance. *Human immunology,* 75**,** 1110-1114.

EISENBEIS, C. F., SINGH, H. & STORB, U. 1995. Pip, a novel IRF family member, is a lymphoid-specific, PU. 1-dependent transcriptional activator. *Genes & Development,* 9**,** 1377-1387.

ESCALANTE, C. R., YIE, J., THANOS, D. & AGGARWAL, A. K. 1998. Structure of IRF-1 with bound DNA reveals determinants of interferon regulation. *Nature,* 391**,** 103-106.

FUJITA, T., REIS, L., WATANABE, N., KIMURA, Y., TANIGUCHI, T. & VILCEK, J. 1989. Induction of the transcription factor IRF-1 and interferon-beta mRNAs by cytokines and activators of second-messenger pathways. *Proceedings of the National Academy of Sciences,* 86**,** 9936-9940.

GAO, J., SENTHIL, M., REN, B., YAN, J., XING, Q., YU, J., ZHANG, L. & YIM, J. H. 2010. IRF-1 transcriptionally upregulates PUMA, which mediates the mitochondrial apoptotic pathway in IRF-1-induced apoptosis in cancer cells. *Cell Death and Differentiation,* 17**,** 699-709.

GEOFFROY, M.-C. & HAY, R. T. 2009. An additional role for SUMO in ubiquitin-mediated proteolysis. *Nature reviews Molecular cell biology,* 10**,** 564-568.

GILL, G. 2004. SUMO and ubiquitin in the nucleus: different functions, similar mechanisms? *Genes & development,* 18**,** 2046-2059.

HAGLUND, K., DI FIORE, P. P. & DIKIC, I. 2003. Distinct monoubiquitin signals in receptor endocytosis. *Trends in biochemical sciences,* 28**,** 598-604.

HAO, B., OEHLMANN, S., SOWA, M. E., HARPER, J. W. & PAVLETICH, N. P. 2007. Structure of a Fbw7-Skp1-cyclin E complex: multisite-phosphorylated substrate recognition by SCF ubiquitin ligases. *Molecular cell,* 26**,** 131-143.

HARADA, H., KITAGAWA, M., TANAKA, N., YAMAMOTO, H., HARADA, K., ISHIHARA, M. & TANIGUCHI, T. 1993a. Anti-Oncogenic and Oncogenic Potentials of. *Science,* 259**,** 12.

HARADA, H., KITAGAWA, M., TANAKA, N., YAMAMOTO, H., HARADA, K., ISHIHARA, M. & TANIGUCHI, T. 1993b. Anti-oncogenic and oncogenic potentials of interferon regulatory factors-1 and-2. *Science,* 259**,** 971-974.

HARADA, H., KONDO, T., OGAWA, S., TAMURA, T., KITAGAWA, M., TANAKA, N., LAMPHIER, M., HIRAI, H. & TANIGUCHI, T. 1994. Accelerated exon skipping of IRF-1 mRNA in human myelodysplasia/leukemia; a possible mechanism of tumor suppressor inactivation. *Oncogene,* 9**,** 3313-3320.

HARIKUMAR, K. B., YESTER, J. W., SURACE, M. J., OYENIRAN, C., PRICE, M. M., HUANG, W.-C., HAIT, N. C., ALLEGOOD, J. C., YAMADA, A. & KONG, X. 2014. K63-linked polyubiquitination of transcription factor

IRF1 is essential for IL-1-induced production of chemokines CXCL10 and CCL5. *Nature immunology,* 15**,** 231-238.

HAY, R. T. 2005. SUMO: a history of modification. *Molecular cell,* 18**,** 1-12.

HILGARTH, R. S. & SARGE, K. D. 2005. Detection of sumoylated proteins. *Ubiquitin-Proteasome Protocols***,** 329-337.

HORIUCHI, M., YAMADA, T., HAYASHIDA, W. & DZAU, V. J. 1997. Interferon regulatory factor-1 up-regulates angiotensin II type 2 receptor and induces apoptosis. *Journal of Biological Chemistry,* 272**,** 11952-11958.

KERSCHER, O., FELBERBAUM, R. & HOCHSTRASSER, M. 2006. Modification of proteins by ubiquitin and ubiquitin-like proteins. *Annu. Rev. Cell Dev. Biol.,* 22**,** 159-180.

KIM, E.-J., PARK, J.-S. & UM, S.-J. 2008. Ubc9-mediated sumoylation leads to transcriptional repression of IRF-1. *Biochemical and biophysical research communications,* 377**,** 952-956.

KIM, P. K., ARMSTRONG, M., LIU, Y., YAN, P., BUCHER, B., ZUCKERBRAUN, B. S., GAMBOTTO, A., BILLIAR, T. R. & YIM, J. H. 2004. IRF-1 expression induces apoptosis and inhibits tumor growth in mouse mammary cancer cells in vitro and in vivo. *Oncogene,* 23**,** 1125-1135.

KIRCHHOFF, S., OUMARD, A., NOURBAKHSH, M., LEVI, B. Z. & HAUSER, H. 2000. Interplay between repressing and activating domains defines the transcriptional activity of IRF-1. *European Journal of Biochemistry,* 267**,** 6753-6761.

KOMANDER, D. 2009. The emerging complexity of protein ubiquitination. *Biochemical Society Transactions,* 37**,** 937-953.

KOMANDER, D. & RAPE, M. 2012. The ubiquitin code. *Annual review of biochemistry,* 81**,** 203-229.

KONDO, S., SCHUTTE, B. C., RICHARDSON, R. J., BJORK, B. C., KNIGHT, A. S., WATANABE, Y., HOWARD, E., DE LIMA, R. L. F., DAACK-HIRSCH, S. & SANDER, A. 2002. Mutations in IRF6 cause Van der Woude and popliteal pterygium syndromes. *Nature genetics,* 32**,** 285-289.

LEE, H. J., OH, Y. K., RHEE, M., LIM, J.-Y., HWANG, J.-Y., PARK, Y. S., KWON, Y., CHOI, K.-H., JO, I. & PARK, S. I. 2007. The role of STAT1/IRF-1 on synergistic ROS production and loss of mitochondrial transmembrane potential during hepatic cell death induced by LPS/d-GalN. *Journal of molecular biology,* 369**,** 967-984.

LEE, J. H., PARK, S. M., KIM, O. S., LEE, C. S., WOO, J. H., PARK, S. J., JOE, E.-H. & JOU, I. 2009. Differential SUMOylation of LXRα and LXRβ mediates transrepression of STAT1 inflammatory signaling in IFN-γ-stimulated brain astrocytes. *Molecular cell,* 35**,** 806-817.

LEUNG, Y. T., SHI, L., MAURER, K., SONG, L., ZHANG, Z., PETRI, M. & SULLIVAN, K. E. 2015. Interferon regulatory factor 1 and histone H4 acetylation in systemic lupus erythematosus. *Epigenetics,* 10**,** 191-199.

LI, W. & YE, Y. 2008. Polyubiquitin chains: functions, structures, and mechanisms. *Cellular and Molecular Life Sciences,* 65**,** 2397-2406.

LI, X., LEUNG, S., QURESHI, S., DARNELL, J. E. & STARK, G. R. 1996. Formation of STAT1-STAT2 heterodimers and their role in the activation of IRF-1 gene transcription by interferon. *Journal of Biological Chemistry,* 271**,** 5790-5794.

LIN, A. W. & MAN, H.-Y. 2013. Ubiquitination of neurotransmitter receptors and postsynaptic scaffolding proteins. *Neural plasticity,* 2013.

LOHOFF, M. & MAK, T. W. 2005. Roles of interferon-regulatory factors in T-helper-cell differentiation. *Nature Reviews Immunology,* 5**,** 125-135.

MAJUMDER, S., ZHOU, L. Z.-H., CHATURVEDI, P., BABCOCK, G., ARAS, S. & RANSOHOFF, R. M. 1998. p48/STAT-1α-containing complexes play a predominant role in induction of IFN-γ-inducible protein, 10 kDa (IP-10) by IFN-γ alone or in synergy with TNF-α. *The Journal of Immunology,* 161**,** 4736-4744.

MAMANE, Y., GRANDVAUX, N., HERNANDEZ, E., SHARMA, S., INNOCENTE, S. A., LEE, J. M., AZIMI, N., LIN, R. & HISCOTT, J. 2002. Repression of IRF-4 target genes in human T cell leukemia virus-1 infection. *Oncogene,* 21**,** 6751-6765.

MATIC, I., VAN HAGEN, M., SCHIMMEL, J., MACEK, B., OGG, S. C., TATHAM, M. H., HAY, R. T., LAMOND, A. I., MANN, M. & VERTEGAAL, A. C. 2008. In vivo identification of human small ubiquitin-like modifier polymerization sites by high accuracy mass spectrometry and an in vitro to in vivo strategy. *Molecular & cellular proteomics,* 7**,** 132-144.

MUKHOPADHYAY, D. & DASSO, M. 2007. Modification in reverse: the SUMO proteases. *Trends in biochemical sciences,* 32**,** 286-295.

MURTAS, D., MARIC, D., DE GIORGI, V., REINBOTH, J., WORSCHECH, A., FETSCH, P., FILIE, A., ASCIERTO, M., BEDOGNETTI, D. & LIU, Q. 2013. IRF-1 responsiveness to IFN-γ predicts different cancer immune phenotypes. *British journal of cancer,* 109**,** 76-82.

NAKAGAWA, K. & YOKOSAWA, H. 2000. Degradation of transcription factor IRF-1 by the ubiquitin–proteasome pathway. *European Journal of Biochemistry,* 267**,** 1680-1686.

NAKAGAWA, K. & YOKOSAWA, H. 2002. PIAS3 induces SUMO-1 modification and transcriptional repression of IRF-1. *FEBS letters,* 530**,** 204-208.

NARAYAN, V., PION, E., LANDRÉ, V., MÜLLER, P. & BALL, K. L. 2011. Docking-dependent ubiquitination of the interferon regulatory factor-1 tumor suppressor protein by the ubiquitin ligase CHIP. *Journal of Biological Chemistry,* 286**,** 607-619.

NEHYBA, J., HRDLIČKOVÁ, R., BURNSIDE, J. & BOSE, H. R. 2002. A novel interferon regulatory factor (IRF), IRF-10, has a unique role in immune defense and is induced by the v-Rel oncoprotein. *Molecular and cellular biology,* 22**,** 3942-3957.

NGUYEN, H., HISCOTT, J. & PITHA, P. M. 1997. The growing family of interferon regulatory factors. *Cytokine & growth factor reviews,* 8**,** 293-312.

NOZAWA, H., ODA, E., NAKAO, K., ISHIHARA, M., UEDA, S., YOKOCHI, T., OGASAWARA, K., NAKATSURU, Y., SHIMIZU, S. & OHIRA, Y. 1999. Loss of transcription factor IRF-1 affects tumor susceptibility in mice carrying the Ha-ras transgene or nullizygosity for p53. *Genes & development,* 13**,** 1240-1245.

OGASAWARA, K., HIDA, S., AZIMI, N., TAGAYA, Y., SATO, T., YOKOCHI-FUKUDA, T., WALDMANN, T. A., TANIGUCHI, T. & TAKI, S. 1998.

Requirement for IRF-1 in the microenvironment supporting development of natural killer cells. *Nature,* 391**,** 700-703.

ORLICKY, S., TANG, X., WILLEMS, A., TYERS, M. & SICHERI, F. 2003. Structural basis for phosphodependent substrate selection and orientation by the SCF Cdc4 ubiquitin ligase. *Cell,* 112**,** 243-256.

PARK, J., KIM, K., LEE, E.-J., SEO, Y.-J., LIM, S.-N., PARK, K., RHO, S. B., LEE, S.-H. & LEE, J.-H. 2007. Elevated level of SUMOylated IRF-1 in tumor cells interferes with IRF-1-mediated apoptosis. *Proceedings of the National Academy of Sciences,* 104**,** 17028-17033.

PENNINGER, J. M., SIRARD, C., MITTRÜCKER, H.-W., CHIDGEY, A., KOZIERADZKI, I., NGHIEM, M., HAKEM, A., KIMURA, T., TIMMS, E. & BOYD, R. 1997. The interferon regulatory transcription factor IRF-1 controls positive and negative selection of CD8+ thymocytes. *Immunity,* 7**,** 243-254.

PERALTA, R. C., CASSON, A. G., WANG, R. N., KESHAVJEE, S., REDSTON, M. & BAPAT, B. 1998. Distinct regions of frequent loss of heterozygosity of chromosome 5p and 5q in human esophageal cancer. *International journal of cancer,* 78**,** 600-605.

PFLUGHEBER, J., FREDERICKSEN, B., SUMPTER, R., WANG, C., WARE, F., SODORA, D. L. & GALE, M. 2002. Regulation of PKR and IRF-1 during hepatitis C virus RNA replication. *Proceedings of the National Academy of Sciences,* 99**,** 4650-4655.

PICKART, C. 1997. Targeting of substrates to the 26S proteasome. *The FASEB Journal,* 11**,** 1055-1066.

PICKART, C. M. & EDDINS, M. J. 2004. Ubiquitin: structures, functions, mechanisms. *Biochimica et Biophysica Acta (BBA)-Molecular Cell Research,* 1695**,** 55-72.

PION, E., NARAYAN, V., ECKERT, M. & BALL, K. L. 2009. Role of the IRF-1 enhancer domain in signalling polyubiquitination and degradation. *Cellular signalling,* 21**,** 1479-1487.

PIZZOFERRATO, E., LIU, Y., GAMBOTTO, A., ARMSTRONG, M. J., STANG, M. T., GOODING, W. E., ALBER, S. M., SHAND, S. H., WATKINS, S. C. & STORKUS, W. J. 2004. Ectopic expression of interferon regulatory factor-1 promotes human breast cancer cell death and results in reduced expression of survivin. *Cancer research,* 64**,** 8381-8388.

RUSSELL, F. M. M. 2013. *Role of C-terminal phosphorylation in the regulation of the tumour suppressor IRF-1.* University of Edinburgh.

SAITOH, H. & HINCHEY, J. 2000. Functional heterogeneity of small ubiquitin-related protein modifiers SUMO-1 versus SUMO-2/3. *Journal of Biological Chemistry,* 275**,** 6252-6258.

SATO, M., SUEMORI, H., HATA, N., ASAGIRI, M., OGASAWARA, K., NAKAO, K., NAKAYA, T., KATSUKI, M., NOGUCHI, S. & TANAKA, N. 2000. Distinct and essential roles of transcription factors IRF-3 and IRF-7 in response to viruses for IFN-α/β gene induction. *Immunity,* 13**,** 539-548.

SCHAPER, F., KIRCHHOFF, S., POSERN, G., KÖSTER, M., OUMARD, A., SHARF, R., BEN-ZION, L. & HAUSER, H. 1998. Functional domains of interferon regulatory factor I (IRF-1). *Biochemical Journal,* 335**,** 147-157.

SCHEFFNER, M., NUBER, U. & HUIBREGTSE, J. M. 1995. Protein ubiquitination involving an E1–E2–E3 enzyme ubiquitin thioester cascade. *Nature,* 373**,** 81-83.

SHANG, F., DENG, G., LIU, Q., GUO, W., HAAS, A. L., CROSAS, B., FINLEY, D. & TAYLOR, A. 2005. Lys6-modified ubiquitin inhibits ubiquitin-dependent protein degradation. *Journal of Biological Chemistry,* 280**,** 20365-20374.

SUN, T., GAO, F., LIN, X., YU, R., ZHAO, Y., LUAN, J., LI, H. & SONG, M. 2014. α-Lipoic acid (α-LA) inhibits the transcriptional activity of interferon regulatory factor 1 (IRF-1) via SUMOylation. *Toxicology in Vitro,* 28**,** 1242-1248.

SUN, Y. & LI, H. 2013. Functional characterization of SAG/RBX2/ROC2/RNF7, an antioxidant protein and an E3 ubiquitin ligase. *Protein & cell,* 4**,** 103-116.

TAKAOKA, A., TAMURA, T. & TANIGUCHI, T. 2008. Interferon regulatory factor family of transcription factors and regulation of oncogenesis. *Cancer science,* 99**,** 467-478.

TAKAOKA, A., YANAI, H., KONDO, S., DUNCAN, G., NEGISHI, H., MIZUTANI, T., KANO, S.-I., HONDA, K., OHBA, Y. & MAK, T. W. 2005. Integral role of IRF-5 in the gene induction programme activated by Toll-like receptors. *Nature,* 434**,** 243-249.

TAMURA, T., ISHIHARA, M., LAMPHIER, M. S., TANAKA, N., OISHI, I., AIZAWA, S., MATSUYAMA, T., MAK, T. W., TAKI, S. & TANIGUCHI, T. 1995. An IRF-1-dependent pathway of DNA damage-induced apoptosis in mitogen-activated T lymphocytes.

TAMURA, T., YANAI, H., SAVITSKY, D. & TANIGUCHI, T. 2008. The IRF family transcription factors in immunity and oncogenesis. *Annu. Rev. Immunol.,* 26**,** 535-584.

TAN, R. S.-P., TANIGUCHI, T. & HARADA, H. 1996. Identification of the lysyl oxidase gene as a target of the antioncogenic transcription factor, IRF-1, and its possible role in tumor suppression. *Cancer research,* 56**,** 2417-2421.

TANAKA, N. & TANIGUCHI, T. The interferon regulatory factors and oncogenesis. Seminars in cancer biology, 2000. Elsevier, 73-81.

TANIGUCHI, T., OGASAWARA, K., TAKAOKA, A. & TANAKA, N. 2001. IRF family of transcription factors as regulators of host defense. *Annual review of immunology,* 19**,** 623-655.

THAKAR, A., PARVIN, J. D. & ZLATANOVA, J. 2010. BRCA1/BARD1 E3 ubiquitin ligase can modify histones H2A and H2B in the nucleosome particle. *Journal of Biomolecular Structure and Dynamics,* 27**,** 399-405.

THROWER, J. S., HOFFMAN, L., RECHSTEINER, M. & PICKART, C. M. 2000. Recognition of the polyubiquitin proteolytic signal. *The EMBO journal,* 19**,** 94-102.

UPRETI, M. & RATH, P. C. 2005. Expression and DNA binding activity of the recombinant interferon regulatory factor-1 (IRF-1) of mouse. *Molecular biology reports,* 32**,** 103-116.

VANDEMARK, A. P. & HILL, C. P. 2002. Structural basis of ubiquitylation. *Current opinion in structural biology,* 12**,** 822-830.

WEI, W., YANG, P., PANG, J., ZHANG, S., WANG, Y., WANG, M.-H., DONG, Z., SHE, J.-X. & WANG, C.-Y. 2008. A stress-dependent SUMO4

sumoylation of its substrate proteins. *Biochemical and biophysical research communications,* 375**,** 454-459.

WELCHMAN, R. L., GORDON, C. & MAYER, R. J. 2005. Ubiquitin and ubiquitin-like proteins as multifunctional signals. *Nature reviews Molecular cell biology,* 6**,** 599-609.

WELCKER, M. & CLURMAN, B. E. 2008. FBW7 ubiquitin ligase: a tumour suppressor at the crossroads of cell division, growth and differentiation. *Nature Reviews Cancer,* 8**,** 83-93.

WILKINSON, K. A. & HENLEY, J. M. 2010. Mechanisms, regulation and consequences of protein SUMOylation. *Biochemical Journal,* 428**,** 133-145.

XU, D., ZHAO, L., DEL VALLE, L., MIKLOSSY, J. & ZHANG, L. 2008. Interferon regulatory factor 4 is involved in Epstein-Barr virus-mediated transformation of human B lymphocytes. *Journal of virology,* 82**,** 6251-6258.

YOSHIDA, K., YAMAMOTO, K., KOHNO, T., HIRONAKA, N., YASUI, K., KOJIMA, C., MUKAE, H., KADOTA, J.-I., SUZUKI, S. & HONMA, K. 2005. Active repression of IFN regulatory factor-1-mediated transactivation by IFN regulatory factor-4. *International immunology,* 17**,** 1463-1471.

IRF1 Gene from NCBI (https://www.ncbi.nlm.nih.gov/gene/3659)

IRF1 Gene Description by Ensembl

(http://www.ensembl.org/Homo_sapiens/Gene/Summary?db=core;g=ENSG00000125347;r=5:132481609-132490798;t=ENST00000245414)